Experimental investigation of hydrogeochemical consequences of gas leakages into shallow aquifers

PhD Thesis

Márton Berta

Kiel University
Faculty of Mathematics and Natural Sciences
Institute of Geosciences
2017

Dissertation
zur Erlangung des Doktorgrades
der Mathematisch-Naturwissenschaftlichen Fakultät
der Christian-Albrechts-Universität zu Kiel

vorgelegt von Márton Berta

Kiel, 2017

Erster Gutacher: PD. Dr. Markus Ebert
Zweiter Gutachter: Prof. Dr. Klaus Wallmann

Tag der mündlichen Prüfung: 11. April 2017

Zum Druck genehmigt: 11. April 2017

gez. Prof. Dr. Natascha Oppelt, Dekanin

Acknowledgements

First, I would like to thank Dr. Frank Dethlefsen for his active commitment to all the tasks involved in this doctoral research project, for endless discussions and spontaneous thinking together as well as for his constant support improving my formal and soft skills in many ways including writing and teamwork. Distinguished thanks also go to PD Dr. Markus Ebert for his constructively critical suggestions on constructing experiments, data evaluation, model development and on our written and presented outcomes; and to Prof. Dr. Andreas Dahmke for his strategic directives regarding this work. I thank all my three *de facto* supervisors for taking me as a doctoral candidate at the beginning, and for leading me through the challenges and discoveries in the past few years as well as creating the frames for the work which opened a way for me in this team to learn many new things and skills I could while getting until the -hopefully successful- end of my doctoral process.

Additionally, I would like to thank the reviewer Prof. Dr. Klaus Wallmann, the examiner Prof. Dr. Romain Bousquet and the chairperson Prof. Dr. Sebastian Bauer for all the work when assessing my Thesis in the doctoral examination committee.

The funding provided by the German Ministry of Education and Research (BMBF) for the ANGUS+ project, grant number 03EK3022, as well as the support of the Project Management Jülich (PTJ) are both gratefully acknowledged. Special thanks go to my supervisors and the Project Coordination for allowing me to finish this PhD Thesis.

I would like to thank all our coworkers contributing to this research: Dirk Schäfer for his remarks, simulations and support in 3D gas leakage modeling; Joachim Lippke for his always cheerful, flexible and effective cooperation to get analytics done; Jutta Salamon for her constantly kind help at measurements; Anke Westphal, Tobias Lienen and Hilke Würdemann (GFZ Potsdam) for the microbial results they provided; Birgit Mohr for her kind and patient training at the SEM; Ulrike Westernströer for precisely investigating trace elements in our samples; Oliver Lischtschenko and Derek Guenther (OceanOptics GmbH) for advising us regarding optical oxygen measurement; Claus-Henning Solterbeck (IMST FH Kiel) for generously providing time and instructions with Raman; Alina Kabuth for the project coordination; Thorsten Kohnert, Wolfgang Jonathal and the Werkstatt members for their effective help at the construction of the experiments; and Birgit Jacobsen as well as Klaus-Dieter Stüwe for their smooth and cheerful help with the bureaucratic challenges.

I am very thankful for my fellow PhD Students: Svea Hausberg for her support especially at the beginning; Klas Lüders for his support in the preparation of this Thesis and for all the random talks on countless issues from various fields in our mighty office; Nicolas Koproch for many happy discussions at second lunch; Bo Wang for his aspects on pyrite oxidation and compressed air storage; Wolf Tilmann Pfeiffer for his points on geological hydrogen storage; Elisabetta Ballarini for her advices during weekends and late evening hours; Tessa Strutz, Kerstin Meier zu Beerentrup, Janin Struß, and Johannes Nordbeck for their general advices; and the whole group of colleagues in Kiel and the other ANGUS+ partners all over Germany.

Master (Karsten Gundske, Saskia Koch, Claus Mascus, Stefan Berger) and Bachelor (René Mommsen, Julia Bußmann, Anne Becker, Adrian Metzgen) students, as well as HiWis (Louisa Lagmöller, Patricia Brandt) working with me contributed together by more than a thousand working hours to the outcomes of the ANGUS+ AP1.7 and this dissertation, for which I am very thankful; and I am also really proud to have most of them as coauthors of papers and posters.

I also thank my former supervisor(s) and colleagues in the LRG lab at the ELTE University in Budapest for helping me become eligible for this doctoral position.

Last, but definitely not least I thank my whole family and all my close and remote friends very much for their kind, diverse, and constant support during my whole quasi-half-a-decade-long stay in Kiel!

I dedicate this PhD Thesis to my Grandmother.

Preface

This cumulative doctoral Thesis is composed by three main chapters (Chapters 2-4) as well as a common introduction (Chapter 1) and common conclusions (Chapter 5). The three main chapters report on the distinct episodes of investigating hydrogeochemical effects of an intrusion of the three investigated gases, namely compressed air, methane, and hydrogen, into a shallow aquifer. All these chapters are based on manuscripts prepared for submission, as indicated after each title. Critiques and remarks suggested by reviewers and journal editors were also incorporated, where available; the published forms of the papers are provided in the Appendix. Beyond the published outcomes, all three chapters were extended by additional results. Although these further aspects were not included in the submitted manuscripts, they are presented here because they still contribute to the topics discussed in the respective papers and because the underlying research was carried out in the frames of this doctoral project. Four Master and four Bachelor theses were also prepared in cooperation with this dissertation. These works are included in the References as well as the raw data gathered during the experimental investigations in the Appendix.

In addition to journal publications and theses, several talks and posters have been prepared and presented at various meetings to additionally spread the results assembled in the frames of this doctoral project: all these talks and posters, along with their corresponding abstracts, can be found on the Appendix CD of this PhD Thesis, too. The work presented in the talk at the meeting of the Hydrogeology Division of the German Geological Society (FH-DGG) in 2014 and the work presented on the poster at the European Association of Geoscientists and Engineers (EAGE) Sustainable Earth Sciences meeting in 2015 were awarded with prizes given by the FH-DGG, and the EAGE, respectively.

The presented doctoral research is part of the ANGUS+ joint research project. The wider context of the project is the globally increasing need for energy storage solutions, with the focus on geological energy storage. Such a focus is justified by various studies predicting that stabilizing future energy networks containing a major share of solar and wind energy production is expected to involve the subsurface along with other technologies. To support the planning and implementation of such geological energy storage facilities, participating ANGUS+ project partners have been investigating various scenarios of using the subsurface space including the side effects subsurface use can have on protected natural goods in the deep and shallow subsurface using mainly experimental and modeling tools. Within the framework on shallow aquifers, potential effects of heat storage and gas leakages were investigated through experiments and modeling in various working packages usually coupled to PhD projects similar to this presented one. The experimental efforts supported both the process understanding and the parameterization workflow for developing numerical models and directly contributed to the evaluation of scenarios of subsurface use. The outcomes of this Thesis support the description of the geochemical consequences of a gas (compressed air, methane or hydrogen) leakage and also provide references for calibrating geochemical reaction models and potential future experimental or field investigations.

A further outcome of this PhD project is, therefore, its contribution to the Final Project Report as well as its input to the ANGUS+ German Guidelines for Subsurface Energy Storage, a collection of recommendations improving the planning, monitoring, and operation practices of geological energy storage systems.

Abstract

The fluctuating energy production of renewable sources, most importantly wind turbines and photovoltaic panels, implies the necessity of energy storage. Already operating possibilities for large scale geological energy storage include storage of compressed air (CAES), methane, and hydrogen. For the safe and sustainable implementation of subsurface energy storage, assessment studies and monitoring strategies are needed, based on proper process understanding and supported by evaluating numerically modeled scenarios of subsurface use. In case of gas storage, this process understanding includes knowledge gaps regarding gas-specific reactions to be expected in shallow aquifers following a leakage of compressed air, methane, or hydrogen. These reactions can change the composition of the groundwater, which potentially leads to conflicts between different ways of utilizing the subsurface. Additionally, groundwater is a natural good protected by law in most developed countries.

Experiments representing reactive hydrogeological environments characteristic to a shallow aquifer influenced by a gas plume were carried out and were evaluated, constituting the main part of this PhD Thesis. The applied experimental approach most importantly included flow-through column experiments using a sediment from a shallow Pleistocene aquifer percolated by the groundwater from the same aquifer as well as auxiliary batch and column experiments with further materials. The water used to percolate the experimental sediment columns was saturated by the respective gas at partial pressures representing the conditions taking place within a dissolved gas plume in a shallow aquifer after a leakage of compressed air, methane, or hydrogen.

Supporting expectations based on literature data, experiments on leakage of compressed air showed pyrite oxidation (at a rate up to 4 μM/h) in the sediment columns. At oxygen partial pressures between 0 and 11 bars kinetically controlled pyrite oxidation therefore caused an increase in sulfate concentration and a decrease in pH. The transfer function on reaction kinetics developed using PHREEQC based on the experimental reaction rates for upscaling the results includes a new surface passivation term describing the inhibition of more than 90% of the pyrite reactivity compared to the reactivity expected based on previously published models. This model was then integrated into a multiphase 3D numerical reactive transport model to investigate potential site-scale effects.

Methane oxidation coupled to reduction of nitrate and especially sulfate is known from various groundwater and marine environments. However, fugitive methane was not oxidized and did not cause detectable changes in the groundwater within one year in the presented flow-through column experiments. This finding acknowledges earlier studies describing no methane oxidation if methane or its electron acceptors are newly introduced into an aquifer, even if methane and its electron acceptors are unlikely to be present in natural conditions concurrently in a steady state.

In contrast to methane, elevated (in the mM range instead of the natural nM range) concentration of hydrogen immediately triggers a series of redox reactions. Changes in groundwater composition were found in experiments with hydrogen partial pressures between 1 and 25 bars. The resulting reduction of ferric iron, nitrate (rates up to 10.4 $\mu M/cm^3$sediment/h), sulfate (rates up to 42 nM/cm^3sediment/h), and carbonate have major effects on groundwater, including the increase of acetate (rates up to 85 nM/cm^3sediment/h), nitrite, and sulfide concentrations and pH (by up to 1.5); along with decreasing (by 150 μS/cm) electric conductivity. Based on these observations, a descriptive reaction model was developed for further modeling applications.

The conclusions of this PhD project have direct applications beyond the description of reactive conditions not explicitly studied before. The observed hydrogeochemical behavior of gas-saturated shallow geological environments improves the state-of-the-art process understanding for gas leakage scenarios and serves as a base for further research efforts. Moreover, geohydromodeling efforts may utilize the presented quantification of geochemical reactions when parameterizing numerical scenarios on geological energy storage for site characterization as well as for developing leakage monitoring strategies. Such investigations are expected to contribute to more sustainable energy storage solutions in future energy networks.

Kurzfassung

Die fluktuierende Energiebereitstellung aus erneuerbaren Quellen, vor allem Wind- und Solarenergie, impliziert die Notwendigkeit einer Energiespeicherung. Bereits verwendete Möglichkeiten für großskalige unterirdische Energiespeicherung sind unter anderem Druckluft- (CAES), Methan- und Wasserstoffspeicherung. Für eine sichere und nachhaltige Umsetzung geologischer Energiespeicherung werden auf einem angemessenen Prozessverständnis und der Auswertung numerischer Nutzungsszenarien des Untergrundes basierende Bewertungstudien und Monitoringmaßnahmen benötigt. Das Prozessverständnis für die zu erwartenden gasspezifischen Folgereaktionen im Falle einer Leckage von Druckluft, Methan oder Wasserstoff aus einem Gasspeicher in einen oberflächennahen Grundwasserleiter ist unvollständig. Insbesondere diese Folgereaktionen können jedoch die Zusammensetzung des in vielen Ländern gesetzlich geschützten Grundwassers verändern.

Zur Verbesserung des Prozessverständnisses bezüglich der potenziellen Folgereaktionen einer Gasleckage in oberflächennahe Grundwasserleiter wurden relevante hydrogeochemischen Bedingungen repräsentierende Experimente durchgeführt, welche den Hauptteil dieser Dissertation ausmachen. Dabei wurden Säulen-, und Batchexperimenten hauptsächlich mit Sediment und Grundwasser aus dem selben flachen, pleistozänen Aquifer durchgeführt. In dem jeweiligen Versuchswasser wurde dann entsprechend der zu simulierenden Partialdrücken Druckluft, Methan oder Wasserstoff gelöst um die Bedingungen in einer Fahne aus gelöstem Gas nach einem Leckageereignis nachzustellen.

Experimente zu Druckluftleckagen zeigten in Übereinstimmung mit Literaturdaten eine Pyritoxidation (mit Raten bis zu 4 μM/h). Bei Sauertoffpartialdrücke von 0 bis 11 bar verursachte eine kinetisch kontrollierte Pyritoxidation eine Zunahme der Sulfatkonzentration und eine Abnahme des pH-Wertes. Die mit PHREEQC auf den experimentellen Ergebnissen basierend entwickelte Transferfunktion für die Reaktionskinetik zur Hochskalierung der Ergebnisse enthält auch einen Term für die Oberflächenpassivierung, mit der die Inhibition von bis zu 90% der anhand von zuvor publizierten Modellen erwarteten Reaktivität beschrieben wird.

Methanoxidation gekoppelt mit einer Reduktion von Nitrat und besonders Sulfat, ist aus verschiedenen Marinen- und Grundwassermilieus bekannt. Jedoch wurde flüchtiges Methan in den vorliegenden Durchfluss-Säulenexperimenten innerhalb eines Jahres weder oxidiert, noch verursachte es Veränderungen in der Grundwasserzusammensetzung. Dieses Ergebnis bestätigt frühere Studien in denen keine Methanoxidation beobachtet wurde, falls Methan oder seine Elektronakzeptoren neu in einen Aquifer intrudierten, auch wenn Methan und seine Elektronenakzeptoren unter natürlichen Bedingungen normalerweise nicht gleichzeitig vorhanden sind.

Im Gegenteil zu Methan, lösten hohe (in der Größenordnung von mM statt der natürlichen nM) Wasserstoffkonzentrationen sofort nach ihren Eintritt ins Grundwasser Redoxreaktionen aus. Veränderungen in der Grundwassersusammensätzung wurden in Experimenten mit 1-25 bar Wasserstoffpartialdruck gefunden. Die resultierende Reduktion von Eisen, Nitrat (bis zu 10.4 $\mu M/cm^3$Sediment/h), Sulfat (bis zu 42 nM/cm^3Sediment/h), und Karbonat haben eine bedeutende Auswirkung auf die Grundwasserzusammensetzung, einschließlich der Zunahme der Acetat- (bis zu 85 nM/cm^3Sediment/h), Nitrit-, Sulfidkonzentrazionen, des pH-Werts (von bis zu 1.5) und der Abnahme der elektrischen Leitfähigkeit (von ca. 150 μS/cm). Basierend auf diesen Beobachtungen wurde ein deskriptives Reaktionsmodell entwickelt.

Die in dieser Dissertation dargelegten, experimentell begründeten Aussagen haben direkte Anwendbarkeit über die Beschreibung bisher nicht untersuchter geochemischer Bedingungen hinaus. Das beobachtete hydrogeochemische Verhalten gasgesättigter oberflächennaher geologischer Milieus verbessert das Prozessverständnis für Gasleckageszenarien und kann als Grundlage für die Charakterisierung neuer Gasspeicher und für die Entwicklung von Monitoringstrategien genutzt werden. In der Geohydromodellierung könnten die quantifizierten geochemischen Reaktionen zur Parametrisierung von numerischen Szenarien zur Energiespeicher im Untergrund verwendet werden.

Contents

1. Introduction

1.1. Energy transition and the need for energy storage

The anthropogenic greenhouse gas emissions increasing since the pre-industrial era have been causing an unprecedented change in the climate of the Earth (IPCC, 2014), especially in terms of temperature. These temperature changes imply an overall warming of the atmosphere and the oceans, as well as a rise in the sea level and an increasing frequency and intensity of extreme weather events. The combination of such climatic impacts results in a wide range of harmful environmental and economic consequences, which shall be diminished by the widening international consensus on the agenda to be followed. Complementary responses given to climate change aiming at a sustainable future may be divided into mitigation and adaptation measures (IPCC, 2014). A main goal of several mitigation strategies is to decrease the emissions of anthropogenic greenhouse gases, most importantly carbon dioxide, which is released mostly when producing energy or power for heating, transport or industrial processes. Additionally to other factors, such as decreasing dependency on energy import, preventing carbon dioxide emissions has been motivating a large-scale development of renewable energy sources in many industrialized nations since the last few decades (BMUB, 2013). This global energy transition suggests a further development also supported by ambitious national and international goals, including for instance a scenario considering at least 85-90% renewable energy production until 2050 in Germany (UBA, 2010).
Within most scenarios on energy systems wind turbines and solar panels represent a significant proportion of both the renewable capacities installed so far and also in the capacities still to be developed. However, a major issue caused by the increasing use of wind and solar energy is the fluctuating energy production caused by these sources on the power supply side (Figure 1.1). On the demand side of the network the energy consumption of end users fluctuates as well, which could be followed by more flexible energy production technologies. Such conventional sources include igniting fossil hydrocarbons as well as using renewable energy sources like biogas or hydropower, which are often limited in capacity by regional conditions. The increasing use of climate neutral energy sources in the upcoming decades is therefore expected to create and propagate a fluctuating gap between supply and demand in power networks. This changing, positive or negative, gap between renewable power production and the consumption of end users is one of the major challenges for both regional and international energy systems, and their operators will have to assess this issue in order to function safely and sustainably in the future.

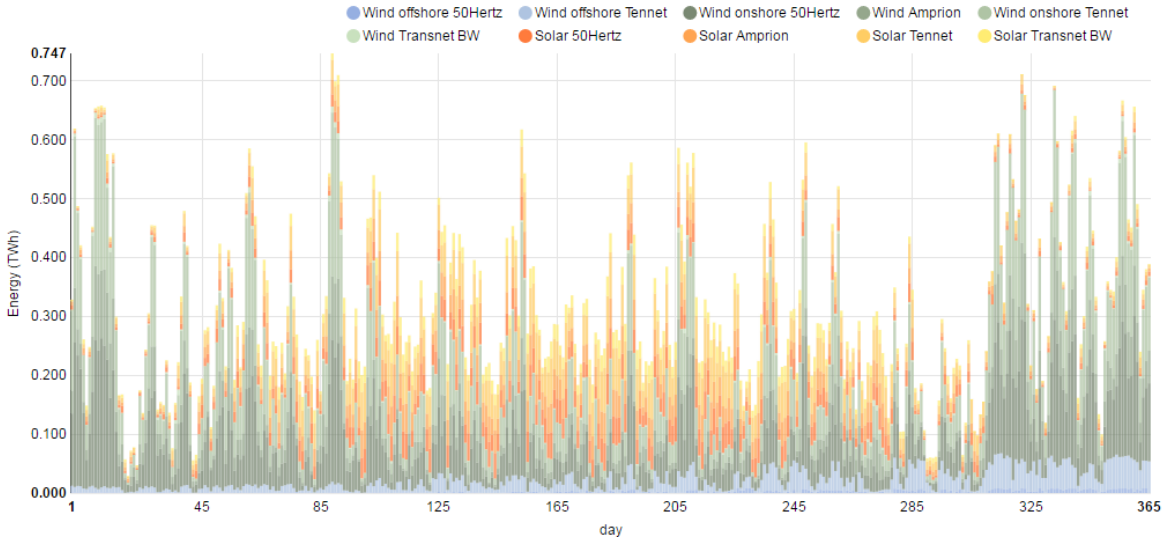

Figure 1.1: Strongly fluctuating daily wind and solar power production in different German networks in 2015 (Fraunhofer, 2016).

Storage of renewably produced energy may balance the fluctuating gaps between overproduction (surplus) and underproduction (shortage) of energy compared to the demand on the market. Considering the described growth in such fluctuations an increasing need for energy storage solutions can be very well predicted. Energy storage in general can be carried out by simultaneously implementing and improving a wide range of already available technologies (Figure 1.2). A synergic structure of various energy storage methods may be installed by combining technologies with different response times (e. g. intraday and seasonal) and volume scales (e. g. household or regional). Several ways to store energy may be based on different working principles (e. g. physical or chemical), which shall be coupled and optimized for sustainable future applications. For example, already at a projected renewable share of 85% in the energy supply network a cooperating storage system including power-to-gas energy storage, heat storage and short-term storage technologies like pumped hydro facilities will be a strict prerequisite for a stable operation (Sterner and Stadler, 2014). As a renewable share of around 85% is needed to fulfill major European climate protection goals by 2050 (UBA, 2010), the development of energy storage technologies, including the construction of large-scale facilities, is probably inevitable.

For an economically and environmentally sustainable application of technologies involved in energy storage detailed evaluation is needed regarding potential operational and unwanted environmental impacts but they also need assessments concerning possible interactions influencing their efficiency (Bauer et al., 2013). Such investigations are especially crucial for large-scale facilities (e. g. pumped hydro, heat or gas storage) because the zones of their implementation may interfere with areas where other ways of resource utilization, most importantly water production, is carried out. Moreover, large-scale energy storage technologies installed in natural systems can potentially cause changes in one or more elements of the environment, for instance in the groundwater. Characterizing such interactions and changes will, therefore, support the efforts for realistically planning and sustainably operating a future renewable-based energy network balanced by energy storage technologies.

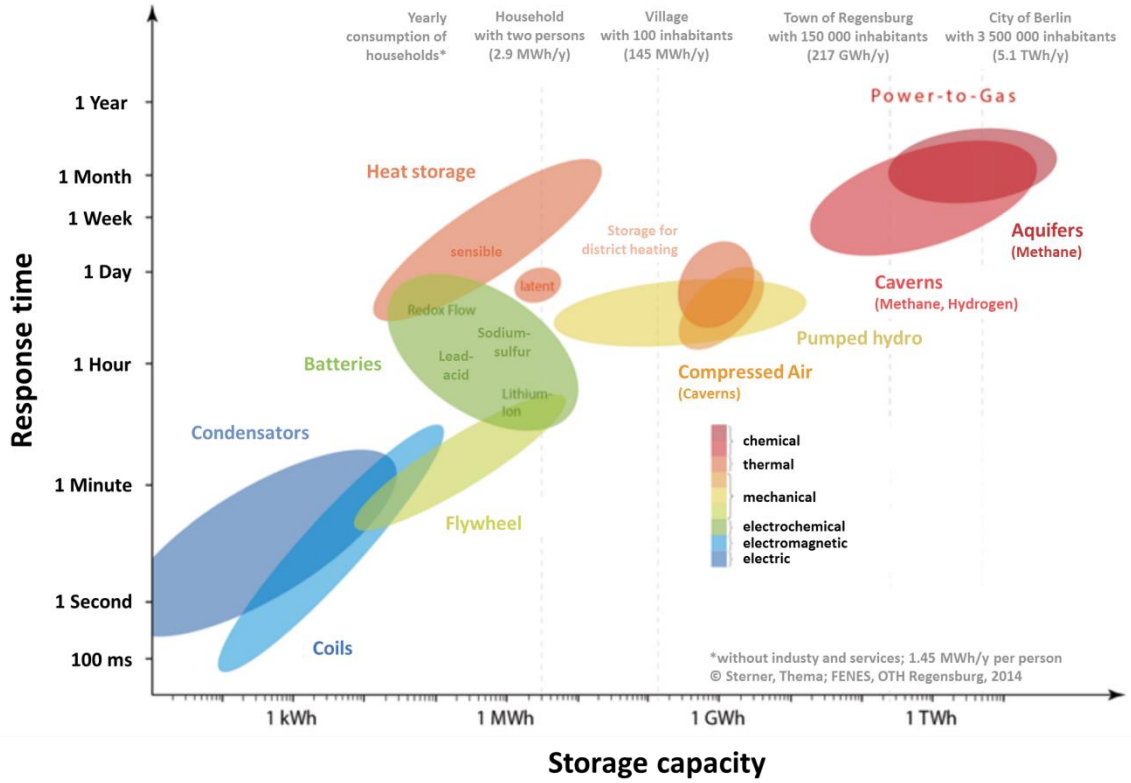

Figure 1.2: Comparison of energy storage technologies installed in Germany based on the response time and capacity ranges they are able to cover (modified after Sterner and Stadler, 2014).

Both amongst large and small scale systems the subsurface offers several possibilities for energy storage in the context of the transition towards a sustainable future energy system (Bauer et al., 2013; Kabuth et al., 2017; Bauer et al., 2015 a and b). Geological energy storage technologies include most importantly storage of heat and gases; both generated from surplus electricity production and termed "power-to-heat" and "power-to-gas", respectively. When using aquifer heat storage injection and production wells installed in the shallow subsurface can provide buffering on up to a seasonal time scale for the heating or cooling needs of up to districts. Constructing power-to-gas plants connected to geological gas storage facilities in the deep subsurface can balance larger power surpluses and shortages in whole regions (Figure 1.2). These subsurface gas reservoirs may be installed in artificial salt caverns or deep confined aquifers to store typically compressed air, methane, or hydrogen.

1.1. Gas storage and impacts of gas leakages

By 2050 in Germany alone, the capacity for power-to-gas energy storage is projected to reach 110 TWh and 514 TWh for hydrogen and methane, respectively (Sterner and Stadler, 2014), which could potentially balance the broad fluctuations taking place in a renewable-intensive energy supply mix (Figure 1.1). The expansion of gas storage capacity in the upcoming decades requires the construction of several geological gas storage sites, involving the operation of various subsurface facilities containing the stored gas under high pressure (e. g. wells, gas caverns, reservoirs, etc.). However, the shallow and deep subsurface is very often used for several purposes other than gas storage simultaneously (Figure 1.3), which can potentially lead to conflicts between concurrent ways of subsurface utilization. Interactions caused by gas storage include those caused by normal operation and by unwanted events, such as accidental gas leakages (Evans, 2008). These thermal, hydraulic, mechanic and chemical effects may lead to changes relevant for the operators of the gas storage site as well as for civil and official stakeholders (Bauer et al., 2013). Therefore, the zone(s) of operation as well as the surrounding zone shall consider the area where the processes induced by gas storage can potentially be identified. In such an area the monitoring of gas storage or identifying potential leakages shall be carried out to observe and follow regular or unwanted changes in- and around geological gas storage facilities (Bauer, 2015a). Beyond the interactions influencing the use of subsurface resources or energy storage operations themselves, gas storage can also have unwanted effects on protected natural goods, such as groundwater in the shallow subsurface. For a wider implementation of power-to-gas energy storage extensive and thorough understanding of the processes potentially changing the conditions of protected natural goods or reservoir conditions is needed to adequately handle potential environmental and operational effects of subsurface gas storage technologies. A highlight of such investigations may be laid on the groundwater, and particularly on potential changes in its composition.

Groundwater, especially in shallow aquifers, is a protected natural good and it is often utilized as a resource for drinking water; therefore potential changes in its flow, temperature, and, most importantly, composition are of distinguished significance and consequently often a matter for major public concern. One or more of these groundwater conditions can potentially be influenced by a gas intrusion originating from a gas storage facility in an underlying reservoir. Stored gases may leak through reactivated faults, broken, forgotten, or poorly sealed wells, or through a not homogenously impermeable cap rock (Evans 2008; Evans, 2009). On the other hand, deep porous reservoirs and salt caverns are still considered to be a comparatively safe and cost-efficient solution for storing major amounts of compressed gases, such as air, methane, or hydrogen (Taylor, 1986).

Therefore, deep saline aquifers and artificial salt caverns may be expected to accommodate large-scale energy storage facilities in the potential vicinity of protected shallow groundwater resources (Figures 1.2 and 1.3). Considering the scenario of an accidental gas leakage from a deep reservoir, the site characterization process before installing new gas storage facilities usually requires the evaluation of potential changes in groundwater conditions, especially in groundwater chemistry, possibly caused by gas leakages.

The chemical composition of the groundwater can be influenced beyond the dissolution of the leaked gas by various geochemical reactions potentially taking place in an aquifer. Although the leakage mechanisms of methane, hydrogen, or compressed air show some similarities to leaky carbon capture and sequestration (e. g. Apps et al., 2010; Dethlefsen et al., 2013; Haase et al, 2014) and hydraulic fracturing (e. g. Osborn et al., 2011) facilities, their geochemical consequences can be expected to be different. So far, only a few studies considered biogeochemical or hydrogeochemical consequences of accidental leakages of compressed air, methane, and hydrogen into shallow aquifers from storage facilities coupled to power-to-gas plants.

As discussed above, well-characterized geochemical processes contribute to a better understanding of various aspects of routine operation and leakage management. For instance, operational and leakage monitoring of subsurface gas storage facilities can very well be supported by identifying geochemical changes known to occur within a dissolved or multiphase gas plume in an aquifer. Also before the actual gas storage would start, the description of such reactions can support site characterization as well as risk assessment efforts by evaluating the potential for the changes geochemical reactions may cause in the subsurface. In order to optimize the planning and the monitoring of geological gas storage systems numerical models are widely applied (e. g. Pfeiffer et al., 2016). By evaluating various scenarios potentially taking place while using the subsurface in defined ways a wider geological and technological context of energy storage can be considered and projections can also be made considering the specific boundary conditions. Including geochemistry in such computer models in general, and geochemical reactions in particular, can provide more realistic results for simulating subsurface environments influenced by gas storage or gas leakages. To reliably support leakage monitoring, storage site assessment, and model parameterization workflows involving hydrogeochemical reactions, such reactions cannot be sufficiently characterized based on general kinetic or even equilibrium data gathered from the literature. However, as discussed above, studies have not been published on geochemical aspects of effects large-scale subsurface storage of hydrogen, methane, or compressed air could have on shallow groundwater in an extent which could provide a well-established base for model parameterization workflows. Therefore, to investigate which geochemical reactions shall be expected to take place in aquifers following a gas intrusion, further process characterization is needed, including the identification of the reactions actually taking place and quantifying their kinetic behavior at aquifer conditions.

Changes, hydrogeochemical changes in particular, can potentially be caused in the subsurface by the intrusion of gases (Bauer et al., 2013; Kabuth et al., 2017; Bauer et al., 2015 a and b). Amongst a series of possible geochemical consequences subsurface energy storage can have (e. g. Lüders et al., 2016), the hydrobiogeochemical interactions potentially taking place when unwanted gas leakages from deep reservoirs intrude shallow freshwater aquifers can have many implications and such scenarios are therefore investigated and discussed here in details (Figure 1.3).

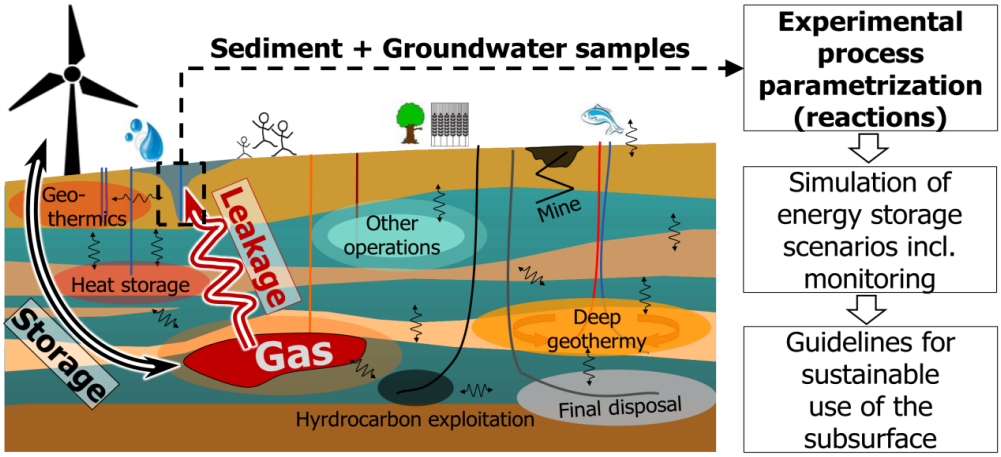

Figure 1.3: Possible conflicts between potential ways of using the subsurface for mass and energy storage (left), and the concept for investigating these interactions (right); the energy storage scenarios as well as the investigation workflows discussed in this Thesis are marked as bold (modified after Bauer et al., 2013).

1.2. Reactions in shallow aquifers following a gas leakage

Amongst various hydrogeochemical and biogeochemical processes able to change the composition of groundwater, redox reactions may be expected to have a deciding impact if a plume of compressed air, methane, or hydrogen would intrude an aquifer (Appelo and Postma, 2010; Bauer et al., 2013). The intrusion of these three gases would potentially affect the redox state of an aquifer by providing additional reducing (electron donating) or oxidizing (electron accepting) reactants. In case of a compressed air leakage oxygen serves as an electron acceptor while fugitive hydrogen and methane can have the role of the electron donor. Reaction partners for processes to take place can be available from the solid phase (e. g. pyrite to be oxidized) or they can be dissolved in the groundwater (e. g. sulfate and nitrate to be reduced) or can be found in both solid and dissolved form (e. g. carbonate to be reduced). The occurrence and the kinetics of aqueous redox reactions is determined primarily by the availability of electron acceptors and electron donors as well as by the activation of a reaction path by thermodynamically favorable conditions or catalysis, for instance by microorganisms.

The evaluation of redox reactions following the leakage of compressed air, methane, or hydrogen, as well as the integration of these reactions in numerical modeling and leakage monitoring workflows require clear identification and proper parameterization of the occurrence and the kinetics of such reactions. The consecutive steps for such a characterization may be realized through collection and synthesis of literature and field data, laboratory experiments, and pilot field investigations.

Leakage of compressed air may result in a high partial pressure of oxygen in aquifers typically depleted in oxygen (Chapter 2). A major part of the oxygen intruding an aquifer is usually consumed by the oxidation of pyrite (Descouvieres et al., 2010), therefore pyrite oxidation can be considered as a potential consequence of an accidental compressed air intrusion into a shallow aquifer. What is known on the kinetics of pyrite oxidation is known mostly from studies investigating acid mine drainage sites (e. g. Williamson and Rimstidt, 1994), where oxygen-saturated, mostly meteoric water intrudes mining or mining waste disposal areas. The waters discharged from such reactive environments are characterized by low pH value, high sulfate content and often a considerable amount of dissolved toxic trace elements. However, in shallow groundwater the changes in pH may be buffered by dissolved or even solid phase carbonates ubiquitously available in aquifers. Investigating the effects of such a buffer on pyrite oxidation kinetics is therefore essential for understanding the hydrogeochemical processes taking place after a compressed air leakage into a shallow aquifer.

In contrast to oxygen, methane of natural, biogenic origin can often be found in shallow and deep aquifers where all electron acceptors are already depleted. Gas leakages may enrich also aquifers in methane, where a substantial amount of electron acceptors, most importantly sulfate (Knittel and Boetius, 2009), is still available, which poses a potential for redox reactions to take place (Chapter 3). The characteristics of microbially mediated anaerobic oxidation of methane coupled to sulfate reduction are known mostly from sulfate-methane transition zones in marine and freshwater environments. At such interfaces the microbial community carrying out the reaction has been well established over a time which is way longer than the few months to few years' time span of a gas leakage. Therefore, additional understanding of the reactive behavior of a freshwater aquifer influenced by a comparatively sudden and extensive methane intrusion is needed for parameterizing site-scale numerical models and to support monitoring as well as the development of their methods.

Hydrogen can also be found in natural aquifers, mostly as an intermediate of microbial redox reactions degrading organic matter. However, usual hydrogen concentrations in aquifers are in the nanomolar range and these very low hydrogen concentrations correlate with the terminal electron accepting reactions taking place in such environments. However, if a gas leakage provides hydrogen at high concentrations of up to several millimoles, the hydrogenotrophic redox reactions known from hydrogen-limited environments may show significantly different kinetic behavior (Chapter 4). Therefore, to enable a realistic understanding and parameterization of redox reactions taking place after the intrusion of hydrogen into an aquifer, further investigation is needed, covering a hydrogen concentration range which is about a million times higher than values in natural systems.

1.3. Aims of this Thesis

In order to gather data enabling such a characterization process beyond the available state of the literature, laboratory experiments were carried out. The applied batch (0 D) and column (1 D) experiments represented the reactive environment of a shallow aquifer influenced by a gas leakage most importantly in terms of the partial pressures of gases, which corresponded to a gas leakage into a shallow aquifer. The experiments were realistic in terms of the sediment and groundwater used, as these materials were gathered mostly from shallow aquifers. The transport (flow) conditions created in column experiments aimed to represent a homogenous flow field within an aquifer, with groundwater flow speeds usually set close to realistic values. Therefore, the applied experimental methods can enable the direct observation of geochemical reactions, the measurement of their rates, and the characterization of their kinetic behavior. Such outcomes will support the process understanding for model development and monitoring efforts considering subsurface gas storage scenarios.

The aim of the investigations carried out in the frames of the presented PhD project was to experimentally identify and parameterize geochemical reactions taking place in a shallow aquifer as a consequence of a gas intrusion originating from a leakage from a storage reservoir. Furthermore, reaction models deducted from experimental results completed the evaluation process. The experimental conditions with three gases (O_2, CH_4, and H_2) at elevated dissolved concentrations investigated effects of compressed air, methane and hydrogen intrusions in originally pristine groundwaters, and delivered a base for interpretation to answer the questions below. These investigations are presented after organizing them into three chapters answering primarily the following main questions:

1. How does pyrite oxidation by oxygen change the groundwater in a shallow aquifer after a leakage of compressed air?
    a. How do the products of pyrite oxidation decrease pyrite reactivity? What factors influence this passivation?
    b. What transfer function can scale up the results from lower, athmospherical pressure experiments to higher, in situ conditions?
2. How can methane be oxidized in a shallow aquifer after a methane leakage and what reaction rates should be considered?
    a. What does the state-of-the-art literature reveal on microbial redox reactions oxidizing methane in aqueous environments?
    b. What is the expected time scale for starting a reaction involving reduction of sulfate or nitrate coupled to methane oxidation?
    c. What should be in the focus of monitoring and modeling efforts for fugitive methane?
3. What biogeochemical redox reactions do elevated hydrogen partial pressures trigger in shallow aquifers and at what rates do these reactions take place?
    a. Is nitrate, sulfate and carbonate reduction dependent on hydrogen concentration?
    b. Are the observations on reactions potentially transferable to deeper aquifer environments?

2. Surface passivation model explains pyrite oxidation kinetics in column experiments with up to 11 bars $p(O_2)$

This chapter is based on a paper published by Berta M, Dethlefsen F, Ebert M, Gundske K, Dahmke A (2016) in Environmental Earth Sciences 75:1175.

2.1. Abstract

Despite decades of research in numerous experimental and field studies, the reaction kinetics of pyrite oxidation is still not characterized for high partial pressures of oxygen and near-neutral pH-levels. These conditions potentially exist in aquifers where oxidative site remediation, temporary water storage, or a leakage from a Compressed Air Energy Storage facility is present. For planning and monitoring of such field operations, their potential side effects on protected natural resources like groundwater have to be characterized.

Thereby, site-scale assessments of such side effects of subsurface use by numerically modeling geochemical changes caused by the presence of oxygen need parametrization. Also, a function transferring results from simple, low pressure experiments to high pressure environments requires experimental bases.

Pyrite oxidation can be the main consequence of oxygen intruding reduced aquifers. In this study, pyrite oxidation kinetics was examined at oxygen partial pressures from 0 to 11 bars, corresponding to an air intrusion in up to 500 m depth, at neutral pH-levels in high and low pressure flow-through column experiments representing aquifer conditions. A reaction rate equation was developed and evaluated with 1D PHREEQC numerical reactive transport models using experimental data as transfer function between high pressure and low pressure experiments. This model development included an improvement of established rate laws with a passivation term, which is, in contrast to previously published functions, dependent on the partial pressure of oxygen. The resulting model on passivated oxidation kinetics of pyrite at high oxygen partial pressures was able to reproduce independent experimental results acquired using different experimental set-ups. This assessment found the passivation to overcome the theoretical increase in pyrite oxidation kinetics caused by elevating oxygen partial pressure.

These findings contribute to future experimental and modeling efforts for risk assessment and monitoring of oxygen-rich plumes in the subsurface.

2.2. Introduction

Pyrite oxidation could be responsible for up to 100% of the oxygen consumption in aquifers at low redox conditions after introducing air-rich waters (Descouvieres et al., 2010). Significant amounts of intruding oxygen and consequently oxygen partial pressures higher than 1 bar will usually not occur in natural systems, but may occur in conjunction with different technical subsurface operations. For example, at in-situ air sparging, air is injected into the subsurface to remove volatile organic contaminants (Thomson and Johnson, 2000; McCray, 2000), or oxygen is injected to accelerate the degradation of those substances (Beckmann et al., 2007). Air at higher pressure than the hydrostatic pressure is required in those applications and this may lead to dissolved oxygen concentration in equilibrium with higher partial pressures than at normal conditions. A total air pressure of about 5 bars is required in order to reach a partial pressure of oxygen of about 1 bar, corresponding to a hydrostatic pressure in a depth of around 50 m.

A further possible source of high oxygen partial pressures in aquifers is connected to Compressed Air Energy Storage (CAES) facilities, as discussed recently in the literature (Bauer et al., 2013; Crotogino et al., 2001; Kabuth et al., 2017; Bauer et al., 2015). The principle of CAES is to compress air and pump it into a subsurface reservoir (e. g. a salt cavern) during periods of surplus power production. The energy stored this way can be recovered in periods of low power production by releasing the compressed air through turbines (Crotogino et al., 2001). CAES is potentially a key technology for storing energy in the subsurface in the frame of changing the energy supply system in Germany ("Energiewende"). Such mass and energy storage technologies, including methane, hydrogen, and heat storage, significantly enhance the sustainability of the energy sector by providing renewably produced energy at the demanded time distribution (Safaei et al., 2013). However, air stored at high pressure in a deep reservoir might infiltrate shallow aquifers accidentally (Al Hagrey et al., 2016). Shallow aquifers are often used for drinking water supply at depths of up to 500 m below surface, and consequently they are highly protected natural goods. An air leakage into those aquifers at total pressures of up to 50 bars will result in comparatively high dissolved oxygen concentrations at groundwater temperatures. At these conditions a strong pyrite oxidation may follow, because pyrite is common in aquifers at a depth of up to 500 m.

Pyrite oxidation studies have focused mainly on acid mine drainage aspects (e. g. McKibben and Barnes 1986; Hammack and Watzlaf 1990, Moses and Herman 1991, Williamson and Rimstidt 1994, Rimstidt and Vaughan 2003). Moreover, natural oxidation of reduced sulfur species in active volcanic regions also results in acidic near-surface waters with high sulfate concentrations (Nordstrom et al., 2009; Varekamp et al., 2009). Based on the findings published so far, it could be assumed that oxygen intruding pyrite-containing aquifers causes a decrease in pH, release of sulfate, iron, and trace elements, therefore potentially affecting the groundwater quality (Equation 1). Most works on pyrite oxidation kinetics applied waters in equilibrium with O_2 partial pressures lower than 1 bar in batch or column experiments. Higher pressures in further studies for hydrometallurgical purposes at up to 20 bars were applied using high temperatures up to 180 °C along with strongly acidic conditions in batch reactors (Papangelakis and Demopoulos, 1991; Long and Dixon, 2004). These studies provided precious knowledge about mechanisms, kinetics, and microbiological effects (e. g. Gleisner et al., 2006) of the pyrite oxidation by oxygen, but no study has covered the pressure, temperature, and hydrogeochemical conditions representing a shallow aquifer so far.

Reliably parametrized, site scale numerical models and laboratory experiments are necessary in order to assess the risks of pyrite oxidation at aquifer conditions and, therefore, the risks potentially associated with CAES (Bauer et al., 2013). Those experiments have to represent the sediment-water ratio and structure, flow, and transport conditions characterizing an aquifer. For these purposes flow-through column experiments are much more adequate than batch tests. Applying oxygen partial pressures corresponding to the depth of the leakage and the interaction zone can yield direct experimental data on air leakages into these shallow aquifers. The investigation presented here improves the pyrite oxidation rate equation (Equation 2.2) from Williamson and Rimstidt (1994), whose equation has been generally accepted and widely used for geohydromodeling.

$$FeS_2 + {}^{15}/_4O_2 + {}^{7}/_2H_2O \rightarrow Fe(OH)_3 + 2SO_4^{2-} + 4H^+ \qquad \textit{Equation 2.1}$$

$$r = 10^{-8.19} \cdot [O_2]^{0.5} \cdot [H^+]^{-0.11} \qquad \textit{Equation 2.2}$$

The goal of the work presented here was to experimentally characterize potential effects of air intrusions on water composition in shallow aquifers and to parameterize the pyrite oxidation kinetics in groundwater temperature and high oxygen partial pressure systems, representing conditions in aquifers of up to 500 m depth. Thereby, the study evaluates the commonly used rate laws for pyrite oxidation and develops an improved rate law applicable to a p(O2) range from 0 to 11 bars. Site scale models can use this transfer function for scenario modelling approaches. Furthermore, the function can be used for upscaling results from low pressure (1 bar system pressure) experiments to high pressure (>1 bar system pressure) conditions which enables more time and cost effective pre-studies for a particular CAES storage site using site specific sediments at normal laboratory conditions.

2.3. Materials and methods

2.3.1. Materials and setup

A sediment composed of quartz sand (grain size 0.2-0.8 mm, Gebrüder Dorfner GmbH, Germany) and 0.5 mass% of pyrite (hydrothermal origin, Krantz GmbH, Germany) was used for all experiments. Crushing and sieving the pyrite resulted in a grain size fraction of 0.25-0.5 mm. This fraction was then repeatedly cleaned using 1 M HCl until the aliquot was clear. After flushing, the grains were rinsed with deionized water several times, the resulting grains were mixed to the sand and the mixture was filled into the experimental columns. The pyrite content of 0.5 mass% is chosen as representative for pyrite-rich Pleistocene and Miocene sediments forming aquifers used as main resource for drinking water in northern Germany (Dethlefsen et al., 2016 a and b). The columns were percolated by tap water from the Kiel University, which is produced from groundwater in a Quaternary aquifer. This water was equilibrated with oxygen at partial pressures $p(O_2)$ of 0, 0.21, 1; and 1, 5, 11 bars for the low pressure and for the high pressure experiments, respectively (Table 2.1). The temperature of the water used for the experimental series was 20 ± 2°C. In the mixing cells, where the water was equilibrated with 0, 0.21, and 1 bar $p(O_2)$ for the low pressure experiments, precipitation of carbonate-containing phases were observed, and removed every few weeks. The tap water was diluted 1:10 with deionized water for the high pressure experiments to prevent any precipitation; this dilution consequently decreases the carbonate pH buffer capacity to $1/10^{th}$ compared to the low pressure experiments. The low pressure experiments were conducted for 164 days, the high pressure experiments for 91 days in total.

Table 2.1: Average composition of the waters used as inflow for the different experiments. Fe^{tot} concentrations were below the detection limit.

Parameter	Tap water	Low pressure inflows			High pressure inflows		
		0 bar	0.21 bars	1 bar	1 bar	5 bars	11 bars
Ca^{2+} [mM]	3.09	1.89	2.29	2.08	0.35	0.31	0.26
Mg^{2+} [mM]	0.36	0.36	0.38	0.37	0.04	0.04	0.05
Na^{+} [mM]	0.64	0.63	0.67	0.65	0.10	0.08	0.09
K^{+} [mM]	0.07	0.07	0.08	0.07	0.01	0.01	0.004
Fe^{tot} [mM]	< 0.01	< 0.01	< 0.01	< 0.01	< 0.01	< 0.01	< 0.01
NO_3^{-} [mM]	0.01	0.01	0.01	0.01	< 0.1	0.004	0.006
SO_4^{2-} [mM]	0.51	0.50	0.53	0.50	0.04	0.03	0.02
Cl^{-} [mM]	0.85	0.84	0.89	0.88	0.08	0.08	0.07
TIC [mM]	5.34	2.86	3.66	3.22	0.52	0.64	0.60
O_2 [mM]	0.152	0.057	0.172	0.628	1.28	6.4	14.08
pH [-]	8.32	8.96	8.73	8.95	7.4	7.4	7.4

Three parallel low pressure column experiments were performed using glass columns (L=30 cm, Ø=6 cm, 5 sampling ports at 5 cm distance, Eydam KG, Germany) and different low oxygen partial pressures ($p(O_2)$= 0, 0.21, and 1 bar). The water free of oxygen was prepared by purging the inflowing water in a mixing cell with nitrogen. Using air and oxygen (purity: 4.8, Air Liquide GmbH) for purging the tap water in a mixing cell resulted in inflow solutions equilibrated to oxygen partial pressure of 0.21 or 1 bar, respectively. Gas tight Viton® tubes were used for all connections in order to prevent or at least to minimize the gas exchange after oxygen enrichment or depletion. An Ismatec IPC high precision peristaltic pump with calibrated Viton® pumping tubes enables constant flow velocity within the column experiments. The pumping rate was adjusted to a flow velocity of 0.6 m/day and later 0.3 m/day within the columns, assuming an effective porosity of 0.35 from tracer tests and experiments using the same quartz sand (Koch, 2014; Becker, 2014). Samples from the inflow and from all sampling ports were taken in order to characterize the hydrogeochemical changes along the flow path in addition to sampling the outflow on the downstream side of the column.

A high pressure ($p(O_2)$= 1, 5, and 11 bars) experimental column (L=50 cm, Ø=4 cm, electrochemically passivated pure titanium Grade 2, from Werner Kluge Engineering GmbH, Germany) with stainless steel and hastelloy fittings and tubes (Swagelok, OH, USA) was percolated with water equilibrated with 1, 5, and 10 bars of oxygen consecutively, while keeping a total system pressure of 22±2 bars to prevent the development of gas phases in the column. The water was

percolated using HPLC pumps (Knauer GmbH, Germany), and only outflow samples were taken. This could be accepted, as in pre-experiments, where the same kind of sediment and set-up was used and sampling included also the five ports along the flow path, proved linear variations of dissolved compounds along the flow-path in the column (Figure 2.1). The flow speed was temporarily decreased during the high pressure experiments in order to evaluate an effect on the reaction rate or the passivation resulting from such a change in transport conditions.

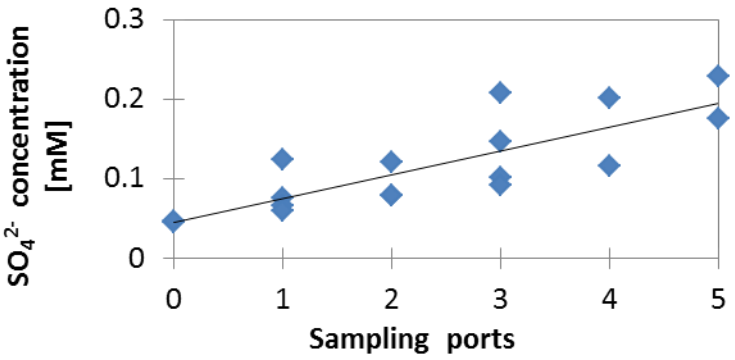

Figure 2.1: Concentration of sulfate increases linearly through the high pressure column in pre-experiments.

Haase et al. (2014) described the same high pressure experimental set-up in detail (Figure 2.2), and calculated an effective porosity of 0.34 after applying tracer tests using the same kind of sand mixture, so that this effective porosity value was accepted in the presented study as well. Considering this effective porosity, the flow velocity was between 0.45 and 0.07 m/day for the high pressure experiments; the residence times and the number of exchanged pore volumes (PV) used for further evaluation and comparison were always calculated based on the actual flow speed for that sampling event.

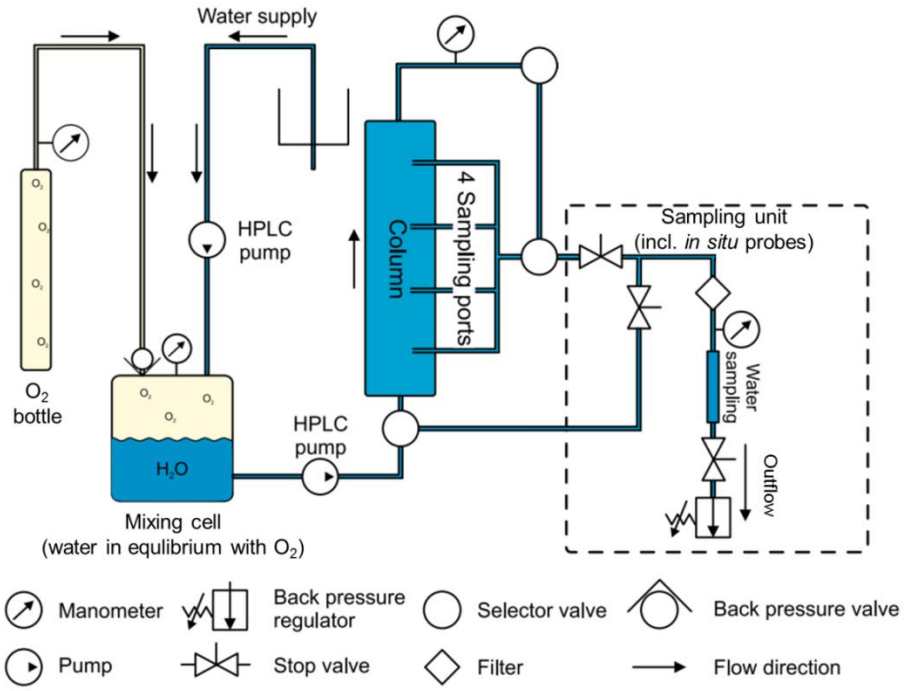

Figure 2.2: Conceptual setup of the column experiment at high pressure (modified after Haase et al., 2014)

2.3.2. Analytics

Redox potential, pH-level, specific electric conductivity, and dissolved oxygen up to 1 bar were measured using WTW devices and electrodes. In order to measure high oxygen concentrations directly at high pressure conditions, a novel method based on collisional quenching instead of the conventional Clark electrode was established (Fospor T1000 TS Neo oxygen sensor, NeoFox Viewer 2.40 software, NeoFox Oxygen Phase Fluorimeter, Bifboro 1000-2 fiber assembly, and device from OceanOptics GmbH). To our knowledge, no oxygen measurement method able to operate under these particular experimental conditions (groundwater temperature, elevated total pressure and comparatively high oxygen concentration corresponding to elevated partial pressure) was applied before. For these high oxygen partial pressures, the application of a novel method and its calibration had to be done (see Figure 2.3 and Equation 2.4 in Results). The optical sensor was calibrated by exposing it to oxygen partial pressures of 0, 0.21, 1, 2, 5, 8, and 11 bars and by developing a calibration function in cooperation with the manufacturers of the hardware thereafter. This function was then tested at three randomly chosen high pressure conditions. To quantify electric conductivity and pH online and under high pressure as well, sensors (Corr Instruments, TX, USA) were placed in the system, and any inflow, sampling port, or outflow sample could be measured using the sensors (Figure 2.2). The presence of sulfide has been sensed organoleptically and photometrically.

All samples for further analyses were collected in a 60 ml polypropylene syringe and injected into vials required by the corresponding analytical devices through filters (NML high flow, 0.2 µm, Sartorius, Germany). The concentrations of anions were determined using a Metrohm IC881 ion chromatograph, the total organic, inorganic, and non-purgable organic carbon concentrations were measured with an Analytic Jena multi N/C 2000 TIC-TOC analyzer, the concentrations of cations were measured with a Varian Vista AX CCD Simultaneous ICP AES (after conservation with sp. cc. HNO_3).

After the end of the experiments, a sediment sample from the middle part of all columns was taken for solid phase analysis. As preparation, the pyrite grains were picked and dried at room conditions. The surface of the pyrite grains was observed using a CamScan-CS-44 SEM after preparing the samples using Au/Pd high vacuum evaporation. For Raman microspectrometry a Bruker Senterra device was applied.

The microbial communities of the sediments and waters from the low pressure experiments were characterized using PCR-DGGE. For this purpose, the outflowing water from the low pressure columns was collected for ca. 24 hours into sterile and closed glass bottles. In total, three samples were taken for this analysis in the first, second, and third month from each of the low pressure experiments.

2.3.3. Modeling

To evaluate the experimental results and to develop as well as to evaluate a rate equation for pyrite oxidation, a PHREEQC 3.1 (Parkhurst and Appelo, 2013; Mommsen, 2013) 1D reactive transport model was parametrized, calibrated and validated. The main model parameters are shown in Table 2.2.

Table 2.2: The discretization of the reactive transport model in PHREEQC. The parameters were not changed for the different runs, except it is marked otherwise.

Number of cells for high pressure	50
Number of cells for low pressure	25
Length of cells (cm)	1
Dispersivity (cm)	0.2
Shifts (0.21 bars, low pressure)	1750
Shifts (1 bar, low pressure)	1750
Shifts (1 bar, high pressure)	800
Shifts (5 bars, high pressure)	300
Shifts (11 bars, high pressure)	2000
Time step (s, high pressure)	1440
Time step (s, low pressure, fast flow)	1440
Time step (s, low pressure, slow flow)	2880
Flow boundary conditions	flux-flux
Initial amount of pyrite (mol/kgw)	0.165

2.4. Results

2.4.1. Calibration of dissolved oxygen measurement at high partial pressure

The calibration was carried out successfully: after the equilibration of the water with the gas phase stable oxygen values could be determined. The resulting function (Figure 2.3) shows a hyperbolical shape due to the nature of the fluorimetric measurement principles (quenching). Consequently, the level to noise ratio decreases towards higher dissolved oxygen concentrations. The calibration function (Equation 2.3) was checked and confirmed at three further partial pressures (4.75, 7, 10.75 bars). Tau_0 represents the Tau value measured at 0 bars partial pressure of oxygen created in a N_2-pruged solution.

$$p(O_2) = \frac{\left(\frac{Tau_0}{Tau} - 1\right)}{0.9752} \qquad \textit{Equation 2.3}$$

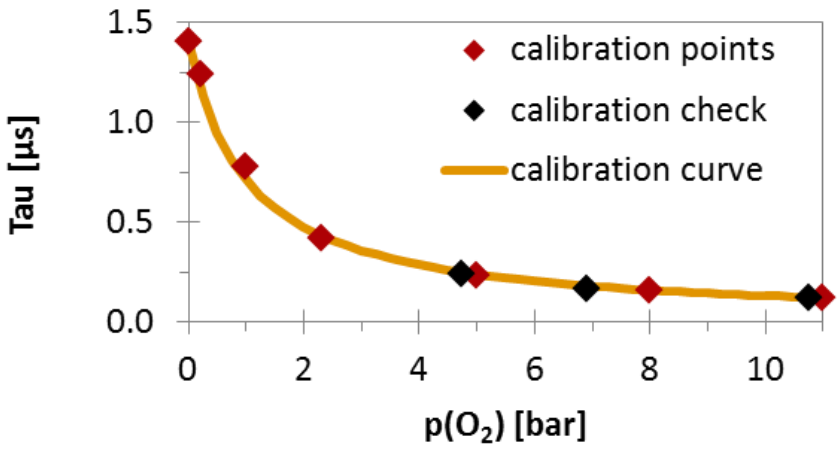

Figure 2.3: The calibration for high partial pressure oxygen measurements.

2.4.2. Low pressure experiments

Effects of pyrite oxidation were observed in all column experiments containing oxygen, starting immediately after the beginning of the experiments. Thereby, mainly monotonously decreasing oxygen and increasing sulfate concentrations along the flow path were indicative for this oxidation reaction (Figure 2.4).

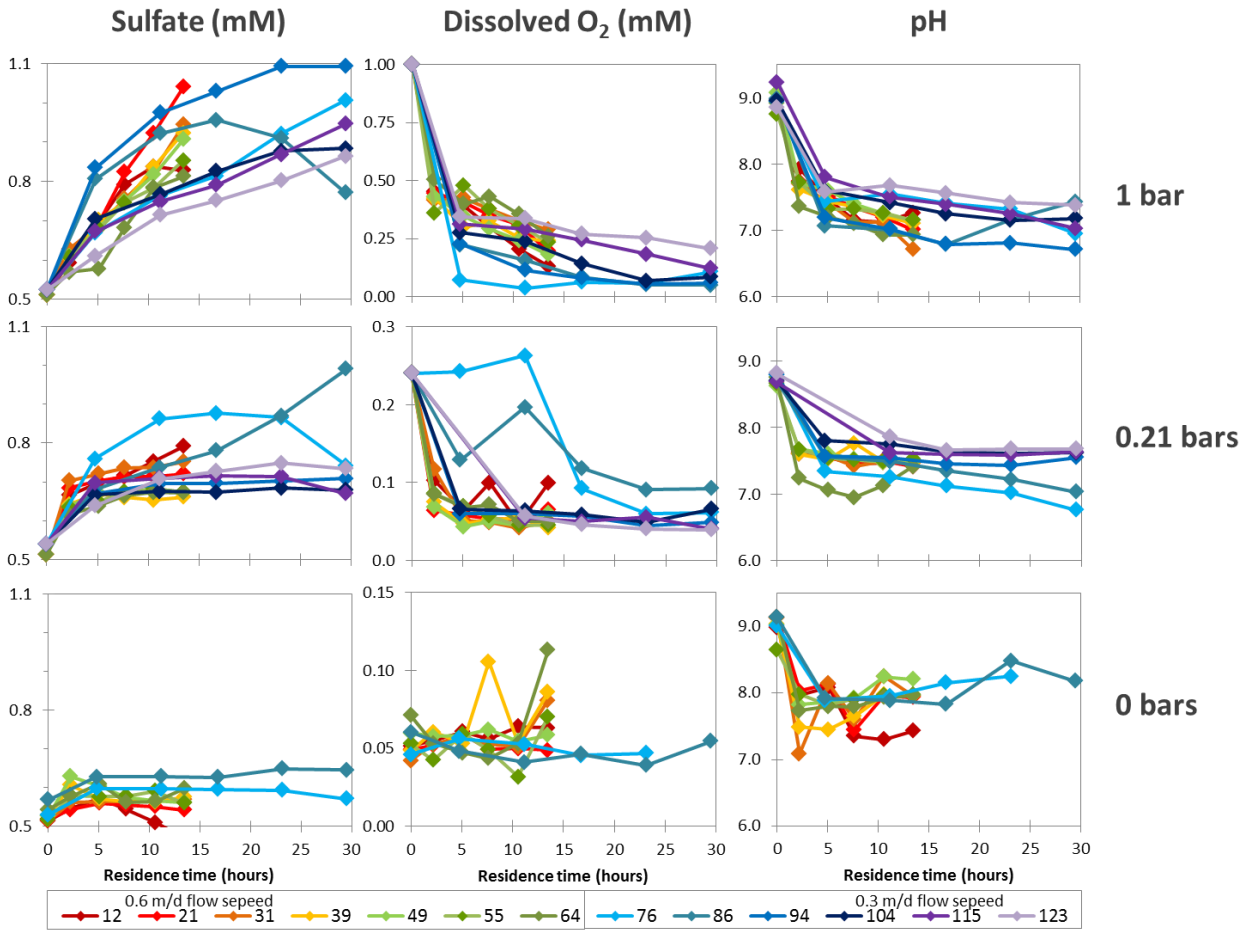

Figure 2.4: Changes in pH, sulfate production, and oxygen consumption in the water flowing through the 0, 0.21 and 1 bar experimental columns. Shorter lines represent experiments with faster flow speed; different lines signify samples taken in the course of the experiment, expressed as exchanged pore volumes in the figure's legend.

No appearance of dissolved Fe^{tot} or significant changes in other dissolved species (nitrate, chloride, Na^+, K^+, Ca^{2+}, Mg^{2+}, Mn^{tot}, Si, or inorganic and organic carbon) and water parameters (redox potential, and electric conductivity) were observed at any time in the experiments. Also, no other sulfur species (e. g. thiosulfate, sulfide, etc.) than sulfate was found in any of the experiments. The lack of any dissolved iron in the solution phase signifies that all the iron produced from pyrite oxidation stayed in the solid phase within the column.

The development of the water composition (i.e. sulfate concentration) indicates the slow but immediate start of pyrite oxidation in both experimental systems containing oxygen. This initial establishment of the reaction is visible by the first data points of the reaction rate series measured in the 1 bar low pressure column experiment and indicted by blue squares on both sides of Figure 2.6. The third column containing no oxygen showed no signs of pyrite oxidation, although nitrate (0.02 mM) was present through the whole flow path.

The increase in sulfate (up to 0.57 mM) and decrease in oxygen concentrations (up to 0.95 mM) showed a ratio with a slope of 1.875 scattering around the stoichiometry of the oxidation of pyrite by oxygen into trivalent iron and sulfate (Equation 2.1) (Figure 2.5). The most probable reason for this scattering is an inaccuracy of the oxygen measurements conducted by the Clark sensors, which is large compared to the precise measurement of sulfate by IC. Additionally, due to the long percolation time, no desorption of sulfate from the sediment can be expected to influence the measured concentration profiles, and there is no suggestion for sulfur of any redox state remaining adsorbed in the solid phase within the column. This suggestion was acknowledged by the control experiments without oxygen (Figure 2.4) and blank runs without pyrite in the sediment. Therefore, sulfate concentration could be stoichiometrically applied as the primary indicator for calculating pyrite oxidation rates due to its more precise and representative measurement.

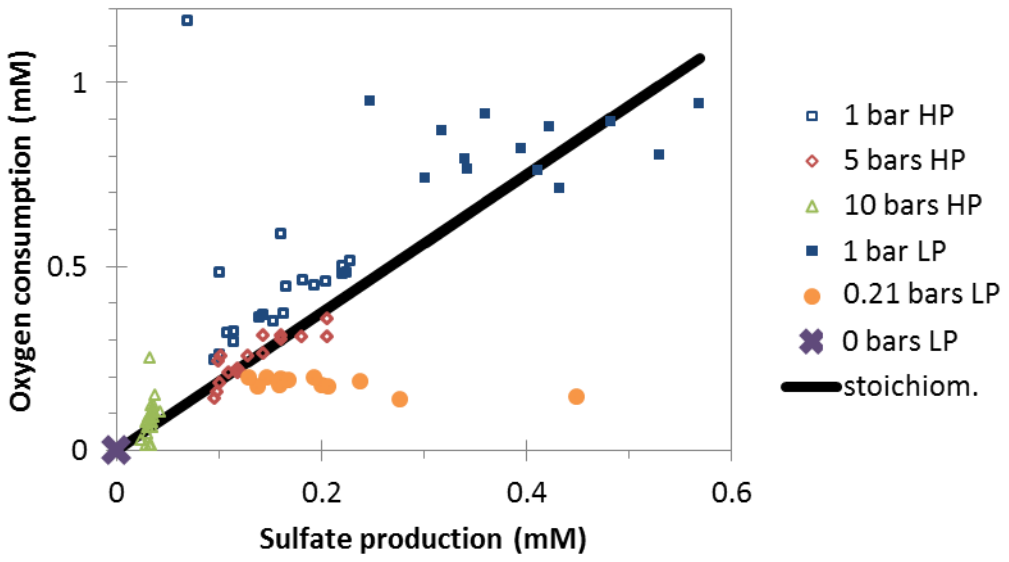

Figure 2.5: Oxygen consumption versus sulfate production in the low (LP) and high (HP) pressure experiments. The continuous line represents the expected stoichiometric ratio according to Equation 1.

The rates of pyrite oxidation were calculated assuming that the reaction in the experimental column is constant, which is supported by a nearly linearly increasing sulfate concentration along the flow path (Figure 2.4). Consequently, the sulfate produced along the entire flow path between inflow and outflow was multiplied by the stoichiometric coefficient between sulfate and pyrite (Equation 2.1), and divided by the corresponding residence times for determining the rate of pyrite oxidation. The rates gathered this way showed that the pyrite oxidation by oxygen was faster by a factor of approximately two when the partial pressure of oxygen was 1 bar (16-5 µM/h) compared to the experiments with 0.21 bars (10-2 µM/h) in parallel columns.

The observed rate of pyrite oxidation decreased versus the amount of pyrite oxidized from the initial 41.4 mmol available (Figure 2.6). This decrease takes place after the initial phase, which is represented by the first data point, and is linearly proportional to the amount of pyrite oxidized per the initial mass of pyrite. However, this decrease can also be observed when plotted against the experimental run time or exchanged pore volumes (Figure 2.6).

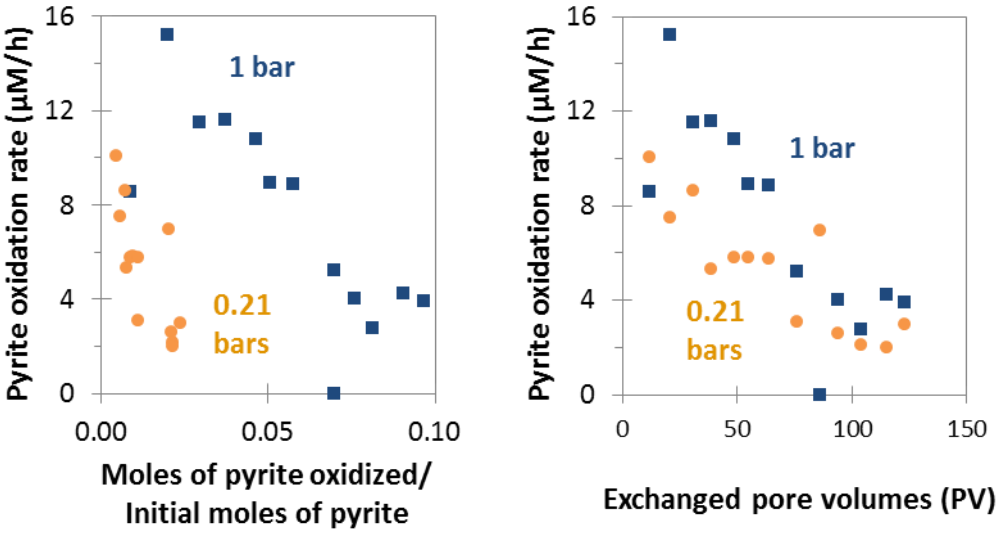

Figure 2.6: Decrease in pyrite oxidation rate in the low pressure experiments versus the ratio of oxidized and initial moles of pyrite (left) and versus the number of exchanged pore volumes (right).

Based on the low pressure experimental results, the geochemical changes influencing the composition of groundwater after an air leakage primarily evolve from a limited (up to 50 mg/l) release of sulfate. A decrease (1.75) in pH was observed in these experiments, but this was also found in the reference experiments without oxygen. Therefore, an acidification related to the pyrite oxidation was not identifiable in this geochemical system.

2.4.3. High pressure experiments

The high pressure column experiments also showed a decrease in oxygen concentrations and production of sulfate along with a slight acidification (Figure 2.7). Oxygen was not completely depleted in the outflows, and stayed rather close to the inflowing concentrations. A further new aspect compared to the low pressure experiments was that the changes in pH became more significant, but the pH at the outflow stayed always higher than 6.2. On the other hand, similarly to the low pressure experiments, no significant changes in any other measured water constituents were observed. Most importantly, still no dissolved iron species were present and no sulfur species other than sulfate were observed.

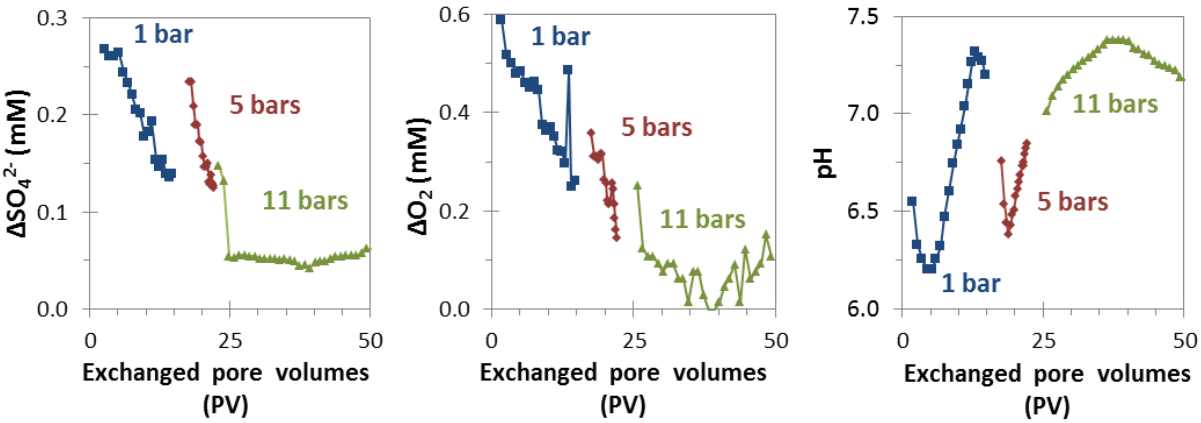

Figure 2.7: Results of online measurements in the high pressure experiment show decreasing sulfate production (left), decreasing consumption of dissolved oxygen (middle), and decreasing pH reduction (right). The depicted differences in concentrations were calculated between water samples flowing into and out of the column.

The increase in sulfate concentration indicates pyrite oxidation as described before, and it was found to proceed linearly within the column such as it was observed in the low pressure experiments. Therefore, the rate calculations were performed in the same way by regarding the difference in concentrations between the columns inflow and outflow and disregarding the sampling points along the flow path in the column. During the experiment, the reaction rate of pyrite oxidation always increased suddenly, when the water flowing into the experimental column was switched to the next and higher partial pressure of dissolved oxygen. Also, the decrease in pyrite oxidation rate (from 8.33 to 2.3 µM/h at 1 bar, from 3.75 to 0.55 µM/h at 5 bars, and from 4.48 µM/h to 1.6 µM/h at 11 bars) was identified in the high pressure conditions. Moreover, this decline apparently accelerated at higher partial pressures of oxygen. This accelerating decline explains the slopes of the trend lines fitted on pyrite oxidation rate getting steeper in the course of the experiment (Figure 2.8). The decelerating reaction rate together with a consecutive increase of the partial pressures in the experiment resulted in a remarkable behavior: the observed (local) maximum rates were seemingly lower towards the higher pressures, instead of the expected increase.

The flow velocity declined during the first phases of the high pressure experiment by approximately a factor of 7. However, by plotting the pyrite oxidation rates against the exchanged pore volumes or mass conversion of pyrite (Figure 2.8), it is exemplified that this variability in the water flow velocity has no effect on the rate of the pyrite oxidation. Therefore, the pyrite oxidation rate as well as its strong decrease is suggested to be independent from the changes in groundwater flow speed.

As the carbonate buffer system was weaker in the high pressure experiments due to the tenfold dilution of the inflowing water, the effect of pyrite oxidation resulted in a minor influence on the pH (values of 6.2 -7.5), even as the pyrite oxidation rates were smaller in the high pressure experiment compared to the low pressure experiments. Another reaction potentially influencing groundwater composition is pyrite oxidation by nitrate as electron acceptor (e. g. Jørgensen et al., 2009), while it is also possible that nitrate is used in the presence of oxygen. However, no nitrate consumption was detected in any of the columns, including even the low pressure experiment where no oxygen was applied.

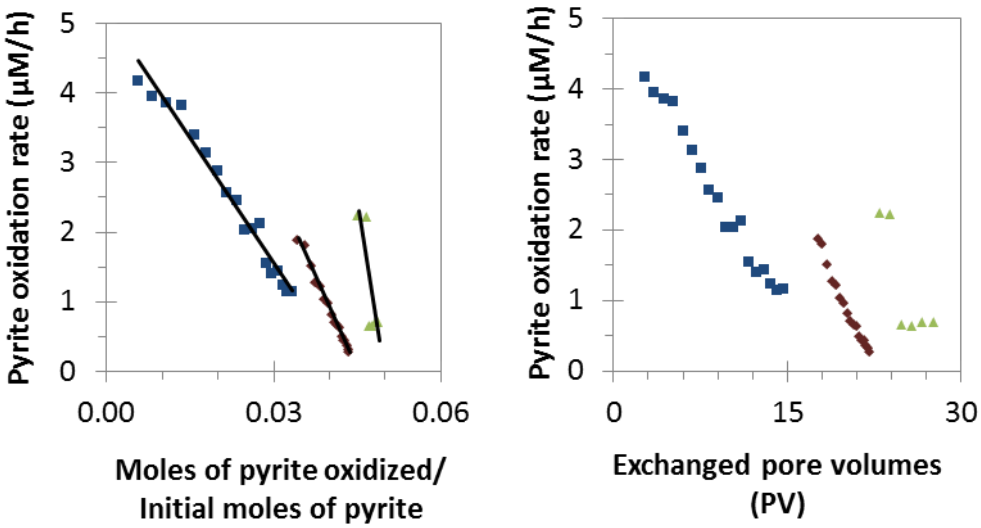

Figure 2.8: The linear decrease in reaction rates versus the moles of pyrite oxidized (which equals to the moles of precipitate) divided by the initial moles of pyrite in the high pressure experimental column (left) and versus the number of exchanged pore volumes (right). The slopes of the fitted black lines are -119 for 1 bar, -177 for 5 bars, and -528 for 11 bars.

The changes in oxidation rates, therefore, seemingly resulted in a pyrite reactivity increasing with the oxygen partial pressure when observed in parallel (low pressure) experiments, but decreasing when the experiments were carried out consecutively (using high pressure experiments). This obviously contradicts the existing reaction models and further considerations were needed for developing a transfer function able to consistently describe these phenomena and to realize the upscaling of the results.

2.4.4. Pyrite grains after the experiments

By SEM analyses conducted using pyrite grains after the experiment, a ca. 3 μm thick layer covering the whole surface of the pyrite could be seen as well as 0.2-0.5 μm large pockmarks on the surface of pyrite where this layer was removed (Figure 2.9). This layer was found to be present in all experiments involving oxygen and to cover nearly the whole surface of the pyrite grains, although fractures crossing it could be seen all over the grains. To characterize the mineral reaction products on the surface of the pyrite grains, Raman spectra were gathered from 90 points of 26 pyrite samples representing all experiments and pre-experimental conditions. Although peaks around 1600, 1335, 270, and 210 cm^{-1} indicated a phase (assemblage) on the pyrite surface different than pyrite (which was also found), this layer could not be mineralogically identified. The presence of iron oxihydroxides, sulfates, carbonates, and elemental sulfur were denied, in contrast to the assumptions of Long and Dixon (2004).

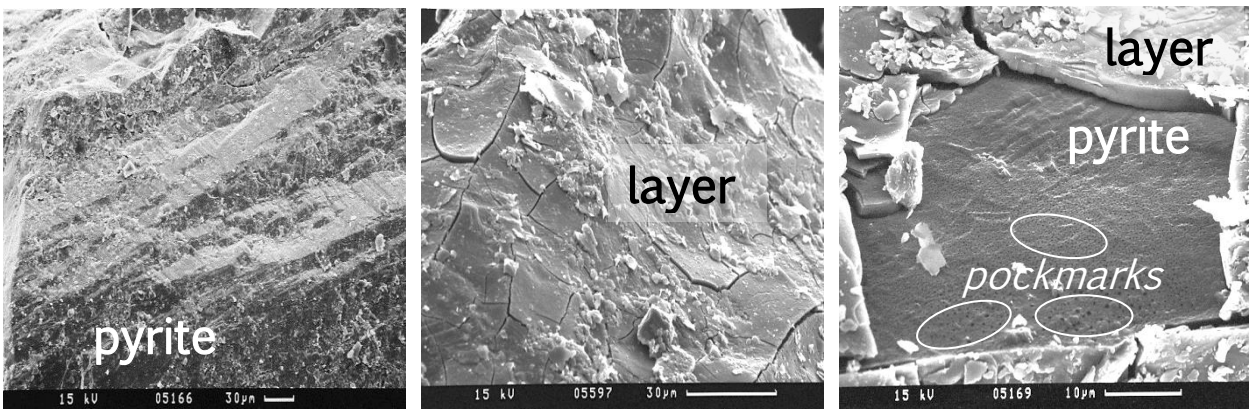

Figure 2.9: Fractured layer completely covering the pyrite grains (in the middle, 0.21 bar experiment). Pockmarks (right, 10 bars experiment) on a bare pyrite surface. These are caused probably by oxidative microbial activity. None of such structures (layer, pockmarks) were observed in the oxygen-free control runs (left, 0 bar experiment) having clear surfaces and sharp edges.

2.4.5. Microbial community

The members of the bacterial community are mostly mesophilic bacteria favoring neutral pH that are mostly known from soils, freshwater, drinking water distribution systems, lakes and groundwater (Lienen et al., 2014). No significant deviation between the 0.21 and the 1 bar oxygen partial pressure conditions were observed regarding the total concentration of DNA as an indicator of microbial biomass in the solutions outflowing the low pressure experimental columns. Genetic fingerprints suggested the presence of iron oxidizing bacteria and, after 2 months of run time, sulfur oxidizing bacteria in the outflows of the low pressure columns. No microorganisms were seen during the SEM investigations.

2.5. Discussion

The well-established rate law from Williamson and Rimstidt (1994) was used in a first attempt for simulating the high pressure column experiments with PHRREQC (Equation 2.4). A k_{obs} of $10^{-7.9}$ was used as a product of the k value and the surface area (SA) and it was fitted to the initial maximal rate at the beginning of the experiment. Furthermore, the shrinking core model was included in the rate equation using an initial mass of pyrite (m_0) of 0.165 mol·kg_{water}^{-1}. Figure 2.10 shows that the model is not able to simulate the experimental results without further adjustments and that the model will strongly overestimate the pyrite oxidation in the investigated system. Obviously, the mass of pyrite which is oxidized during the experiment is not high enough to induce a remarkable decrease in the simulated oxidation rate and, therefore, the shrinking core model shows nearly a constant oxidation rate during the first phase of the experiment (pO_2 = 1 bar). Consequently, the model shows an increase of the oxidation rate in case of increasing oxygen concentration in the next two phases of the experiment ($p(O_2)$=5 and 11 bars), which is not supported by the experimental data. The simulation results converge to the data only if the initial mass of pyrite is drastically reduced to nearly 1% of the actual mass in the experiment. This indicates a limited reactivity of the pyrite, or a limited or strongly decreasing reactive surface area of the pyrite.

$$r_{\text{Williamson and Rimstidt (1994)}} = k_{obs} \cdot [H^+]^{-0.11} \cdot [O_2]^{0.5} \cdot \left(\frac{m}{m_0}\right)^{\frac{2}{3}} \quad and$$

$$k_{obs} = k \cdot SA$$

Equation 2.4

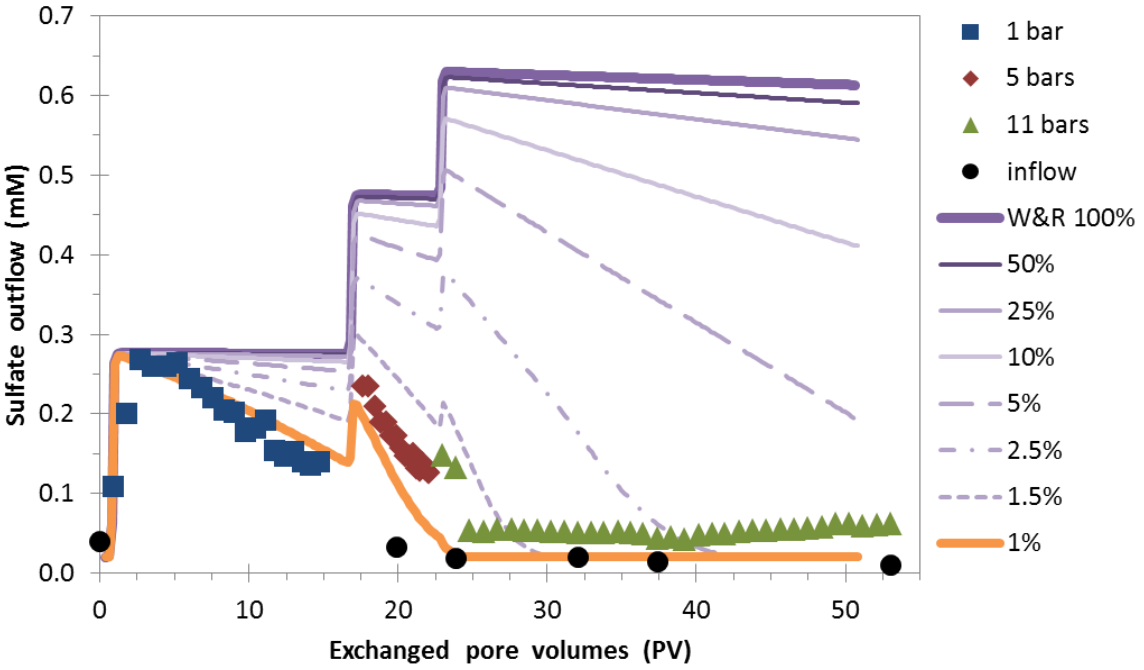

Figure 2.10: Sulfate concentration in the outflow of the high pressure (1, 5, and 11 bars) experiment (symbols); and modeling attempts using an unmodified Williamson and Rimstidt (1994) model with decreased amounts of pyrite and a k_{obs} of $10^{-7.9}$ (lines).

According to the literature, pyrite oxidation at near neutral pH conditions results in the formation of Fe(III)-oxyhydroxide coatings on the surface, reducing the oxidant's diffusion coefficient by more than five orders of magnitude (Huminicki and Rimstidt, 2009; Perez-Lopez et al., 2009 and Courtin-Nomade et al., 2010). The formation of such a passivation layer, containing Fe(III) minerals or sulfur, will lead to strongly decreasing reaction rates due to the decreasing reactive surface area. All of the pyrite grains showed a precipitated layer after the experiments containing O_2. The layer is probably responsible for the strong decrease in reaction rates observed in the low and high pressure experiments. It can be assumed that the precipitates mainly contain Fe(III) oxihydroxide phases because dissolved iron was not detected in any of the samples. However, the mineralogical characterization of these layers was without results. Huminicki and Rimstidt (2009) found a surface passivation following a square-root dependency on the amount of pyrite oxidized, based on stirred batch experiments conducted for several hours. In our column experiments, the passivation was found to be linear versus the amount of pyrite oxidized and additionally the passivation seemed to be dependent on the partial pressure of oxygen (Figure 2.7). Zhukov et al. (2015) developed a non-linear passivation function based on the data of Long and Dixon (2004) for acidic conditions: $(1\text{-}X)^n$ with X being the conversion of pyrite due to oxidation and n a fitting parameter. This function was tested, but it was unable to describe the experimental results, most probably due to the comparatively high pH and the variation of oxygen partial pressure (Figure 2.10).

Therefore, a new passivation term *pass* is introduced in the rate law, depending on the mass of pyrite oxidized (m_0 - m), the partial pressure of oxygen ($p[O_2]$) and the fitting parameters f_1, f_2, and f_3 (Equation 2.5):

$$pass = \left(1 - \frac{m_0 - m}{m_0} \cdot f_1 \cdot e^{f_2 \cdot p[O_2]}\right)^{f_3} \quad and \quad 1 \geq pass \geq 0$$

Equation 2.5

The results of the high pressure experiment indicate that the development of a passivation layer becomes nearly complete by the first few days of the experimental phase where 11 bars of oxygen partial pressure was applied (Figure 2.10), but a constant residual electron transfer is still ongoing. This causes a continuous sulfate release from the column experiment of around 0.05 mM. Fractures crossing the developing layer as observed by SEM (Figure 2.8) can be responsible for this residual pyrite oxidation. This remaining reaction rate is independent from the degree of the passivation and, therefore, a term considering the rest reactivity is also included in the rate law for the pyrite oxidation (Equation 2.6).

$$r_{pyrite} = \left(f_{rest} + f_{pass} \cdot pass\right) \cdot r_{Williamson\&Rimstidt(1994)}$$

Equation 2.6

The best model fit (Figure 2.11) shows that the fraction of un-passivated pyrite f_{rest} = (1 - f_{pass}) is 0.025, while the fraction of passivated pyrite (f_{pass}) is 0.975. A fitting factor f_2 = -0.015 was gathered and adjusted from the slopes found on Figure 2.8 expressing the increasing passivation intensity with increasing partial pressure of oxygen. The fitting factor f_1 = 100 was used, signifying that the passivation is linearly dependent on the percentage of pyrite oxidized relative to the initial amount of pyrite. Finally, the factor f_3 = 0.75 was estimated by best model fit, found to be in the range of 0.45-2.0 that was used by Zhukov et al. (2015).

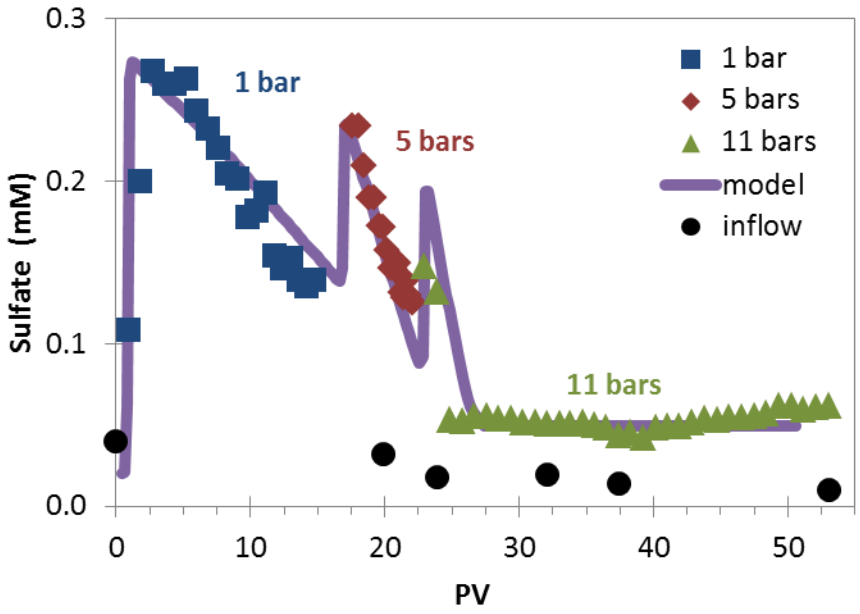

Figure 2.11: The decrease of sulfate concentration in the outflow of the high pressure experiments shows a decreasing pyrite oxidation rate. Measured experimental data is marked by symbols; the line shows the modeling results.

The developed function (Equation 2.6) reproduced the results from the high pressure experiment well without any further modifications (Figure 2.11). Using the amount of pyrite oxidized $(m_0 - m)$ implies the stoichiometric transformation of iron ions from pyrite into the passivating layer and, therefore, it could be replaced by a term including a mineral formation dependent on a saturation index. Dissolved iron was not detected in any of the samples from the experiment; therefore the assumption of a stoichiometric relation between the mass of oxidized pyrite and the mass of precipitated minerals is suitable. At the beginning of the experiment, an increasing reactivity was observed, indicated by increasing sulfate concentration, until the maximum oxidation rate was reached after ~3 PV (Figure 2.11). This increasing reactivity was not included in the model and might be explained by an initial increase in the reactive surface area due to the formation of holes at the surface. This is supported by SEM images showing the surface of the pyrite grains when the passivating layer was detached (Figure 2.9) and also by other studies (Tichomirova and Junghans 2009; Blight el al., 2000; Gleisner et al., 2006; Lefticariu et al., 2007). However, the effect of the passivation layer becoming tighter towards higher oxygen partial pressures, to our knowledge, has not been described in the literature so far and it is important considering this effect in the context of a risk assessment when water qualities are evaluated at compressed air storage facilities in the subsurface.

The model was used to simulate the results of experiments using 1 bar and 0.21 bars of oxygen partial pressure in the low pressure experiments in order to evaluate the scalability of the developed rate equation (Figure 2.12). A good fit was reached by setting the k_{obs} to $10^{-7.3}$ and the fitting parameter to $f_1 = 8$. The higher observed rate coefficient k_{obs} and the smaller f_1 value might be necessary due to the difference in experimental set-up and water composition between low pressure and high pressure experiments, even if the same sediment and oxygen partial pressure was used (1 bar). Different microbiological effects (e. g. lower concentration of trace nutrients) also cannot be excluded as a reason, because microbial screening was performed only in the low pressure experiments. However, the resulting model reproduces the results from two different flow speeds in the 1 bar low pressure experiment well, only by modifying these two parameters.

The pyrite oxidation in the experiments using water in equilibrium with 0.21 bars oxygen partial pressure was underestimated by the passivation model near the starting phases, probably because in that case the overall reaction is limited by the availability of oxygen instead of being controlled through a surface passivation. The later experimental results are more affected by passivation and, therefore, the model fits better on this phase of the experiment.

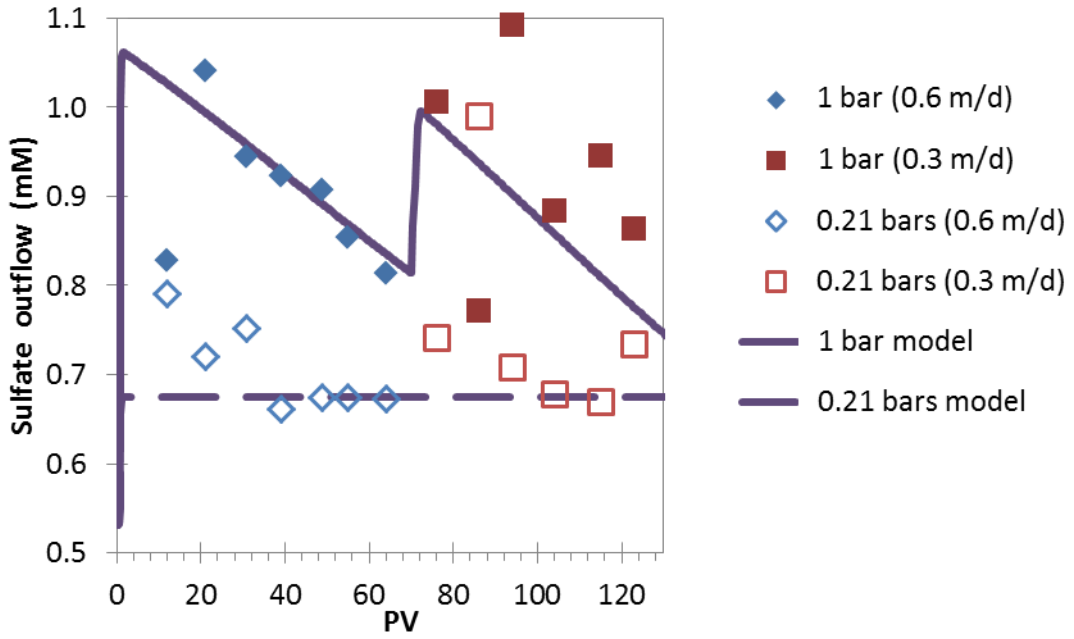

Figure 2.12: The model developed based on the results from the high pressure experiments describes the results from the low pressure experiments at two different flow speeds after modifying the $k_{observed}$ and the passivation parameter. The symbols represent measured data, the lines show the model results.

Additionally to the considerations described above, for the development of multiphase reactive transport models effects of water saturation and geotechnical aspects of pyrite oxidation might be helpful to consider. The water saturation (0% is dry gas, 100% is water only) of the pore space has been described to have a major influence on pyrite oxidation rates. According to Leon et al. (2004) the reaction rate at 25% saturation is ca. 3 times higher in comparison to 95%, while almost no reaction was found at 0.1%. Based on the stoichiometry of a carbonate-cemented aquifer rock, if 0.5mass% pyrite content of the sediment is totally oxidized, then ca. 0.8% carbonate content could balance the generated acidity entirely when dissolving. This slight dissolution can hypothetically cause minor changes in rock stability. The iron-containing reaction products precipitating within a few micrometers from the pyrite surface suggest that possible changes in the pore space geometry, and therefore in porosity and permeability, remain negligible due to pyrite oxidation itself. Even if there is enough time for the decelerating reaction to be completed, pyrite can pseudomorphically transform to goethite (Huminicki and Rimstidt, 2009) resulting in no change in mineral volume.

2.6. Conclusions on pyrite oxidation and air leakages

The high pressure experiment represents conditions that potentially appear in a sedimentary system reached by a front of a progressing oxygen-rich plume, which is a typical scenario for an aquifer downgradient of a compressed air leakage into a shallow aquifer. This is marked by a consecutively increasing oxygen partial pressure for a certain sediment part. Overall, the experimental results and the model simulation indicate that two antagonistic effects have to be considered in case of an impact assessment regarding a potential leakage from compressed air storage on pyrite containing sediments. Increasing oxidation rates of pyrite as well as an increasing passivation effect have to be acknowledged, while both are dependent on increasing dissolved oxygen concertation. The results show that at slightly alkaline condition, i.e. carbonate buffered aquifers, the passivation due to the formation of surface precipitation prevails over the acceleration of the oxidation reaction induced by higher oxygen concentration. Furthermore, the results show a stronger passivation reaction at increasing oxygen partial pressure. Consequently, a leakage of compressed air into a near surface (< 500 m depth) pyrite containing aquifer will not necessarily induce an acidification of the ground water, at least if the pH buffer capacity is high enough to make an initial formation of surface precipitations possible. In case of smaller pH-buffer capacities or an exhaustion of the buffer capacity over time, the oxidation rate of pyrite might suddenly increase, because surface precipitates may be not be formed or may be re-dissolved.

The extended pyrite oxidation rate law including passivation is applicable to an oxygen partial pressure of up 11 bars and, therefore, up to a total air pressure of 50 bars, reflecting a hydrostatic pressure of around 500 m. The rate law might be used for modelling subsurface utilization scenarios in order to assess the geochemical effects of accidental compressed air leakage into shallow aquifers (Bauer et al., 2013; Kabuth et al., 2017; Bauer et al., 2015). Furthermore, the scalability of the rate law between 1 and 11 bars of oxygen partial pressures enables the possibility to investigate the pyrite oxidation for a particular aquifer sediment in column experiments at low pressure conditions, which will drastically reduce the experimental effort and allows more simple pre-studies in order to provide risk assessments for a planned compressed air storage facility.

2.7. Implementation of the experimentally developed transfer function into 3D site-scale modeling

2.7.1. Further motivation

Additionally to the evaluation discussed in Chapters 2.1-2.6 and published in Environmental Earth Sciences, further utilization of the experimental results and of the deducted passivation model was carried out in the frames of the ANGUS+ project by PD Dr. Dirk Schäfer. The goal of these additional investigations was to evaluate the capabilities of an integrated experimental and modeling workflow for assessing the hydrogeochemical consequences of a compressed air leakage on a shallow aquifer at a realistic scale. The outcomes of this chapter will be presented at the EGU meeting after this Thesis has been handed in (Berta et al., 2017).

2.7.2. Modeling method and setup

To create a model simulating similar aquifer conditions to the conditions represented by the experiments, a site-scale 3D numerical model using OpenGeoSys was built (Schäfer, unpublished). This model incorporated the improved reaction rate equation (Figure 2.14, Eqs. 2.5-2.6) to describe pyrite oxidation kinetics, as well as a hypothetical site parameterized based on a typical Upper Lignite Sand Formation (Dethlefsen et al., 2016 a and b) common in Northern Germany. To evaluate the effect of the passivated pyrite oxidation on groundwater composition on site scale in comparison to non-passivated kinetics a model including a pyrite oxidation term without passivation was also considered (Eq. 2.4, Figure 2.15). The applied boundary conditions represented the aquifer conditions of the experiments and the parameters considered for process model development using PHREEQC. These boundaries included pyrite content of the aquifer sediment, oxygen dissolution kinetics, groundwater composition including the carbonate buffer, and diffusive and advective transport parameters. The simulated site was a 130 to 160 m deep confined aquifer with a thickness of 30 m, a width of 50 m and a length of 100 m (Schäfer, unpublished). The two modeled leakage scenarios include a fixed gas phase providing a continuous supply of dissolved oxygen in a column above the modeled leakage spot as well as a groundwater flow of 0.216 m/day (Schäfer, unpublished). The location of the compressed air leakage source and the direction of the flow are illustrated on Figures 2.14 and 2.15.

2.7.3. Results and discussion

The results of the presented 3D site-scale multiphase reactive transport model revealed the spatial distribution of geochemical parameters to be expected after an intrusion of compressed air into a pyrite-containing lignite sand aquifer. The dissolved concentrations of redox-sensitive substances such as oxygen and sulfate as well as the pH value and the concentration of pyrite in the solid phase suggest that the effects of pyrite oxidation on groundwater composition are well recognizable in both scenarios (Figures 2.14 and 2.15). The calcite concentration in the aquifer material, however, showed only a minor decrease which was mostly limited to the zone where surplus oxygen was available. An increase in the electrical conductivity of the groundwater may also be observed in both compressed air leakage scenarios involving pyrite oxidation, most probably caused by the increasing dissolved concentration of sulfate.

Comparing the two modeled scenarios, the one with and the one without considering the influence of the surface passivation effect on pyrite oxidation kinetics demonstrates several further findings. The primary observation, according to the expectations, is that pyrite oxidation, indicated by sulfate concentration, proceeds way faster if the reaction kinetics is not limited by passivation.

The site-scale models also suggest that the presence of oxygen originating from the leakage is mostly limited to a few tens of meters from the leakage source. Therefore, the majority of pyrite oxidation, also indicated by the depletion of pyrite, may be expected to take place within the near-leakage zone. Consequently, the zone where pyrite oxidation takes place is slightly larger if a slower pyrite oxidation rate allows the transportation of oxygen from the source zone to slightly larger distances. In both investigated scenarios calcite dissolution was considered as an equilibrium process, therefore it only took place in the near-leakage zone where pyrite oxidation delivered H^+ ions in the groundwater.

Despite its deciding role, it is yet unknown how the passivation would be effected if the carbonate buffer depleted or missing entirely in an aquifer environment. These conditions may also characterize a long term leakage scenario with pyrite oxidation taking place in a more extensive manner. A reaction rate higher than the ones found in the presented investigations may be caused by, for instance, higher pyrite content or higher specific surface area of pyrite; and a similar overall effect is potentially caused by slower groundwater flow or a significantly higher oxygen partial pressure. In such a hypothetical scenario, the pH value could possibly decrease way below the levels measured and simulated in the scenarios studied here. If this decrease would reach a pH of ca. 4, the oxihydroxides precipitated on the surface of pyrite would potentially dissolve in the groundwater (Figure 2.13), thus eliminating the coating which limited the oxidation rate. The removal of the passivation layer would result in a transition from the passivated pyrite oxidation scheme to the quicker, non-passivated process kinetics known from acid mine drainage sites.

The limits of validity for the presented integrated experimental and modeling concept are therefore marked by the restrictions implied by the boundary conditions, such as the pH buffer capacity, the amount and specific surface area of pyrite, the transport conditions, and the partial pressure of oxygen. However, these restrictions can be characterized more in details if a deeper process understanding is gathered by for instance studies applying new experimental conditions or if the presented investigations are completed by a pilot-scale field study.

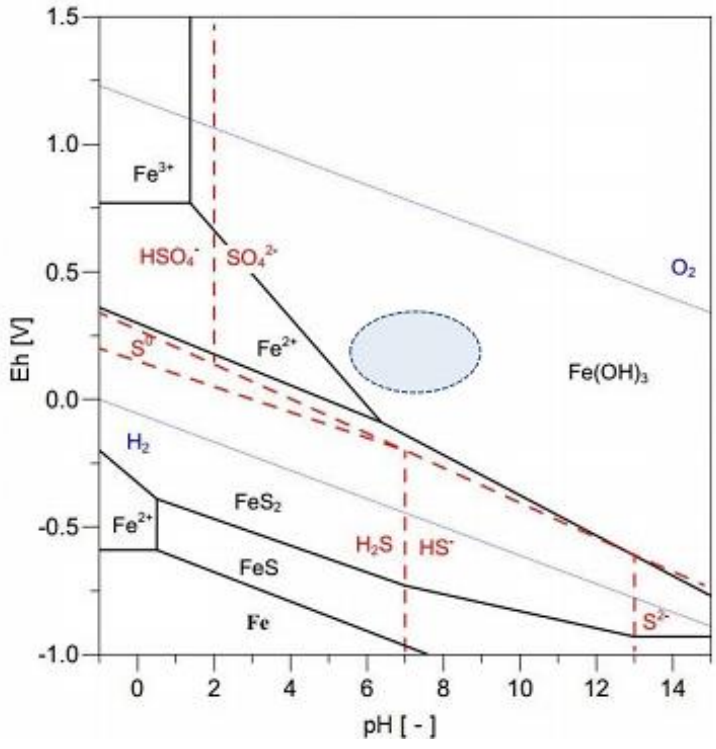

Figure 2.13: E_H-pH diagram for the stability relation in the Fe-S- H_2O system at 25°C, after Levenspiel (1972) taken from Nagy (2008) by Gundske (2013). pH and redox conditions of the column experiments on pyrite oxidation are marked by the light blue ellipse.

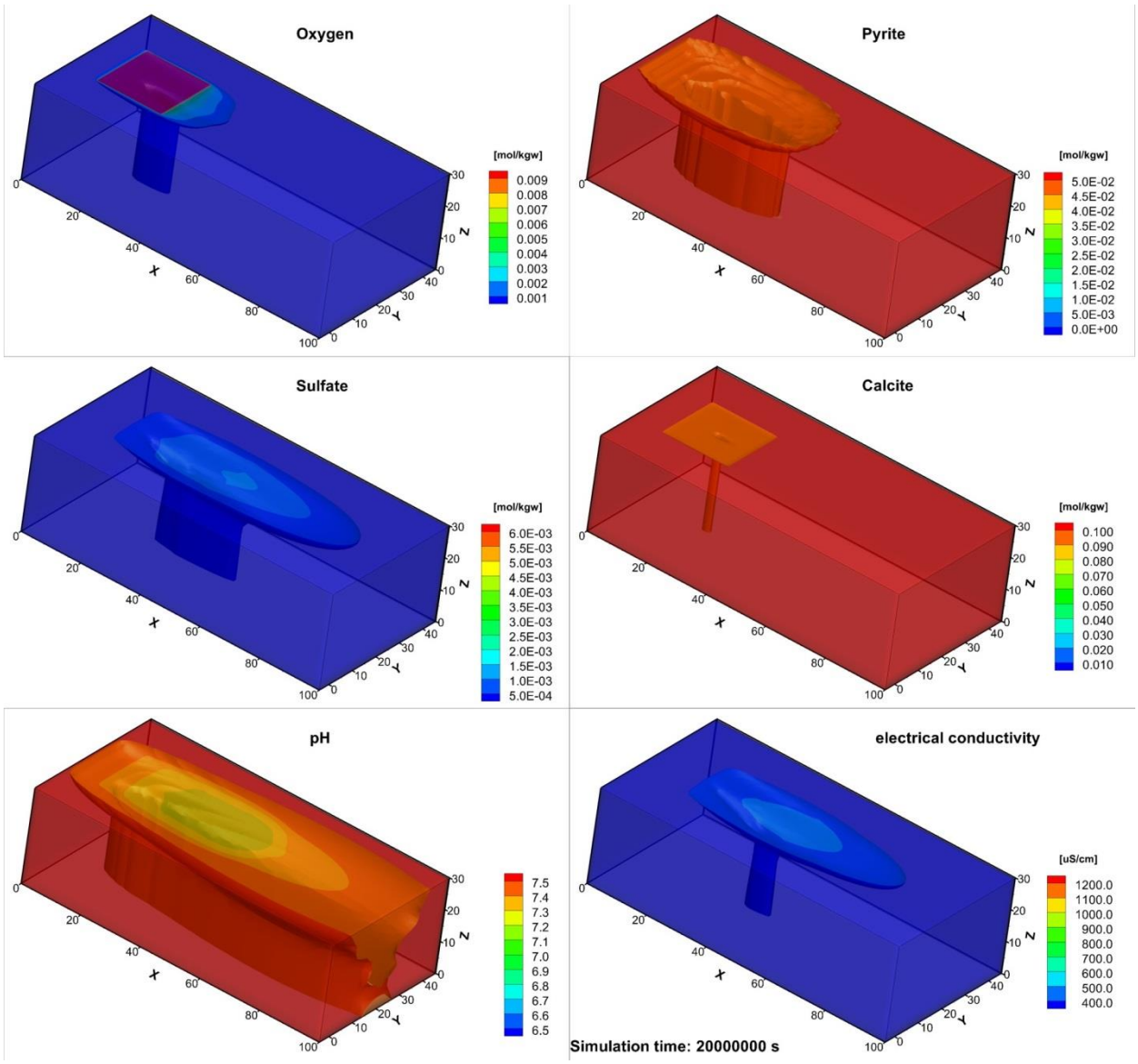

Figure 2.14: Development of dissolved oxygen and sulfate concentrations, the moles of pyrite and calcite in the solid phase per kg of groundwater, as well as the pH value and the electrical conductivity of the groundwater after ca. 230 days. This scenario was calculated ***with*** *passivation effect (courtesy of Dirk Schäfer, unpublished data), the distances are given in meters. For videos showing the development of the plumes please refer to the CD Appendix.*

A coupled experimental and modeling approach can also deliver outcomes for potentially direct applications for leakage management (Schäfer, unpublished) and monitoring. Most importantly the presented results (Figures 2.14 and 2.15) suggest that direct detectability of an air leakage by measuring only oxygen in downstream observation wells may not be a suitable solution for monitoring because the abundance of oxygen is limited to the near-leakage zone by pyrite oxidation. Such a limitation highlights the importance of developing geochemical and geophysical monitoring methods using proxies, for instance sulfate concentration and electrical conductivity, respectively. Moreover, the decrease of pH is a common concern when pyrite oxidation is discussed, however, even if there is no passivation slowing the oxidation of pyrite, the acidification stays within the threshold limits for drinking water (TrinkwV).

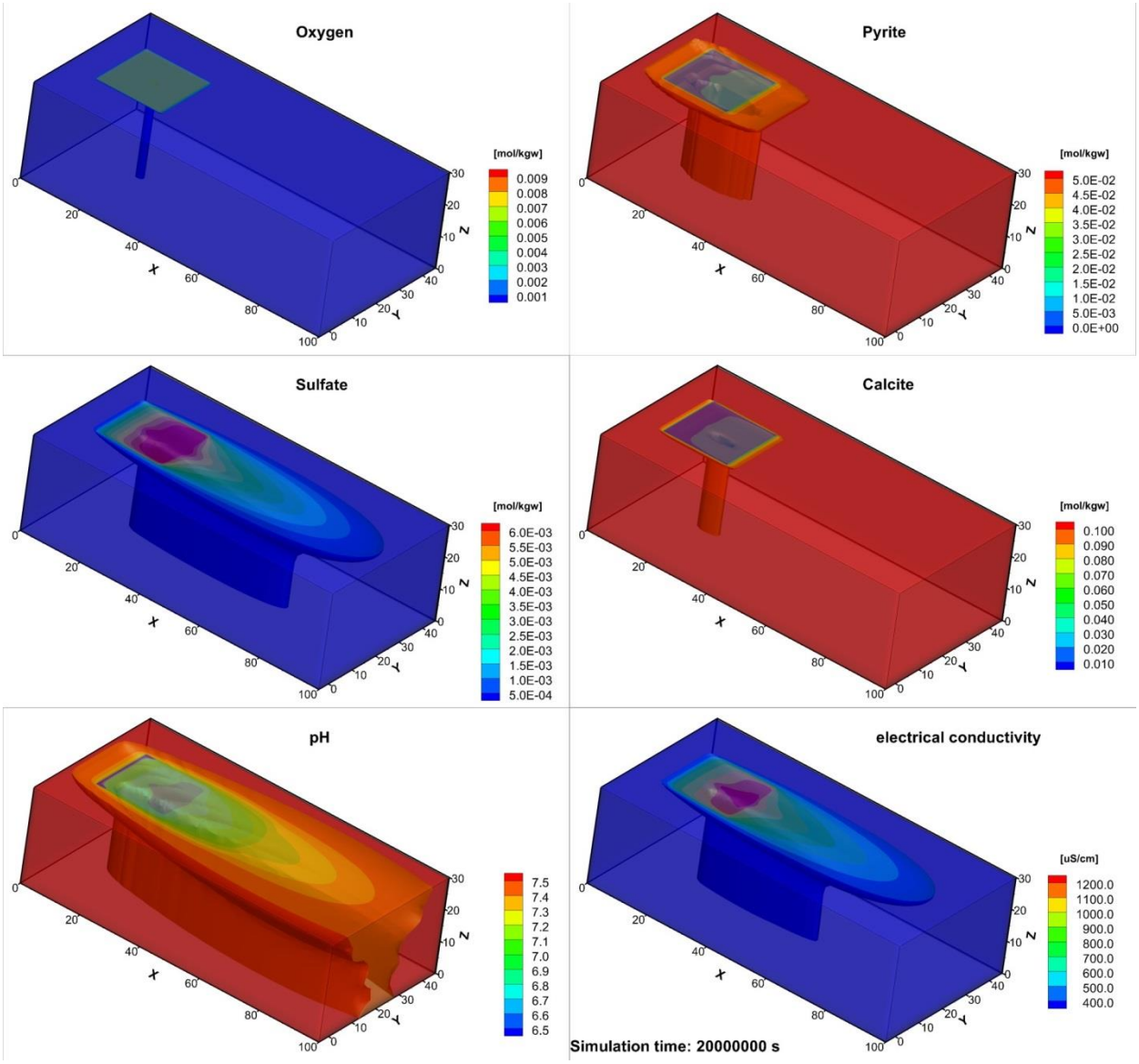

Figure 2.15: Development of dissolved oxygen and sulfate concentrations, the moles of pyrite and calcite in the solid phase per kg of groundwater, as well as the pH value and the electrical conductivity of the groundwater after ca. 230 days. This scenario was calculated ***without*** *passivation effect (courtesy of Dirk Schäfer, unpublished data), the distances are given in meters. For videos showing the development of the plumes please refer to the CD Appendix.*

2.7.4. Implications for the integrated experimental and modeling assessment of gas leakages

This additional chapter demonstrated that the changes in dissolved concentrations of sulfate and oxygen as well as in pH and electrical conductivity observed in laboratory column experiments were reproduced by the models applying the same boundary conditions for site-scale investigations of a compressed air leakage. Thus, it is suggested that the combination of laboratory experiments and numerical models is an appropriate tool to estimate the geochemical consequences of gas leakages on the site scale (Schäfer, unpublished). This conclusion suggests the feasibility of the presented integrated approach also for evaluating comparable gas storage and gas leakage scenarios involving methane and hydrogen plumes based on experimental results gathered similarly.

3. Changes in groundwater potentially following methane intrusions into shallow aquifers

3.1. Sulfate reduction coupled to methane oxidation in aqueous environments – a review

3.1.1. Outline

The increasing global energy demand and the shift to renewable energy sources implies the need for novel natural gas production and renewable energy storage technologies involving methane, while the subsurface has a large capacity for gas storage and recovery in various reservoirs. Establishing subsurface operations utilizing these potentials for methane storage often induce rising public and political concern mainly regarding accidental gas leakages and especially their potential effects on the safety of communal groundwater supplies. These safety questions need to be addressed by detailed field, experimental and modeling studies, resulting in a guideline for the sustainable use of the subsurface. Evaluating potential changes in groundwater quality is especially important because groundwater is a highly protected natural good in most developed countries, mainly due to its common exploitation as a source of drinking water.

Numerical scenarios are developed for the risk assessment for constructing or operating a methane storage site and for planning possible leakage monitoring actions. As direct field data regarding the hydrogeochemical effects of methane ingress into shallow aquifers hardly exist, analogue studies describing the expected geochemical reactions, most importantly methane oxidation coupled to sulfate reduction, from different environments are reviewed to understand the redox processes expected to occur in shallow aquifers following such gas leakages. Pristine potable aquifers usually contain either methane or a considerable amount of electron acceptors, most likely sulfate. Intrusion of an aquifer by methane can therefore result in the reduction of the available sulfate, resulting in production of sulfide. Similarly, reduction of nitrate to nitrite or N_2/N_2O may be expected in near-surface freshwater aquifers.

Here, the state-of-the-art process understanding concerning microbially mediated anaerobic methane oxidation coupled to sulfate reduction is reviewed. The focus is on the expected reaction rates potentially following accidental methane intrusions into shallow aquifers. To complete and specify, to what extent methane oxidation coupled to sulfate reduction has to be expected experimental methods exemplified in the next chapter may be used. This chapter shows that for the oxidation of poorly reactive methane by sulfate reduction, the presence of a slowly developing, extensive, initial methane-oxidizing microbial community is most probably needed; therefore, a prompt geochemical reaction will not necessarily follow a sudden methane leakage. The low reactivity of methane in case of a leakage suggests that monitoring efforts to find fugitive methane may focus on methane itself, instead of looking for reaction products; and that methane can therefore be modeled as a potentially conservative gas.

3.1.2. Introduction

The increasing use of the subsurface for conventional and unconventional energy production and energy storage already shapes the future of the global energy sector considerably. Further development potentially includes scenarios with intensive development of renewable energy sources, like the German goal of gaining all electricity solely from renewable sources by 2050 (UBA, 2010). To balance the natural fluctuations of power production from renewable energy sources such as wind and solar, power-to-gas systems may electrolyze hydrogen from water using surplus energy. This hydrogen can either be fed directly into a hydrogen- based energy system (Reitenbach et al., 2015), or it can be used to produce methane via the Sabatier-process (Müller et al., 2013). In this way, the supply in a regional power network can be balanced on a seasonal time scale. Although this system includes conversion losses, the potential for economic benefits still motivates for development: for example the process of direct hydrogen generation, storage and re-electrification has an efficiency of between 12 and 55% (Bosse, 2006; Luo et al., 2014; Gao et al., 2014). Overall, storage of renewable energy through the power-to-gas technology is expected to be a deciding part of future energy supply networks, and methane is expected to continue playing a deciding role.

Methane may be generated in the order of several millions of normal cubic meters to balance fluctuations lasting between several days to a few months (Sterner and Stadler, 2014). When such large gas volumes are to be stored within a region, underground technologies are both safer and cheaper per kWh compared to the surface facilities usually having a capacity lower by orders of magnitude (Evans, 2009; Taylor et al., 1986). However, establishing a geological reservoir to store methane possibly involves conflicts between different ways of subsurface use: these potential conflicts have to be regarded in order to plan a sustainable use of the subsurface space (Bauer et al., 2013).

Amongst the potential risks posed by such geological storage facilities, hydrogeochemical reactions following an accidental gas leakage into an overlying shallow aquifer are of distinguished significance, as these aquifers are often used for drinking water production. Gas leakage rates may range between 0.04 m^3/d and more than 100 m^3/d (Roy et al., 2016 and refs therein). Such unwanted presence of methane in the groundwater may be caused by for instance unsealed wells or poor performance of the cap rock formation (Jackson et al., 2013a). The nature of these leakages can be similar to leakages of CO_2 from subsurface reservoirs (e. g. Apps et al., 2010, Berest, 2002) regarding the source and the path of the leakage (e. g. Roy et al., 2016 and refs therein), implying a comparable need for leakage monitoring (Dethlefsen et al, 2013; Schäfer et al., 2013). A further analogue may be found at leakages of CH_4 related to unconventional hydrocarbon production (e. g. Osborn et al., 2011); both of them potentially influencing groundwater quality. After a leakage event, the fugitive gas will probably quantitatively remain available for subsurface transport processes (Cirpka et al., 2015), and also for geochemical reactions.

Microbial methane oxidation has been investigated for decades, and microorganisms generally tend to successively utilize the energetically most favorable electron acceptor (EA) available and establish a redox sequence (Table 3.1) by reducing the EAs oxygen, nitrate, $iron^{III}$, $manganese^{IV}$, and sulfate, in the same way bacteria can oxidize other organic compounds (Stumm and Morgan, 1981). Oxygen is the most favorable electron acceptorfor oxidizing methane, but its presence may be restricted to near-surface, unconfined aquifers (Roy et al., 2016). In oxygen-free shallow aquifers, nitrate can be a suitable electron acceptorfor the oxidation of methane (Eisenträger et al., 2001; Raghoebarsing et al., 2006; Ettwig et al., 2009; Modin et al., 2010; Deutzmann and Schink, 2011; Islas-Lima et al., 2004). Methane oxidation may also take place using nitrite as oxidant (Rasigraf et al., 2012). Following $manganese^{IV}$ (Beal et al., 2009; Ettwig et al., 2016), which generally shows a low concentration in shallow aquifers, $iron^{III}$ is the next relevant oxidant (Beal et al., 2009; Ettwig et al., 2016) used in the suggested redox sequence, followed finally by sulfate (Knittel and Boetius, 2009).

Table 3.1. The gatherable Gibbs free energy yields from the reactions involving methane and electron acceptors in comparison to other organic substances (McCarty, 1971 and Thauer et al., 1977 in Edwards et al., 1992[1-4]; Lovley and Phillips, 1988[5]; Thauer et al., 1989[6]; Raghoebarsing et al., 2006[7]; Wang et al., 2010[8]; Beal et al., 2009[9-10]; Deutzmann, 2011[11])

	Reaction			ΔG^0_r [kJ/mol]
1	Aerobic toluene oxidation	$C_7H_8 + 9\ O_2$	→ $7\ CO_2 + 4\ H_2O$	-3807
2	Aerobic xylene oxidation	$C_8H_{10} + 10.5\ O_2$	→ $8\ CO_2 + 5\ H_2O$	-4435
3	Toluene oxidation coupled to sulfate reduction	$C_7H_8 + 4.5\ SO_4^{2-} + 3\ H_2O$	→ $4.5\ HS^- + 7\ HCO_3^- + 2.5\ H^+$	-229
4	Xylene oxidation coupled to sulfate reduction	$C_8H_{10} + 5.25\ SO_4^{2-} + 3\ H_2O$	→ $5.25\ HS^- + 8\ HCO_3^- + 2.75\ H^+$	-267
5	Acetate oxidation coupled to sulfate reduction	$CH_3COO^- + SO_4^{2-} + H^+$	→ $HS^- + 2\ CO_2 + 2\ H_2O$	-63
6	Acetotrophic methanogenesis	$CH_3COO^- + H^+$	→ $CH_4 + CO_2$	-36
7	Methane oxidation coupled to denitrification	$5\ CH_4 + 8\ NO_3 + 8\ H^+$	→ $4\ N_2 + 5\ CO_2 + 14\ H_2O$	-765
8	Methane oxidation coupled to sulfate reduction	$CH_4 + SO_4$	→ $HS^- + H_2O + HCO_3^-$	-19
9	Methane oxidation coupled to iron reduction	$CH_4 + 8\ Fe(OH)_3 + 15\ H^+$	→ $8\ Fe^{2+} + 21\ H_2O + HCO_3^-$	-270
10	Methane oxidation coupled to manganese reduction	$CH_4 + 4\ MnO_2 + 7\ H^+$	→ $4\ Mn^{2+} + 5\ H_2O + HCO_3^-$	-556
11	Aerobic methane oxidation	$CH_4 + 2\ O_2$	→ $CO_2 + 2\ H_2O$	-819

Although numerous studies from marine and freshwater environments suggest that methane oxidation should be expected after a leakage into a shallow aquifer, not all aquifers with a methane ingress showed a significant metabolic activity. In the region in which the Marcellus Shale (Pennsylvania, USA) was subject to extensive conventional gas production and in which unconventional gas production activity has commenced some years ago, methane in aquifers has been monitored for a few years, although not only unconventional gas production (Dusseault and Jackson, 2013) but also poorly built conventional wells in general have a potential to leak hydrocarbons into shallow aquifers (Kelly et al., 1985; Holzman, 2012; Schwartz, 2014). In the Marcellus Shale region, high concentrations of thermogenic methane were found in areas close to hydrocarbon production wells, but no sulfate reduction was identified based on $^{12}C/^{13}C$-methane isotopic compositions in the affected aquifers (Osborn et al., 2011), even when no other EAs than sulfate were available. Despite the thermogenic origin of methane probably related to the gas production, higher dissolved methane concentrations in the area were elevated in valleys (Molofsky et al., 2013) and not in the vicinity of hydrocarbon wells (Jackson et al., 2013b).

Additionally, median sulfate concentrations were observed to inversely correlate with dissolved methane concentrations, along with increased dissolved Fe^{tot} and Mn^{tot} concentrations (Molofsky et al., 2013). This would support the mutual exclusion of methane and its electron acceptors in a steady state (McIntosh et al., 2014). Although the origin of the methane in this (e. g. Brantley et al., 2014) and other regions (e. g. Roy et al., 2016 and refs therein) is still debated, significant geochemical reactions between methane and sulfate are not reported in distances larger than a few 100 meters away from the gas production facilities lying beneath these shallow aquifers. On the other hand, microbial activity may degrade hydrocarbons even at reservoir conditions (Gniese et al., 2014). However, at an aquifer gas storage site in Western Europe, also no methane oxidation coupled to sulfate reduction was identified despite the presence of up to 0.2 mM sulfate, being partially used for degradation of BTEX at trace concentrations (Chiquet, 2015).

Any of the reactions in Table 3.1, but most likely sulfate reduction coupled to methane oxidation would result in a change in the groundwater composition and would also attenuate a potential groundwater contamination by methane. On the other hand, the absence of microbial methane oxidation at a specific site might also cause a long-term impact on the groundwater quality, which would be of distinguished importance because groundwater is classified as a protected natural resource by the EU Water Framework Directive (European Parliament and Council, 2000).

The aim of this chapter is, therefore, to compile the state-of-the-art literature regarding the likeliness and available rates for methane oxidation following a methane ingress into a shallow aquifer as a consequence of a leakage from a gas storage site in the deeper subsurface. In this context, the presented study focuses on the methane oxidation coupled to sulfate reduction, because sulfate is typically the most widespread electron acceptor for methane oxidation in aqueous environments (Knittel and Boetius, 2009). As only very few studies describe such a situation, analogues from other scenarios and other environments are also consulted in this review, and their expressiveness for evaluating potential processes in the groundwater influenced by a methane leakage are discussed.

3.1.3. Analogues for consequences of a methane leakage

Origin and presence of methane

Methane is often present in pristine shallow aquifers. The natural sources of methane in a shallow aquifer may be biogenic or thermogenic. Thermogenic methane can leak into shallow aquifers from deeper reservoirs (Melchers, 2009). Sources of biogenic methane can be the aquifer itself or an underlying shallow aquifer. For instance, in Lower Saxony, North Germany the vast majority of ca. 1000 investigated wells showed the presence of only biogenic methane in concentrations below 1 µl/l, based on ^{13}C isotope and gas composition measurements (Schloemer et al., 2016). On the other hand, there is still a need for studies to deliver a reliable monitoring baseline on methane concentrations in Northern Germany (Figure 3.1).

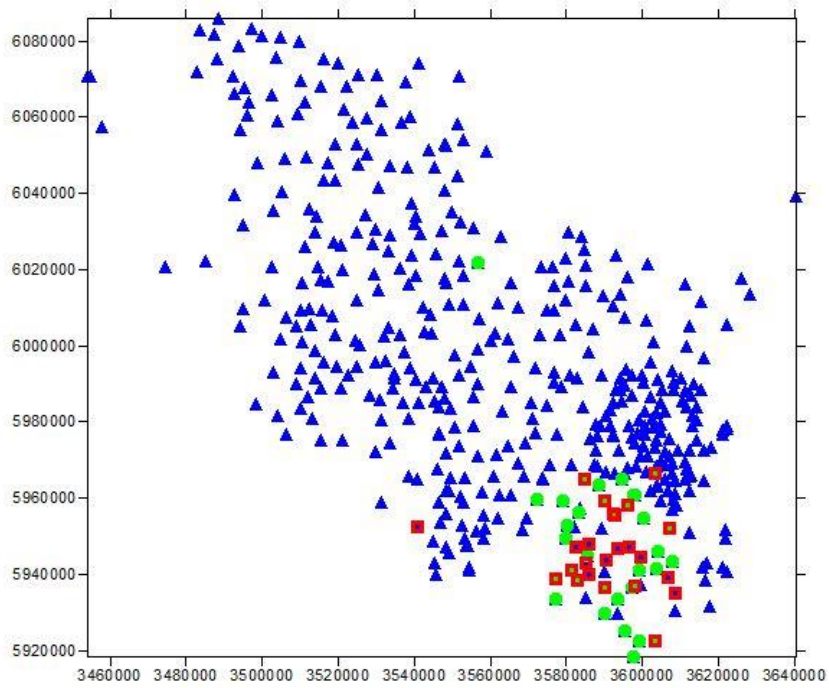

Figure 3.1: Methane in groundwaters of the federal state of Schleswig-Holstein (Germany). Blue triangles (▲) indicate wells not monitored for methane at all, green dots (●) mean wells where no methane (under 0,1 mg/l detection limit) was found, and red empty rectangles (□) mean wells where methane was detected (average: 0.5 mg/l, median:0.2 mg/l). Apart from 3 wells, every methane-containing water was measured only once. Amongst different aquifers, the most methane occurrences are in the Obere and Untere Braunkohlensand formations, and ablin the shallow (0-25 m) but confined aquifers. Overlapping red and green symbols indicate sampling locations where methane is detected only in one of the aquifers. Data source: LLUR database (Dethlefsen et al., 2017).

In aquifers being in a redox steady-state, either the presence of methane or the presence of an electron acceptorwas observed (McIntosh et al., 2014, van Stempvoort et al., 2005), depending on which of the reaction partners had been in surplus. Strict mutual exclusion between EAs and methane was observed in the studies above. This means the presence of either methane at ca. 10% in situ saturation or 300 mg/l sulfate or 10 mg/l nitrate concentrations or 20% in situ oxygen saturation. This mutual exclusion is also valid for aquifers with an external methane supply where methane is present in a high dissolved concentration of up to 2.8 mM due to a long term natural seepage (Melchers, 2009). Additionally, waters produced from reservoirs of hydrocarbons are typically deficient in sulfate (Pelak and Sharma, 2014), suggesting that the mutual exclusion of methane and sulfate to be valid for deeper aquifers as well.

Therefore, dissolved methane is expected to prevail within an aquifer only if sulfate, commonly the electron acceptorpresent in the highest concentrations, is already depleted (Zhang et al., 1998).
On the other way around, methanogenesis, as a processes opposed to methane oxidation, is only taking place at a sulfate concentration of approximately 30 μM or below (Lovley and Klug, 1986). Presence of methane may be expected in aquifers if these main preconditions, namely methane ingress and sulfate depletion, are fulfilled. If there is no methane but sulfate in an aquifer, it can either be a consequence of methanogenesis being inhibited by the availability of sulfate or the methane being oxidized using sulfate as an electron acceptor. For a gas leakage scenario, the reactions consuming methane, their lag phases or reaction rates, and the environments they take place in are highly relevant. Although methane suddenly intruding a shallow, sulfate-containing aquifer is very unusual in natural systems, this is exactly what is expected after a methane leakage from a reservoir e. g. through a poorly constructed well casing. Because of this rareness, there are only a few studies (van Stempvoort et al., 2005; Kelly et al., 1985) available which show and directly describe events when methane intruded a shallow aquifer triggering sulfate reduction. These studies could be potentially used for estimating the occurrence of methane oxidation coupled to sulfate reduction, completed by studies on similar environments, potentially contributing to this estimation (Table 3.2).

Rates of methane oxidation coupled to sulfate reduction in subsurface environments
Due to the widespread availability of sulfate, anaerobic oxidation of methane coupled to sulfate reduction is regarded as the main process for the degradation of methane in both marine and freshwater environments (Knittel and Boetius, 2009). Anaerobic oxidation of methane coupled to the reduction of sulfate is a biogeochemical phenomenon that was assessed theoretically (e. g. Dale et al., 2006; Kasten and Jørgensen, 2000; Treude et al., 2003) and observed at a number of marine sites worldwide (Niewöhner et al., 1998; Treude et al., 2005b; Reeburgh, 2007; Iversen and Jørgensen, 1985; Jørgensen et al., 2001; Siegert et al., 2011; Bussman and Suess, 1998) with reaction rates between 10^{-4} and 10^{5} nmol/cm^3/day, if sulfate is available in marine and freshwater environments (Table 3.1). This redox reaction mostly occurs in sulfate-methane transition zones (SMTZ) in seafloor sediments as well as in deep sea microbial mats (dense layers of microorganisms) and it is catalyzed by syntrophic consortia of uncultured methane oxidizing Archaea and sulfate reducing bacteria (Knittel and Boetius, 2009). As sulfate reduction coupled to methane oxidation can be expected in both saline and freshwater sediments (Knittel and Boetius, 2009), characterization of the microbial communities and their densities in both environments potentially carrying out this metabolism provide a good base to estimate how sulfate reduction by methane oxidation behaves in methane-contaminated potable aquifers. The methane oxidizing Archaea in the consortia serve as the partner activating the methane; the sulfate reducing bacteria shuttle electrons to the electron acceptorthat function as electron sinks (Boetius et al., 2000; Knittel and Boetius, 2009). The time needed for increasing reaction rates, if an increasing amount of substrate (sulfate and/or methane) becomes available, is determined by the growth potential of this microbial community. Methane oxidation by sulfate reduction in high pressure batch incubations showed a 7-months-long doubling time of the microorganisms (Nauhaus et al., 2007). This doubling time was found to be 3.8 months in membrane bioreactor experiments (Meulepas et al., 2009), and 1.1 as well as 2 months in continuous flow and in shaken batch tests, respectively, using sediments from marine sulfate-methane transition zones (Girguis et al., 2005; Krüger et al., 2008).

Table 3.2. (see the next double page) Rates of anaerobic oxidation of methane coupled to sulfate reduction in different environments in nmoles of methane oxidized per cm^3 of water and/or sediment per day. ANME means groups of anaerobic methane-oxidizing archaea and SRB means groups of sulfate reducing bacteria.

Environment	Anaerobic methane oxidation rate (nmol/cm^3/day)	Methane (µM)	Sulfate (mM)	Microbial community	Microbial density	References
Black Sea microbial reefs	1000–20900	1800-2800	17	ANME-1, ANME-2 and SRB	n. d.	Michaelis et al., 2002; Treude et al., 2007 in Knittel and Boetius, 2009
Seeps with surface hydrates	100–5500	0-2500	0-28	Beggiatoa	0.5-1.5·10^8 aggregates/g$_{sediment}$	Joye et al., 2004; Treude et al., 2003 in Knittel and Boetius, 2009
Mud volcanoes, gas chimneys	10–1500	0-5700	0-27	ANME-1, ANME-2, ANME-3 and SRB	10^7-3.6·10^9 cells/cm^{3}sediment	Niemann et al., 2006b; Omoregie et al., 2008 in Knittel and Boetius, 2009
Coastal SMTZ	1–50	0-5000	0-22	ANME-1, ANME-2 and SRB	5.1·10^6-1.4·10^8 cells/cm^{3}sediment	Knab et al., 2008; Parkes et al., 2007; Treude et al., 2005a; Wegener et al., 2008 in Knittel and Boetius, 2009
Continental margin SMTZ	0.1–15	0-8000	0-30	ANME-1, ANME-2 and SRB	1.5·10^8-1.45·10^7 cells/cm^{3}sediment	Niemann et al., 2005; Niemann et al., 2006a; Niemann et al., 2006b; Treude et al., 2005b in Knittel and Boetius, 2009
Subsurface SMTZ	0.003–0.16	0-12500	0-26.5	n. d.	n. d.	Sivan et a., 2007 in Knittel and Boetius, 2009
Marine anoxic water columns	0.0001–0.01	0-15	n. d.	ANME-1, ANME-2, Bacteria	n. d.	Reeburgh, 2007; Schubert et al., 2006 in Knittel and Boetius, 2009
Lake water and lake sediment	0.0001–1	n. d.	n. d.	n. d.	n. d.	Schubert, unpublished in Knittel and Boetius, 2009
Landfill leachate plume in an aquifer	0.049–0.63	100-1400	0.2-9	n. d.	n. d.	Grossman et al., 2002
Hydrocarbon well leakage in an aquifer	1.59	625-68.7	3.9-3.1	n. d.	n. d.	van Stempvoort et al., 2005
Methane hydrate ridge batch incubation	500-5000 (pressure dependent)	0-15000	46753	Archaea and SRB	9·10^7 consortia/g$_{sediment}$	Nauhaus et al., 2002

(continued)

Environment	Anaerobic methane oxidation rate (nmol/cm^3/day)	Methane (µM)	Sulfate (mM)	Microbial community	Microbial density	References
Reactors with marine sediment	0.3-286000	1440	15-25	ANME-1, ANME-2	10^2-10^6 rRNA copies/$g_{sediment}$	Meulepas et al., 2009; Girguis et al., 2005; Krüger et al., 2008
Marine sediment in lab column	96-1025 (flow dependent)	1-4	0-20	ANME	n. d.	Steeb et al., 2014
Marine sediment in lab column	20-162 (temperature-dependent)	133-2849	n. d.	ANME-1	n. d.	Wankel et al., 2012
Marine sediments	49	2006	20	n. d.	n. d.	Bussman et al., 1999 in Roy et al., 2016
Marine sediments	88	2618-5281	0.5-26	n. d.	n. d.	Devol et al., 1984 in Roy et al., 2016
Marine sediments (warm)	15	2	n. d.	n. d.	n. d.	Hansen et al., 1998 in Roy et al., 2016
Marine sediments (warm)	12	1506	n. d.	n. d.	n. d.	Hoehler et al., 1994 in Roy et al., 2016
Marine sediments	0.002-12	3-1000	15-25	SRB (assumed)	n. d.	Iversen and Jorgensen, 1985 in Roy et al., 2016
Lake	0.05-0.08	53	n. d.	n. d.	n. d.	Iversen et al., 1987 in Roy et al., 2016
Marine sediments (cold)	0.021-0.98	201-9500	1.3-28.3	n. d.	n. d.	Koisur and Warford, 1979 in Roy et al., 2016
Marine sediments (cold)	0.11-9.19	6500	20	n. d.	n. d.	Reeburgh, 1980 in Roy et al., 2016
Wetland	265.625	2000	1.15	Archaea and bacteria	n. d.	Segarra et al., 2015 in Roy et al., 2016

The overall coupled methane oxidation - sulfate reduction rate and also its growth potential are also determined by the availability of the reactants. According to Valentine (2002), diffusion is the dominant process delivering dissolved sulfate and dissolved methane to the sulfate-methane transition zones, causing orders of magnitudes of differences in reaction rates between sediments around marine seeps by diffusive mixing and in methane vents by advective mixing. Flow-through column experiments using sediment from a marine SMTZ may be relevant for aquifer conditions: Steeb et al. (2014) found reaction rates to be an order of magnitude higher at faster flow compared to slower transport conditions. Apart from variations in pressure and transport, experiments conducted using different pressure and temperature conditions represent methane oxidation in aquifers at different depths. With the methane partial pressure increased from 0 to 11 bars, sulfate reduction increased linearly (Nauhaus et al., 2002). This suggests that the reaction potentially has a first order dependency on the partial pressure of methane within aquifer conditions as well, although the majority of other studies only provide zeroth order rate constants due to the low number of comparable experiments, often only one, with different methane partial pressures. Moreover, the reaction rate is most probably primarily dependent on the density of the microorganisms; although further research will be needed to make site-specific and time-dependent estimations.

A few considerations may contribute to the evaluation of the reaction rates gathered from various aqueous environments (Table 3.2). Because anaerobic oxidation of methane coupled to sulfate reduction is a redox reaction entirely mediated by microorganisms, it may seem plausible to recognize the increasing reaction rates if a higher microbial density is present. However, due to the major variations in the phylogenetic composition of the communities investigated at different sites, in the partial pressure of methane and in the concentration of sulfate may prevent to consider this trend a direct correlation. A knowledge gap for future studies is that for aquifer environments where methane oxidation coupled to sulfate reduction took place have not been investigated for the microbial community carrying out the geochemically identified reaction. On the other hand, such studies comparatively investigating the microbial reactivity of marine SMTZs and sulfate-rich aquifers intruded by methane may be reasonable because the methane and especially sulfate concentrations measured at many marine sites with a considerable reaction rate are easily high enough to fall in the strict mutual exclusion range of sulfate and methane identified for aquifers.

When predicting processes in methane-containing groundwater, reactions occurring in freshwater aquifers contaminated by organic substances such as solvents can yield additional information. A reason for this approach is that methanotrophic bacteria are ubiquitous and some can metabolize aliphatic and aromatic compounds and even a few chlorinated solvents (Brigmon, 2001). Also, cultured marine strains could degrade toluene in petroleum-contaminated sediments (Bolliger et al., 2001) and a methanotrophic groundwater community was able to metabolize larger (C_{10}) organic substances as well (Hrsak and Begonja, 2000). Moreover, contaminants may co-occur with methane in a landfill leachate plume, creating an environment which is well studied and relatively close to the conditions expected after a methane leakage (Grossman et al., 2002). This suggests anaerobic methane oxidation first via reduction of iron^{III}, then coupled to sulfate reduction, which was identified in distinct zones of a contaminated aquifer (Grossman et al., 2002). Feisthauer et al. (2012) found isotopic evidence for the degradation of BTEX using sulfate as electron acceptorwith ongoing methanogenesis and subsequent anaerobic methane oxidation in an aquifer. Therefore, shallow aquifers contaminated by organic solvents are also potentially showing some of the processes also expected to occur after a methane leakage; consequently, the characterization of sulfate reduction found in such contexts should also be included in a methane leakage scenario as well.

In contrast to numerous papers on marine SMTZs or freshwater sites contaminated by organic solvents, geochemical reactions following an anthropogenic methane intrusion, such as the leakage of thermogenic or synthetic methane into such aquifers, are described by only a few field case studies (van Stempvoort et al., 2005; Kelly et al., 1985; Kotelnikova, 2002; Grossmann et al., 2002). An accident at a gas production well in Lloydminster, Alberta, Canada, resulted in anaerobic oxidation of methane coupled to sulfate reduction after seven years (van Stempvoort et al., 2005).

A multiphase flow modeling study based on the neighboring and similar Lindbergh site from the same region (Roy et al., 2016) showed that the concentration of dissolved methane decreased by up to 100 mg/l within 5 years after a natural gas leakage. After a blowout at another gas well in North Madison, Ohio, USA, sulfate reduction was found to commence within a week, and batch experiments using groundwater from this site partially reproduced the methane oxidation coupled to sulfate reduction observed in the aquifers (Kelly et al., 1985). This suggests an enormous difference in the lag phase durations of reactions taking place at different leakage cases. Regarding factors potentially determining the reactions, *in-situ* redox tracer experiments on freshwater sulfate reduction at the interface between sulfate and its electron donors highlighted the importance of mixing the reactants (Kneeshaw et al., 2011), which is usual for hydrogeochemical reactions following the intrusion of a potentially reactive substance (Meckenstock et al., 2015). Furthermore, a few authors (Kneeshaw et al., 2011) acknowledged a lag phase of 2.4 to 22 h before sulfate reduction started in the aquifer, which is quick on the time scale of processes initiated by regional subsurface leakage and transport of a leaked gas. Additionally, Engle and Rowan (2014) suggested sulfate reduction stimulated by injecting sulfate-rich fracking fluid. Sulfate reduction, therefore, may play a main role in the metabolism of leaked methane in field studies, but several factors like the availability of nutrients and initial density and composition of the microbial community seem to influence the length of the lag phase and the rate of the reaction, taking up to several months or years to commence.

3.1.4. Conclusions and Lessons Learned

The summarized literature data shows that microbially mediated sulfate reduction coupled to methane oxidation can be of deciding significance in methane leakage scenarios, although this reaction is not expected to take place in all environments, spontaneously and at a considerable rate.

Low reactivity of methane

Methane was found to belong to the less reactive groundwater contaminants considered here, similarly to other poorly bioavailable organic contaminants or slowly metabolized natural sources of organic carbon. The low reactivity of methane is probably caused by the comparatively low thermodynamic energy yield of anaerobic methane oxidation (Table 3.1) barely sufficient to synthetize one ATP (adenosine triphosphate), the main energy carrying molecule in biochemical processes and the low efficiency of the microorganisms to assimilate the consumed carbon. These two factors result in a very slow (month-years) doubling time of anaerobic methane oxidizers. For an aquifer environment, this suggests a comparatively low bioavailability of methane as an electron donor resulting in slow reaction rates and difficult establishment of syntrophic microbial consortia metabolizing methane, especially if the aquifer initially lacks methane oxidizing microorganisms. This low reactivity can inhibit spontaneous microbially mediated sulfate reduction and methane oxidation in groundwater composition after a methane leakage.

Rates of sulfate reduction coupled to methane oxidation in shallow aquifers

Based on this review it may be suggested that the characterization of the metabolic potential of shallow aquifers at sites where a methane leakage may be expected shall be first carried out based on studies available on relevant environments (Table 2) and direct investigations. As direct microbial sampling of aquifers implies difficulties (Basso et al., 2005), laboratory experiments on methane attenuation exemplified here may complete such characterizations. For parameterizing numerical modeling scenarios beyond reaction rates from the literature (Table 3.2), experimental investigations need to be operated long enough to represent the time for which the studied aquifer is potentially exposed to fugitive methane, typically for a few months to a year.

If it takes place, oxidation of methane coupled to sulfate reduction can influence the groundwater quality due to the production of sulfide. The coupled sulfate reduction – methane oxidation rate is expected to lie in the range of reactions taking place in shallow aquifers and reviewed here (0.05-1.6 nmol/cm^3/day), although other environments represent a way broader, up to nice orders of magnitude wide range of reaction rates (Table 3.2). Also, the reaction rate order has not been investigated directly by studies adequate for a methane leakage scenario, however, based on Nauhaus et al. (2002) it should be linearly dependent on the partial pressure of methane, meaning that the sulfate reduction coupled to methane oxidation will be faster in a methane leakage plume developing in a deeper aquifer. The flow speed of the groundwater may also play a deciding role, as advective transport was found to have a major influence on the reaction rate (Table 3.2).

Long lag phases before sulfate reduction coupled to methane oxidation would start

A long initial phase on the scale of months to years without any observable reactions is supported by the reviewed field experience. Moreover, even in natural aquifers the strict mutual exclusion between sulfate and methane mostly takes place at higher, at least 300, but up to a few 1000 mg/l sulfate concentrations (McIntosh et al, 2014), suggesting that the leaked methane may persist in freshwater aquifers with typically lower sulfate content. The slow response of a microbial community to develop after a methane intrusion justifies scenarios where methane can be considered as conservative gas in numerical reactive transport simulations. For leakage monitoring purposes, methane itself may be the main substance to focus the efforts on, instead of potential reaction products.

3.2. Experiments showed no reactions coupled to methane leaked into shallow aquifers

This chapter is based on a paper published by Berta M, Becker A, Dethlefsen F, Ebert M, Koch S, Dahmke A (2015) in First Break 33, 93-95.

3.2.1. Abstract

As discussed in previous chapters, geological energy storage has the potential to balance fluctuations in the energy network by using the subsurface for gas storage. A major public concern about underground gas facilities culminates around effects of potential accidental gas leakages into shallow aquifers, especially if these aquifers are used for drinking water production. The biogeochemical reactions potentially caused by gas leakages are revealed by several literature sources. However, for assessing the impact such leakages can have on the protected groundwater experimental efforts can mean a deciding contribution.

Based on earlier works on marine and freshwater environments, dissolved methane may cause the reduction of ferric iron, nitrate, and sulfate while being oxidized by microorganisms. Flow-through column experiments were used in the presented study to observe these reactions in different sediments percolated by different, methane-enriched, groundwaters. This experimental setup created an environment similar to the conditions expected at a methane leakage into a shallow freshwater aquifer.

These one-year-long experiments showed no significant oxidation of methane by any of the electron acceptors available, meaning that the microbial methane oxidation is inhibited at the studied conditions. These findings regarding the impact of potential methane leakages underline the necessity to evaluate the impact of such gas leakages separately and in detail. Thus, a basis for parameterizing numerical scenario analyses simulating the potential impact of methane leakages is provided.

3.2.2. Introduction

The need for subsurface energy storage to balance the fluctuations in power production using renewable sources already exists, and based on the current deployment rate of wind and solar power stations, scenarios with a renewable share of up to 80% of the German energy production were developed for the next decades (UBA, 2010). Due to the known, fluctuating character of renewable energy production, storage of gases including compressed air, methane, and hydrogen may play a deciding role in the geological energy storage mix (Bauer et al., 2013). As discussed in previous chapters, in case of a methane storage concept, the gas is generated from surplus renewable electricity via the Sabatier process, stored underground in deep porous reservoirs or salt caverns, and retrieved and used in the existing energy system when needed. Any geological gas storage operation may result in leakages of the stored gas into shallow geological compartments due to various reasons like well failure (Evans, 2009). Experimental evaluation of hydrogeochemical reactions following such a potential accidental methane leakage into shallow aquifers are of particular importance for ensuring a good groundwater quality, especially if the overlying shallow aquifers are used for drinking water production.

Changes in groundwater chemistry following an intrusion of methane are probably controlled by the metabolic response of the subsurface microbial community. In aquifers not affected by leakage incidents, methane practically does not appear together with potential electron acceptors (e. g. McIntosh et al., 2014), therefore redox reactions consuming biogenic or thermogenic methane intruding such aquifers can be expected. In these processes, oxygen (Smith et al., 1991), nitrate

(Raghoebarsing et al., 2006; Eisentraeger et al., 2001; Ettwig et al., 2010), ferric iron (Beal et al., 2009), and sulfate (Kelly et al., 1985; van Stempvoort et al., 2005) can serve as electron acceptors while methane is oxidized to CO_2. Amongst these processes, sulfate reduction is the most influential on groundwater quality due comparatively high concentrations of dissolved sulfate (Dethlefsen et al., 2016 a and b) and the potential of sulfide production. However, the process is mostly known from marine environments in so-called "sulfate-methane transition zones (SMTZ)", summarized for instance by Knittel and Boetius (1999). In such environments, microbial communities could establish on long, perhaps geological time scales. On the other hand, some groundwater environments, such as aquifers overlying hydrocarbon reservoirs that are being exploited for a comparatively short time span, suggest that a response may not take place if the encounter of methane and an electron acceptor is rather sudden (e. g. Osborn et al., 2011, Ziemkiewicz and He, 2015).
As the reactions potentially triggered by methane have not been studied in laboratory experiments representing groundwater conditions so far, the goal of the work presented in this chapter was to experimentally characterize geochemical effects of methane intrusion on shallow aquifers; similarly to studies regarding the hydrogeochemical effects of compressed air and hydrogen, both being parts of this Thesis.

3.2.3. Materials and methods

Flow-through column experiments were carried out to represent the hydrogeological conditions of a shallow aquifer, using four 30x6 cm glass columns that were filled with sediment and percolated with groundwater (Figure 3.2). Each column was equipped with five sampling ports along the flow path. The groundwater was equilibrated with methane at 1 bar partial pressure, resulting in methane concentrations of up to 1.2 mmol/L at 20±2°C, before this water was pumped into the columns. The residence times, determined using a LiBr tracer test, were between 13 and 16 hours and considered when calculating reaction rates.
These column experiments were run to investigate geochemical effects of methane-saturated water (Table 3.3.) intruding to a shallow aquifer.

Table 3.3. Chemical composition of the waters used for the experiments (LW: Tap water, NMS: Groundwater from a well near Neumünster, GPS-Coordinates: N 54,0773; E 10,0750).

Parameter	LW	NMS
Na^+ [mmol/l]	0.62	0.7
K^+ [mmol/l]	0.09	0.03
Mg^{2+} [mmol/l]	0.36	0.23
Ca^{2+} [mmol/l]	0.42	3.43
Fe^{tot} [mmol/l]	< 0.00035	< 0.00035
Mn^{tot} [mmol/l]	< 0.0002	0.0036

Parameter	LW	NMS
Cl^- [mmol/l]	0.82	28
NO_3^- [mmol/l]	0.016	< 0.003
SO_4^{2-} [mmol/l]	0.5	0.9
O_2 [mmol/l]	0.17	0.084
E_H [mV]	478	308
pH [-]	7.47	7.5
Conductivity [µS/cm]	683	715

Sediments for two columns originated from a core drilled into a shallow (4-12 m below ground level, 10°C) Pleistocene aquifer near Neumünster (Germany) (NMS1 and NMS2 columns). For an additional column, marine sediment material was taken from a SMTZ site in the Kieler Förde near Tirpitzhafen using the *RV Alkor*. This marine sediment had a share of one third, while two thirds of commercial quartz sand (0.3-0.8 mm) was added and the resulting mixture was homogenized under Ar atmosphere (MAR column). Finally, the fourth column was filled with quartz sand containing 0.5 wt% goethite (Bayferrox 920) (GOE column).

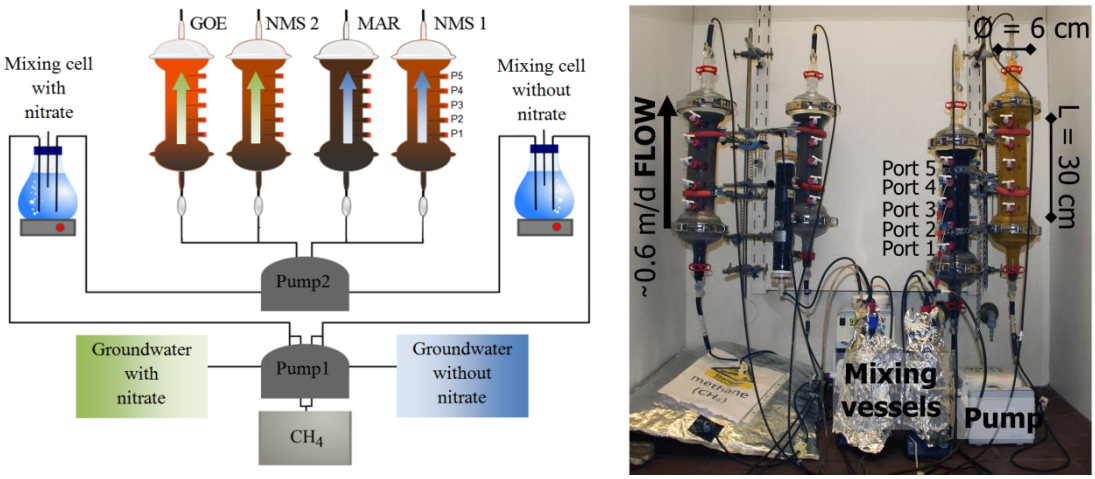

Figure 3.2: Sketch (left) and photo (right) showing the experimental setup. CH_4 gas was used to bubble the groundwater in the mixing cells. From there, the CH_4-saturated water is pumped into the columns. Samples were taken from the five ports along the flow path and from the inflows.

For the first 11 weeks, a near-surface aquifer environment was simulated in these four columns by percolation with tap water from a Pleistocene aquifer at Kiel University. Dissolved oxygen (up to 100 µmol/L), nitrate (20 µmol/L), and sulfate (500 µmol/L) were present in the columns' inflow. After this first aerobic period, sulfate-containing (1000 µmol/L), nitrate- and oxygen-free (<8µmol/L) groundwater from the same NMS aquifer where the sediment was taken from was used to allow the development of a more anoxic environment in the columns NMS1 and MAR. In a further step after approximately 400 exchanged pore volumes, a pre-column filled with Fe^0 grains was added to reduce the redox potential of the inflowing waters of the NMS1 and MAR columns. Moreover, for the two columns GOE and NMS2, up to 70 µmol/L of nitrate was added to the inflowing water.

3.2.4. Results

The column experiments showed no reproducible decrease in methane concentrations during percolation of the sediments (Figure 3.3) in the whole, one-year runtime. On the other hand, three of the four columns (MAR, NMS2, GOE) showed a slight consumption of electron acceptors. From the beginning, denitrification (0.6 and 1 µmol/L/h) was determined in the GOE and NMS2 columns, respectively (Figure 3.3). Nitrate reduction rates remained nearly constant over the experimental runtime measured over the flow path within the columns, regardless the variation of the nitrate concentration between 13 and 72 µmol/L. However, the nitrate reduction rate was higher and increasing from 2 to 12 µmol/L/h and from 4 to 20 µmol/L/h, respectively, between the inflow and first sampling port of both columns percolated with nitrate containing water (Figure 3.3). Ammonium concentrations showed no change versus the flow path based on a sampling event when it was also measured; and nitrite was detected in none of the samples.

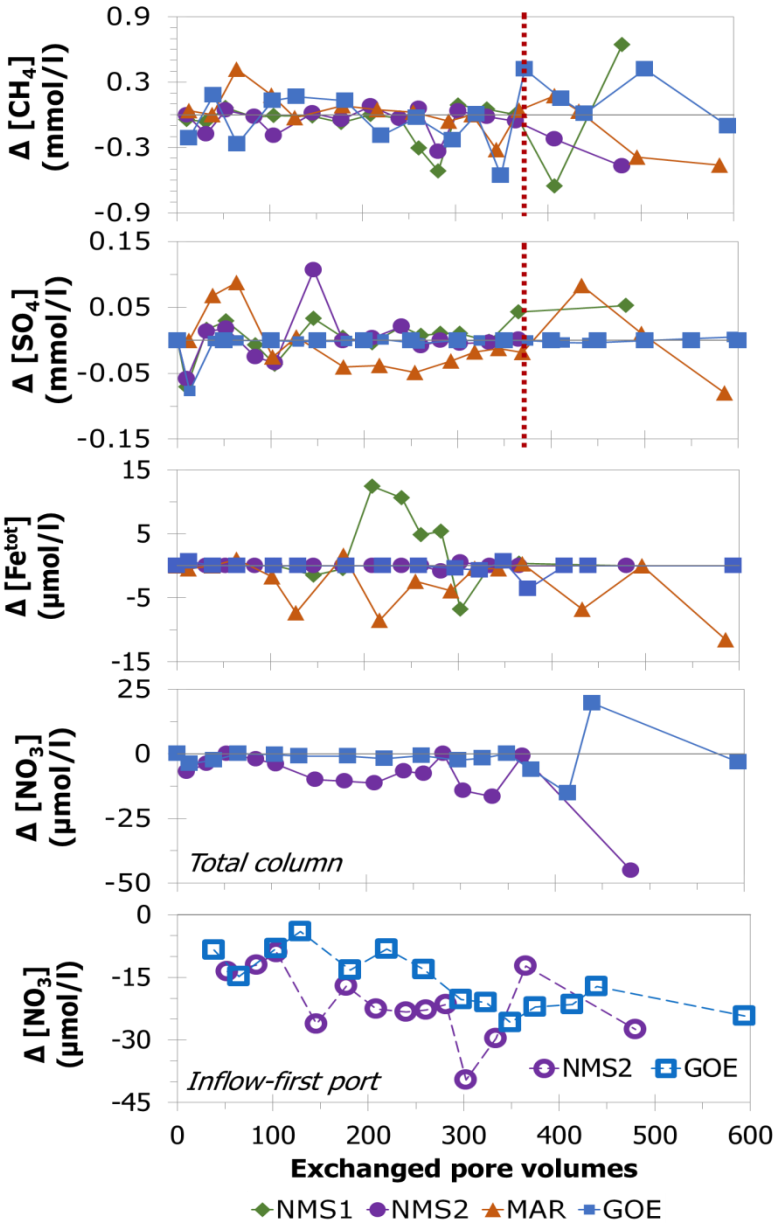

Figure 3.3: The difference in concentration of dissolved methane, sulfate, total iron, and nitrate in the groundwater flowing through the experimental columns. One exchanged pore volume is completed in approx. 12 h. Nitrate reduction rates increase between the inflow and the first sampling port (right), but not within the columns (between first and fifth port). The dashed red lines show the time when the Fe^0 pre-column was attached.

The MAR column showed sulfate reduction (up to 3.8 µmol/L/h) after switching to the anaerobic groundwater. Smell of sulfide production in the MAR column was identified along with decreases of up to 150 mV in redox potential and 0.15 in pH. However, sulfide concentration stayed below the level of determination of 5 µmol/L.

Concentration of dissolved Fe^{2+} varied along the flow path increasing by up to 12.4 µmol/L in the NMS1 column and decreasing by up to 8.5 µmol/L in the MAR column, which were both percolated by nitrate-free groundwater. Mn^{2+} concentrations were increased in all columns by up to 1-1.5 µmol/L. Within the measured values no further changes were observed in electric conductivity, pH, and redox potential; total dissolved organic carbon; dissolved ions (Na^+, K^+, Ca^{2+}, Mg^{2+} and Cl^-); furthermore no bromide, acetate, nitrite, or thiosulfate was detected in any of the samples. Thus no methane oxidation by any electron acceptor could be detected in any of the columns.

3.2.5. Discussion

Although the experimental conditions were considered suitable for the expected methane oxidation, the series of results showed that significant aerobic or anaerobic methane oxidation did not take place in the represented hydrogeological conditions. Other works showed that the experimental setup is adequate for studying methanogenic (Jesußek et al., 2012) redox processes as well as reductive processes caused by dissolved hydrogen, as presented in the next chapter of this Thesis. Anaerobic methane oxidation rates stoichiometrically corresponding to the observed sulfate reduction (up to 48 μmol/L during one pore volume exchange) and denitrification (up to 39 μmol/L) rates would balance to 48 and 24 μmol/L methane consumption, respectively. These changes supporting this calculated mass and electron balance were not identified in the experimental results. The reduction of sulfate and nitrate established in the experimental columns could also have been linked to oxidation of organic material that was potentially released from the sediments or possibly suspended in the inflow water, corresponding to up to 91 and 48 μmol/L C_{org}, respectively. Decreasing redox potential also could have been an indicator for anaerobic methane oxidation coupled to sulfate reduction as mentioned for instance by van Stempvoort et al. (2005), but the measured data suggests that the redox potential in the columns did not decrease below the typical level for nitrate reducing conditions (350 ±60 mV for NMS1-2 and GOE). Therefore, it is exemplified in the presented study that in a year only a slow and uncertain response, if any at all, can be expected following a methane introduction into an aquifer in conditions represented in these experiments.

This long lag phase before any establishment of a redox reaction is potentially similar to sulfate reduction slowly establishing in column experiments on reactive Fe^0 barriers (Ebert, 2004). This indicates that methane oxidation needs the presence of a pre-existing community adapted for the aquifer conditions in order to show a consumption of methane in a time period of up to months, as it was also recognized in (Smith et al., 1991).

Reasons for this slow response in sulfate reduction may include i) the high doubling time of up to 7 months of the microbial consortia (Knittel and Boetius, 2009), which is mainly caused by; ii) the low (only ca. 1%) rate of assimilation of the carbon consumed by the microorganisms carrying out anaerobic methane oxidations (Nauhaus et al., 2007); and iii) the low energy yield of the reaction barely enough for synthetizing a single ATP, the elementary energy transfer substance in cells (Wang et al., 2010). Regarding field experience on sulfate reduction coupled to methane oxidation, the reaction was not identified in shallow aquifers with thermogenic methane near unconventional hydrocarbon exploitation (Marcellus Shale, Pennsylvania, USA; Osborn et al., 2011). In a Canadian aquifer, more than seven years after a methane leakage from a gas well still high (up to 1.25 μmol/L) methane concentrations were observed, and seven more years were necessary to observe a decrease (up to 0.18 μmol/L) coupled to sulfate reduction (van Stempvoort, 2005). However, a response within less than a month followed a gas well blowout in Ohio, but efforts to experimentally reproduce the reactions were only partly successful (Kelly et al., 1985).

In the initial, aerobic period methane oxidation was also not observed, which is consistent with the conclusions of Smith et al. (1991), suggesting that such a response is determined by the resident microbial population. This proposes that even aerobic methane oxidation also needs the presence of a pre-existing community in an aquifer to show a prompt consumption of methane. Nitrate reduction without apparent methane oxidation took place in both experimental columns percolated with groundwater enriched with nitrate. This reduction apparently resulted in the production of N_2, as no ammonium or stop at nitrite were detected. This is in agreement with the results of Raghoebarsing et al. (2006).

3.2.6. Summary and conclusions

After a potential leakage of geologically stored methane into a shallow aquifer, no rapid oxidation of methane can be expected. A most probable reason is the slow metabolic response of the shallow subsurface biogeochemical system for a sudden methane intrusion, inhibiting methane oxidation within at least one year under the conditions described in the presented study. Therefore, the presented chapters suggest that the response of the subsurface depends most probably on the initial density and the growing potential of the microbial community oxidizing methane and reducing the electron acceptors. This is in contrast to the leakage effects of hydrogen and compressed air stored in the subsurface.

The quasi inert nature of methane that was identified in this chapter results means that i) site vulnerability assessments should include experimental and also field studies. For the later, a push-pull redox tracer test is suggested using a site where anaerobic methane oxidation is already established. ii) Modelling efforts may consider methane as a conservative gas as a first approach. iii) Leakage monitoring efforts must focus on methane itself, instead of possible reaction products.

4. Geochemical effects of millimolar hydrogen concentrations in groundwater

- an experimental study in the context of subsurface hydrogen storage -

This chapter is based on a paper submitted by Berta M, Dethlefsen F, Ebert M, Berger S, Dahmke A (2017) to Environmental Science and Technology.

4.1. Abstract

Hydrogen storage in geological formations is one of the most promising technologies for balancing major fluctuations between energy supply from renewable energy plants and energy demand of customers. If hydrogen is stored in a porous medium or if it leaks into a shallow aquifer, redox reactions can oxidize hydrogen and reduce electron acceptors such as nitrate, Fe^{III} and Mn^{IV} (hydro)oxides, sulfate, and carbonate. These reactions are of key significance, because they can cause unintentional losses in hydrogen stored in porous media and they also can cause unwanted changes in the composition of protected potable groundwater. To represent an aquifer environment enclosing a hydrogen plume, laboratory experiments using sediment-filled columns were constructed and percolated by groundwater in equilibrium with high (2-15 bars) hydrogen partial pressures. Here we show that hydrogen is consumed rapidly in these experiments via sulfate reduction (18±5 µM h^{-1}) and acetate production (0.030 ± 0.006 h^{-1}), while no methanogenesis took place. The observed reaction rates were independent from the partial pressure of hydrogen and hydrogen consumption only stopped in supplemental microcosm experiments where salinity was increased above 35 g l^{-1}. The outcomes presented here are implemented for planning the sustainable use of the subsurface space.

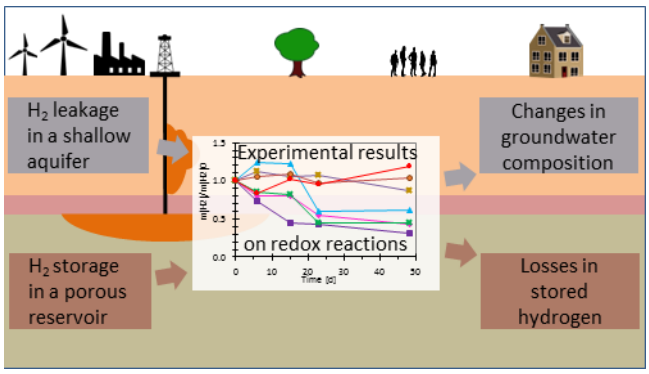

Graphical Abstract: A general investigation concept sketch for this chapter.

4.2. Introduction

The energy production by wind turbines and solar panels fluctuates due to variable wind velocity and solar radiation, while the energy demand of consumers also varies creating a significant challenge for the stability of future energy supplies based mainly on renewable sources. One concept to address this issue is the "power to gas" approach, where the generation of a gas with high energy content uses the excess electrical energy at times where the public energy demand is smaller than the produced energy. Large scale gas storage is potentially necessary in this concept, allowing the gas to be reused when the demand for energy exceeds the supply. The overall difference between the amount of energy supplied by renewable energy sources and the amount of energy demanded usually varies in time, but this gap may reach 10 GWh - 10 TWh, calculated for days to months on a regional scale power network (Sterner and Stadler, 2014). Electrochemical generation, storage, and consumption of hydrogen has the potential to balance such fluctuating gaps (Pfeiffer et al., 2016; Sterner and Stadler, 2014). The volume of hydrogen corresponding to the amount of energy to be balanced in an energy network ranges between tens to hundreds of millions normal cubic meters (Pfeiffer et al., 2016). The subsurface offers a comparatively cost-efficient and safe option for storing such large quantities of gaseous hydrogen (Bauer et al., 2013; Bauer et al., 2015; Dethlefsen et al., 2016; Evans, 2008; Gao et al., 2014; Kabuth et al., 2016, submitted; Pfeiffer et al., 2016; Taylor et al., 1986). Moreover, sustainable renewable-based energy systems will likely require a series of subsurface energy storage technologies, i.e. chemical (hydrogen, synthetic methane), mechanical (compressed air), or heat energy storage, facing the considerable amount of energy that needs to be stored and because of lacking other available storage technologies in the short or medium term fulfilling the requirements (Sterner and Stadler, 2014).

Power-to-gas energy storage including geological hydrogen storage is expected to play an increasing and deciding role in future energy networks, considering that estimations for instance on future German energy supplies project (UBA, 2010) up to 100% renewable power generation by 2050. Overview studies on technical aspects of subsurface hydrogen storage were published in the last few years (Audigane et al., 2015; Bünger et al., 2016; Gniese et al., 2014; Panfilov, 2016) as a part of an increasing research interest, but field or experimental studies specifying potential environmental impacts or operational issues linked to storing large amounts of pure hydrogen at elevated pressures are missing so far. However, studies on hydrogen-containing gas mixtures stored in porous town gas reservoirs hint to the potential of hydrogenotrophic redox reactions consuming hydrogen at such conditions (Buzek et al., 1994; Morozova et al., 2011; Panfilov, 2010, 2016; Reitenbach et al., 2015; Smigáň et al., 1990). These reactions may cause losses from the stored gas and they may also change the groundwater composition in the surroundings of a gas reservoir. Furthermore, accidental leaking of hydrogen into shallow aquifers (Evans, 2009) may result in conditions where an enlarged hydrogen partial pressure (i.e. equal to the hydrostatic pressure in case of a pure hydrogen gas phase) will cause a high dissolved hydrogen concentration in the shallow groundwater, probably initiating typical redox reactions associated with hydrogen oxidation.

Hydrogen-driven redox reactions, mostly microbiologically catalyzed (Truche et al., 2013), are well known from aquatic geosystems, where hydrogen is the electron donor and O_2, NO_3^-, Fe^{III} and Mn^{IV}(hydr)oxides, SO_4^{2-}, or dissolved CO_2 are usually the terminal electron acceptors (Table 3.1). These redox reactions may produce NO_2^-, N_2O, N_2, NH_4^+, Mn^{II}, Fe^{II}, H_2S, CH_3COOH, or CH_4, which might be released into the pore water or precipitated as various mineral phases. Reaction products such as NO_2^-, H_2S or CH_4 may have a negative effect on the composition of the groundwater in terms of its usability for other applications, e. g. drinking water production (Trinkwasserverordnung, 2001). Moreover, an induced excessive production of these components probably creates an issue because groundwater itself is usually a protected good. In pristine aquifers, fermentative degradation of peptides, saccharides, and further organic substances produces hydrogen (Hoehler et al., 1998), while other microorganisms consume it, usually resulting in nanomolar concentrations of dissolved hydrogen (Chapelle et al., 1996; Chapelle and Lovley, 1992; Chapelle et al., 2002; Conrad, 1999; Conrad et al., 1987; Cordruwisch et al., 1988; Heimann et al.,

2007; Hoehler et al., 1994; Hoehler et al., 1998; Jakobsen et al., 1998; Jørgensen, 2000; Kotelnikova, 2002; Lin et al., 2005; Lovley et al., 1994; Smith et al., 2005; Telling et al., 2015; Zinder, 1993). A competition for hydrogen may then result in the development of a typical redox sequence (i.e. decreasing redox potential with increasing time or flow path length) because the electron accepting processes coupled to hydrogen oxidation with the higher energy yield (e. g. sulfate reduction) outcompete the others (e. g. acetogenesis) by keeping the hydrogen concentrations below a threshold concentration required for that process (Table 3.1). Furthermore, the kinetics of the redox reactions usually depends on the concentration of dissolved hydrogen in those hydrogen-limited environments.

In-situ remediation of contaminated aquifers may lead to elevated dissolved hydrogen concentration, e. g. during zero valent iron (ZVI) applications (Ebert, 2004; Reardon, 2005; Schütz et al., 2013), by the application of hydrogen releasing compounds (Sandefur and Koenigsberg, 1999), in hydrogenotrophic denitrification systems (Ergas and Reuss, 2001; Ergas et al., 1999; Liessens et al., 1992; Smith et al., 1994; Xia et al., 2010), or during a sulfidogenic treatment of wastewater containing dissolved metal ions (Nevatalo et al., 2010; van Houten et al., 2009). Increased dissolved hydrogen concentration is thereby either an aim of the technology (e. g. denitrification or sulfidogenic treatment) or a side-effect (e. g. ZVI application for reductive dehalogenation). However, those systems usually show the establishment of redox sequences known from pristine aquifers, and redox kinetics also depend on the hydrogen concentration (Lovley and Goodwin, 1988). Furthermore, the hydrogen concentration is mostly limited to a few hundred micromoles per liter.

In the context of the storage of pure hydrogen gas in the subsurface, dissolution of hydrogen may result in concentrations of up to several millimoles in the groundwater due to the roughly linear correlation between increasing depth and increasing pressure as well as between increasing pressure and increasing gas solubility. Also an unintended leakage of pure hydrogen gas into a shallow or medium deep aquifer (up to 140 m depth) will result in a much higher dissolved hydrogen concentration than usually present in aquifers. This will probably result in a surplus of hydrogen and the microbial community, which is usually striving for hydrogen, may start its consumption rapidly through a series of redox reactions (Lovley, 1985; Lovley and Goodwin, 1988) or through simultaneous redox processes (Mascus, 2015) without the establishment of typical redox sequences. On the other hand, the groundwater in the vicinity of a gas storage reservoir may have an elevated salt content (Hassannayebi and Azizmohammadi, 2015) and a salt water intrusion might accompany a gas leakage into a shallow aquifer potentially inhibiting the microbiologically catalyzed redox reactions due to a limited halotolerance of the present microorganisms (Dincer and Kargi, 2001; Omar et al., 1994; Oren, 2001, 2008; Uygur and Kargi, 2004; Wichern et al., 2006; Windey et al., 2005; Yan et al., 2015).

In order to estimate the potential effects the subsurface storage of hydrogen can have on groundwater, including the effects following an unintended leakage into shallow aquifers, an improved understanding of hydrogenotrophic redox reactions at high dissolved hydrogen concentration is required, but investigations on those systems are missing so far (Table 4.1). The knowledge of the establishment of redox sequences, reaction kinetics, or reaction products is necessary for any risk assessment, spatial planning attempts, or modeling efforts on a regional scale (Bauer et al., 2015; Kabuth et al., 2016, submitted). Furthermore, monitoring strategies for a gas storage site require the knowledge about the fate of the stored gas in shallow aquifers and also an estimation of the impact the stored gas may have through gaseous redox reaction products (e. g. H_2S or CH_4).

Table 4.1. Hydrogen oxidizing reactions with associated Gibbs free energy yields under standard conditions, and the concentrations of hydrogen typical for environments with characteristic metabolic processes.

Reactions		**ΔG^0 [kJ·mol$(H_2)^{-1}$]**	**H_2 [nmol·l^{-1}]**	**References**
Aerobic hydrogen oxidation	$2\ H_2+O_2 \rightarrow 2\ H_2O$	-237	n.d.	(Thauer et al., 1977)
Hydrogen oxidation coupled to denitrification producing N_2	$5\ H_2+2\ H^++2\ NO_3^- \rightarrow N_2+6\ H_2O$	-224	0.03	(Hoehler et al., 1998; Lovley and Goodwin, 1988; Thauer et al., 1977)
Hydrogen oxidation coupled to nitrate reduction producing NH_3	$4\ H_2+2\ H^++NO_3^- \rightarrow NH_4^++3\ H_2O$	-150	<0.05	(Cordruwisch et al., 1988; Thauer et al., 1977)
Hydrogen oxidation coupled to Mn^{IV} reduction	$H_2+MnO_2 \rightarrow Mn(OH)_2$	-163	<0.05	(Conrad and Wetter, 1990; Hoehler et al., 1998; Lovley and Goodwin, 1988)
Hydrogen oxidation coupled to Fe^{III} reduction	$H_2+2\ Fe(OH)_3 \rightarrow 2\ Fe(OH)_2+2\ H_2O$	-114	0.2	(Hoehler et al., 1998; Lovley and Goodwin, 1988; Thauer et al., 1977)
Hydrogenotrophic sulfate reduction	$4\ H_2+H^++SO_4^{2-} \rightarrow HS^-+4\ H_2O$	-57	1-2	(Cordruwisch et al., 1988; Hoehler et al., 1998; Lovley and Goodwin, 1988; Thauer et al., 1977)
Hydrogenotrophic methanogenesis	$4\ H_2+H^++HCO_3^- \rightarrow CH_4+3\ H_2O$	-34	5-10	(Cordruwisch et al., 1988; Hoehler et al., 1998; Lovley and Goodwin, 1988; Stevens and Mckinley, 1995; Thauer et al., 1977)
Hydrogenotrophic acetogenesis	$4\ H_2+H^++2\ HCO_3^- \rightarrow CH_3COO^-+4\ H_2O$	-26	100<	(Cordruwisch et al., 1988; Hoehler et al., 1998; Stevens and Mckinley, 1995)

The study presented here shows results of a high pressure column experiment using natural aquifer materials and groundwater equilibrated with hydrogen partial pressures of 2-15 bars, representing a scenario of hydrogen gas leakage into a shallow or medium deep aquifer. The results enabled the development of a reaction scheme describing simultaneous redox reactions at elevated dissolved hydrogen concentrations at flow through conditions, including reaction kinetics and rate coefficients. Furthermore, results of a simple testing routine for estimating the halotolerance of a microbial community are shown. The outcome of the study is a first step in an improvement of the understanding of hydrogen oxidizing redox reactions in the context of hydrogen gas storage and will be integrated into a Guideline for Subsurface Energy Storage facilitating future improvements in the planning of subsurface use, which is part of the ANGUS+ research project (Bauer et al., 2013; Bauer et al., 2015; Kabuth et al., 2016, submitted).

4.3. Materials and Methods

4.3.1. Experimental set-up

A sediment from a pristine shallow Quaternary aquifer (WGS84: N54.0773, E10.0750, Table 4.2) obtained from drilling cores between 4 and 12 mbgs was used in the experiments. The sediment was homogenized and stored wet in Ar-atmosphere in order to preserve the redox conditions as well as possible. A pre-experiment using the sediment (i.e. flow through batch reactor (Mascus, 2015) at normal total pressure and in equilibrium with a partial pressure of hydrogen, $p(H_2)$, of 1 bar) conditioned the material before the high-pressure column experiment started. The batch experiments for halotolerance testing contained unconditioned sediment. Groundwater from the same well the sediment cores originated from was sampled periodically (Table 4.3) and stored in HDPE canisters before utilizing in the column experiment, or in gas tight Al-impregnated bags (Tesseraux) for the batch experiments. Vacuum filtration (cellulose nitrate membrane 0.45 µm, Sartorius) and dilution using deionized water (1 : 2.5) of the groundwater prevented the formation of precipitates potentially clogging the pumps and capillary tubes supplying the column experiment. Equilibrating this initial solution of diluted groundwater to various $p(H_2)$ in a flow through mixing cell directly upstream the column generated in-line the inflow solution for the high-pressure column experiment (Table 4.3).

Table 4.2. Chemical composition of the middle grained sandy sediment (concentrations in $g \cdot kg^{-1}$)

Na (1)	**K** (1)	**Ca** (1)	**Mg** (1)	**Mn_{tot}** (1)	**Fe_{tot}** (1)	**Fe^{II}** (2)	**Fe^{III}** (2)	**S_{red}** (3)	**C_{org}** (4)	**C_{inorg}** (4)
3.68	8.8	23.2	0.797	0.121	3.91	< 0.02	0.39	0.49	0.27	4.9

(1) after total digestion of sediment sample in hydrochloric acid, nitric acid, hydrofluoric acid, and perchloric acid
(2) after 21 days of extraction in 5 M HCl according to Heron et al. (1994)
(3) analyzed as Chromium Reducible Sulfur (CRS) similar to Canfield et al. (1986)
(4) analyzed with Ströhlein Coulomat Type 702

The basic set-up of the high-pressure column experiment itself is described in detail elsewhere (Berger, 2015; Berta et al., 2016; Haase et al., 2014). In short, the high pressure column used (Ø=4 cm, L=50 cm, electrochemically passivated titanium Grade 2, with 4 ports along the flow path, from Werner Kluge Engineering GmbH, Kiel, Germany) was equipped with stainless steel and hastelloy fittings and tubes (Swagelok, OH, USA) allowing an investigation in a gas tight system at total pressures of up to 100 bars. One HPLC pump (Knauer GmbH, Berlin, Germany) pumped the initial solution into a mixing cell where hydrogen (grade 5.0) was added at a constant pressure. A second HPLC pump pumped the generated inflow solution through the column from the bottom to the top. A variable backpressure valve at the end of the flow line ensured a total pressure in the system of up to 10 bars higher than the applied gas pressures in order to prevent degassing in the experimental apparatus.

In the experiments presented here, hydrogen gas at $p(H_2)$ between 2 and 15 bars was applied during different experimental stages. A pumping rate of 0.5 ml min^{-1} created a flow speed of approximately 2 m d^{-1}, assuming an effective porosity of 0.3 ± 5 % based on equivalent experiments (Berta et al., 2016; Haase et al., 2014), which results in a total residence time of approximately 6.3 hours. The total run time of the column experiment was 242 days. A technical issue with the HPLC pumps interrupted the flow through the column at day 105 for 40 days, but in this phase the total pressure in the column experiment was kept constant and after that discontinuity the groundwater percolation in the experiment was resumed.

Table 4.3. Composition of the groundwater and the inflow solution of the column experiment (mean and standard deviation from n analyses, n.m.: not measured)

Parameter	Unit	Groundwater			Inflow solution		
		mean	stdv	n	mean	stdv	n
Elec. cond.	[µS cm^{-1}]	721	± 9	16	630	± 38	7
pH	[-]	7.2	± 0.2	16	8.5	± 0.3	8
O_2	[mg l^{-1}]	0.011	± 0.007	12	n.m.		
EH_{SHE}	[mV]	-122	± 59	16	n.m.		
T	[°C]	9.8	± 0.2	16	20	± 2	
Na^+	[mmol l^{-1}]	0.72	± 0.03	13	0.33	± 0.08	21
K^+	[mmol l^{-1}]	0.04	± 0.001	13	0.02	± 0.01	21
Ca^{2+}	[mmol l^{-1}]	3.49	± 0.06	13	1.2	± 0.5	21
Mg^{2+}	[mmol l^{-1}]	0.234	± 0.005	13	0.11	± 0.03	21
Si_{tot}	[mmol l^{-1}]	0.468	± 0.008	13	0.21	± 0.03	21
Fe_{tot}	[µmol l^{-1}]	32	± 7	13	0.3	± 1.2	20
Mn_{tot}	[µmol l^{-1}]	3.77	± 0.06	13	0.5	± 1.0	20
Cl^-	[mmol l^{-1}]	0.81	± 0.03	15	0.315	± 0.007	22
SO_4^{2-}	[mmol l^{-1}]	0.95	± 0.04	15	0.33	± 0.04	22
NO_3^-	[µmol l^{-1}]	6	± 37	14	0.9	± 2.0	22
PO_4^{3-}	[µmol l^{-1}]	< 1.05		14	< 1.05		22
F^-	[µmol l^{-1}]	< 5.3		14	< 5.3		22
Br^-	[µmol l^{-1}]	< 1.25		14	< 1.25		22
CH_3COO^-	[µmol l^{-1}]	< 3.33		14	30	± 38	25
CH_4	[µmol l^{-1}]	3	± 1	12	< 1		20
TIC	[mmol l-1]	5.4	± 0.2	15	1.5	± 0.2	22
TOC (1)	[mmol l^{-1}]	n.m.			0.26	± 0.09	22
NPOC (2)	[mmol l^{-1}]	0.4	± 0.1	14	n.m.		

(1) TOC calculated from TC and TIC measurements

(2) NPOC: non-purgeable organic carbon, measurement of TC after acidifying (HCl) and stripping (O_2) the sample for 5 min

A pressure-resistant sampling cell (Berger, 2015; Berta et al., 2016; Haase et al., 2014) was used to sample the in- and outflowing solutions as well as solutions from the sampling ports along the flow path without discharging pressure in the sediment column. After a controlled pressure release in the sampling cell the water was sampled, treated, and analyzed for cation, anion, and total as well as inorganic carbon concentrations. Before samples for hydrogen analyses were extracted from the sampling cell, they were diluted under in situ pressure with the hydrogen free initial solution in-line within the sampling cell in order to minimize a possible loss of the highly fugitive gas. Pressure resistant sensors (Corr Instruments, San Antonio, TX, USA) connected to the sampling cell enabled the measurement of pH and electrical conductivity during each sampling event at in-situ pressure conditions.

For the halotolerance test 115 ml glass serum vials were used as microcosms and filled with 50 g untreated sediment and 75 g groundwater. An enrichment of the groundwater with $CaSO_4$ and NaCl salt adjusted a TDS level between 0.35 and 350 g l^{-1} (Table 4.4). A thorough sparging with pure hydrogen gas for several minutes ensured an initial dissolved hydrogen concentration nearly in equilibrium with $p(H_2)$ = 1 bar. Furthermore, by sealing the vials using aluminum crimps with a Teflon plated butyl rubber septum as fast as possible after the sparging a nearly pure hydrogen atmosphere in the headspace was prepared. The microcosms were stored still and upside down in dark boxes at room temperature (20 ± 2°C) and samples for hydrogen analysis were taken after distinct time intervals from the free water phase after shaking and opening a serum vial. Three separate batches were prepared for each sampling event, which took place after 0, 6, 15, 23, and 48 days.

Table 4.4: TDS-Level and added salt concentration (in mg l^{-1}) in the halotolerance testing schedule

TDS Level	$CaSO_4$	NaCl
350	0	0
1 100	375	375
3 500	1 575	1 575
11 000	2 000	8 650
35 000	2 000	32 650
110 000	2 000	107 650
[(1)]350 000	2 000	347 650

[(1)] A minor fraction of the salt did not dissolve

4.3.2. Sample preparation and analytics

Hydrogen concentrations were measured by gas chromatography (7890B GC, 7697A Headspace Sampler from Agilent Technologies) using up to 3 parallel and unfiltered samples, typically within an hour after sampling. All other samples were filtered (0.2 µm, regenerated cellulose, Sartorius) and filled into vials for cation, anion (HDPE), and inorganic and organic carbon (glass, sealed with a septum crimp) measurements. Cation samples were acidified (cc. HNO_3 s.p.) and all samples were stored at 4°C in the dark until the measurement. An ICP-AES (Vista AX, Varian) analyzed the cations, an ion chromatograph (Metrohm 881) the anion concentrations, and a TIC-TOC analyzer (multi N/C 2000 from Analytik Jena) measured the total inorganic carbon (TIC), total carbon (TC) as well as the non-purgeable organic carbon (NPOC) concentrations. Ammonium concentrations were measured photometrically, following DIN 38406E5.

4.4. Results and Discussion

The column experiment was started using an inflow solution in equilibrium with a $p(H_2)$ of 5 bars and after 56 days the hydrogen partial pressure was increased to 15 bars for 18 days. Then, after the distribution of geochemical parameters in the column had reached steady-state, the partial pressure of hydrogen was decreased back to 5 bars for 17 days followed by experimental phases with even lower $p(H_2)$ of 2 and 3 bars for 16 and 42 days, respectively. Finally, a third 5-bars-period of 22 days completed the experiment. The results indicate that the flow interruption of 40 days between the 2-bars- and 3-bars-period did not affect the system significantly and, therefore, the time interval of the flow interruption was neglected and the results are shown on a continuous time scale (Figure 4.1). The results show a continuous change between in- and outflow in dissolved concentrations of sulfate, acetate, total inorganic carbon species (TIC), calcium, and hydrogen, starting without any detectable lag time at the beginning of the experiment. Figure 4.1 indicates decreasing concentrations of sulfate (by on average 160±100 μM; n = 77), calcium (500±400 μM, n = 79), TIC (800±400 μM, n = 73), and dissolved hydrogen (1700±700 μM, n = 47), while the acetate concentration increased (180±50 μM, n = 61).

These changes in the groundwater composition are in a good agreement with the assumption of an established hydrogenotrophic microbial community. This community apparently oxidized hydrogen mainly by reducing sulfate and reducing carbon dioxide through acetogenesis. Moreover, the decrease in calcium concentrations linked to increasing pH-values along the flow path suggested the precipitation of a calcium carbonate mineral, which also contributed to the decrease in TIC (Figure 4.2). The dissolved Fe_{tot} concentrations stayed below the detection limit of 0.02 mg l^{-1} in all samples while the concentration of dissolved Mn_{tot} exceeded the detection limit of 0.01 mg l^{-1} only in a few samples, suggesting that Fe^{III} and $Mn^{III/IV}$ reducing processes were of minor importance. However, solely measuring dissolved Fe_{tot} concentrations is only a weak indicator for identifying Fe^{III}-reduction processes, because precipitating mineral phases (i.e. FeS, $FeCO_3$) may limit the solubility of Fe^{II}. The same is valid for any $Mn^{III/IV}$ reduction processes. As the experiments are ongoing, mineralogical evaluation of the solid phase was beyond the subjects of this work and, therefore, the role of Fe^{III}- and $Mn^{III/IV}$ reduction is not conclusively evaluated. However, the comparatively small Fe^{III}-content of the solid phase (0.55±0.39 g kg^{-1}) supported the assumptions on a minor importance.

The pH usually increased from 8.7 to 9.6 along the flow path and up to 11.8 during the 15 bars-period of the experiment. The concentrations of other groundwater constituents (i.e. sodium, potassium, magnesium, chloride) showed no mentionable differences between the in- and outflows of the column experiment, apart from an unsteady Si^{tot} increase (50±80 μM, n = 62). A consequence of the observed hydrogeochemical processes was a decrease in the electrical conductivity of the groundwater by 150 μS cm^{-1}.

The composition of the inflow solution varied slightly due to a repeated renewal of the stock in freshly produced groundwater that was used for its preparation, reflecting the background fluctuation of a natural aquifer. The variable hydrogen inflow concentration caused by different applied $p(H_2)$ shows no correlation with these fluctuations. Furthermore, the extent of concentration changes in dissolved species between the in- and outflow generally shows no correlation to the hydrogen inflow concentration, and variations in these changes did not show a clear trend either. An exception is the loss in sulfate concentration, where a temporarily decreasing tendency was observed between day 56 (ΔSO_4^{2-} = 80 μM) and day 78 (ΔSO_4^{2-} = 22 μM), followed by a reestablishment to initial values and then a slight increasing tendency at the beginning of the 3-bars period of the experiment (Figure 4.1). However, the variations in sulfate decrease show no correlation to the dissolved hydrogen concentration in the inflow, these fluctuations are possibly caused by variations in microbial activity not controlled by any of the monitored parameters.

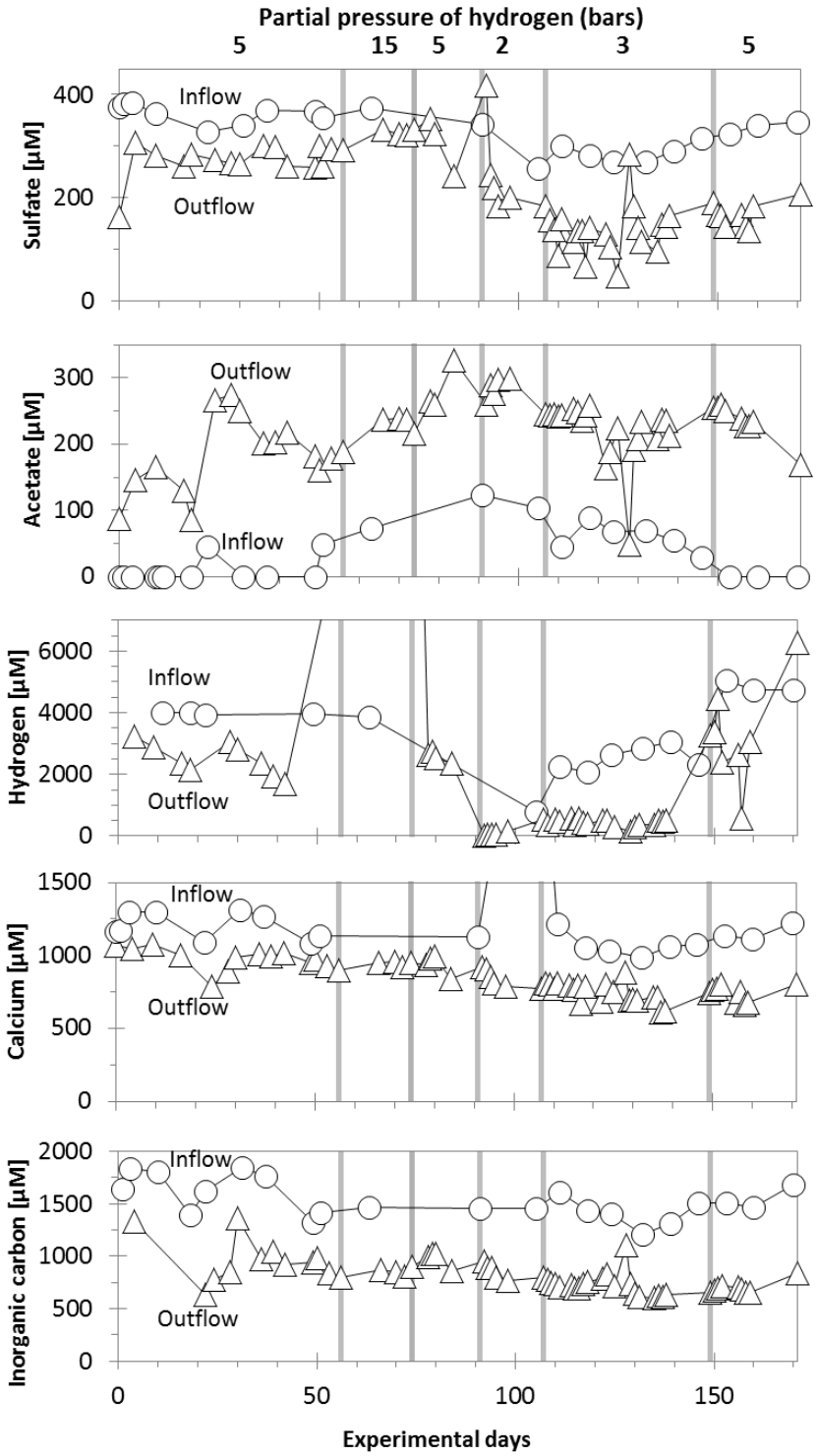

Figure 4.1: Dissolved concentrations of sulfate, acetate, hydrogen, calcium, and total inorganic carbon species (TIC) in the column`s in- and outflow solutions versus the experimental run time in days. Vertical gray lines show the consecutive $p(H_2)$ changes in the inflowing solution.

The concentration profiles along the flow path gathered during all six experimental phases (Figure 4.2) support the assumption that redox reactions, most probably catalyzed by microorganisms, were responsible for the observed changes in dissolved concentrations of hydrogen, sulfate, and acetate. Moreover, the concentration profiles also suggest an independency of the reaction rates from the initial dissolved hydrogen concentration, as already derived from monitoring the in- and outflow concentrations (Figure 4.1).

All concentration profiles show an average decrease in dissolved concentration of sulfate from 0.33 to 0.22 mM, of TIC from 1.45 to 0.70 mM, of calcium from 1.13 to 0.84 mM, and of hydrogen by 1.2 mM as well as an average increase in acetate concentration from 0.05 to 0.2 mM slowing down towards the end of the flow path. The results imply that all reactions started immediately and concurrently at the beginning of the flow path. The simultaneous reaction progress established throughout the total length of the column indicating that a classical redox sequence, i.e. subsequent and separate sulfate reducing and acetogenic zones, was not established in the column experiment. Furthermore, the almost linear decrease in hydrogen, sulfate, TIC, and calcium concentration suggests that the reactions responsible for the concentration changes proceeded more or less evenly along the total length of the flow path. Only the acetate formation decreased towards the end of column.

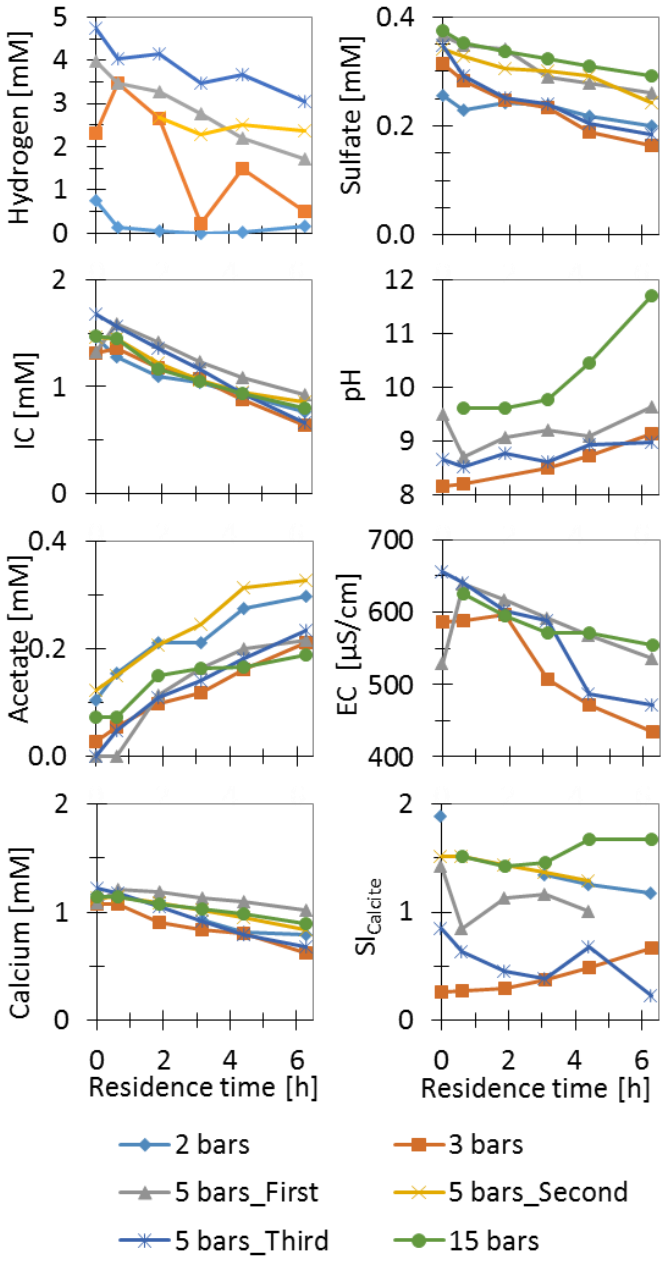

Figure 4.2: Dissolved hydrogen, sulfate, total inorganic carbon species, acetate, and calcium concentrations, and pH, electrical conductivity as well as the saturation index of calcite for the solutions percolating the high pressure column plotted versus the residence time in the experiment. Different profile lines represent consecutive experimental phases using diluted groundwater equilibrated with different hydrogen partial pressures as inflowing solution.

The concentration profiles provide an estimation of an average net hydrogen consumption rate of 0.25 mM h^{-1}, which is nearly balanced by the 0.2 mM h^{-1} that was calculated based on the stoichiometry of hydrogenotrophic sulfate reduction and acetogenesis. The gap in this redox balance is probably due to a loss of hydrogen during the sampling procedure or due to a diffusive loss through pumping heads, tubes, connectors, etc. of the system apparatus, reflecting the serious challenge to work with the highly fugitive hydrogen gas dissolved at pressures much higher than the ambient pressure. However, other hydrogen oxidizing processes cannot be totally excluded but the results do not suggest any other relevant reaction.
Methane (detection limit: 1 µM) or formate (detection limit: 4 µM) production were never detected. The increasing pH-value from 8.7 to 9.6 along the flow path of the column experiment might have inhibited methane formation because pH-levels above 7-9 can prevent methanogenic activity (Cai et al., 2004; Yuan et al., 2006). Studies at town gas storage sites and hydrogen-limited aquifers have also shown methane formation at conditions comparable to the column experiment (Buzek et al., 1994; Panfilov, 2010, 2016; Smigáň et al., 1990). Usually, methane production is known to take place at rates of up to a third of the acetate production rates (Conrad, 1999) and even the presence of acetate itself in the column experiment made methane production expectable (Jesußek et al., 2012). Therefore, the high pH-value characterizing the experiment probably in combination with a lack of specialized microbes could be the reason for suppressed methane formation. Interestingly, earlier predictions assumed a groundwater acidification as a consequence of a surplus in molecular hydrogen (Reitenbach et al., 2015), which is clearly denied by the experimental results.
Overall, the column experiment represents a flow through system characterized by the surplus of dissolved hydrogen and dominated by spontaneously starting hydrogen oxidizing reactions, mainly parallel sulfate reduction and acetogenesis catalyzed by microorganisms. Dissolved hydrogen was depleted in the column only during the 2-bars-period of the experiment, indicated by a non-linear decrease in hydrogen concentration along the flow path (Figure 4.2) and small concentrations of hydrogen in the outflow (between 27 and 158 µM) (Figure 4.1). However, the depletion of dissolved hydrogen did not stop acetate production, pH increase, or calcium precipitation. No dependency of the observed reactions on the initial $p(H_2)$ was detected indicating that the system reached quasi steady-state conditions, meaning that the established microbial community was apparently not sensitive to the pressure variations applied in the experiment at least as long as a surplus of dissolved hydrogen was provided (see also on Figure 4.3).

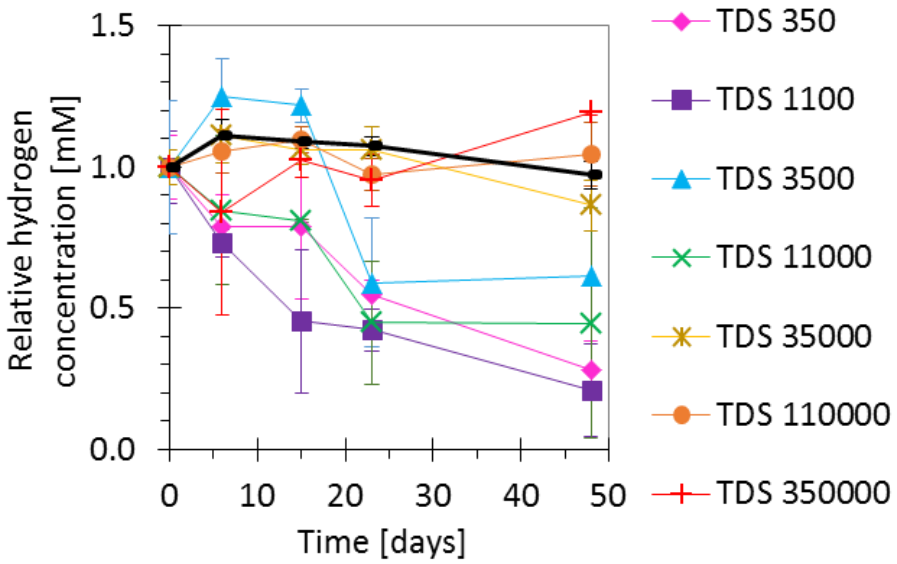

Figure 4.3: Development of dissolved hydrogen concentrations normalized to the initial total moles of hydrogen at different total dissolved solids (TDS, mg l^{-1}) concentrations (black line: blank series with quartz sand and deionized water, standard deviation from triplicate samples).

The results of complementary batch experiments applying a range of different total dissolved solids (TDS) concentrations show that high concentration of TDS inhibited hydrogen-consuming redox reactions (Figure 4.3). The microcosms containing groundwater with TDS higher than 35 g l^{-1} showed constant hydrogen concentrations during a time span of at least 48 days, which were equivalent to the blank experiments containing quartz sand and hydrogen-saturated deionized water. In microcosms containing TDS of 11 g l^{-1} or less a significant and similar decrease in hydrogen concentration was observed after a lag time of less than 6 days. The relative concentration of dissolved hydrogen reached values between 60 and 30% after 48 days in these batch series. Thereby, all these microcosms exhibited comparable hydrogen consumption rates in the different experimental series. Hydrogen consumption being inhibited by increasing the salinity indicated that microbial processes were responsible for hydrogen oxidation. This furtherly suggests that a particular TDS limit may control if microbial activity takes place and that particular TDS limit will probably depend on the site-specific microbial community of an aquifer.
The microbially mediated redox reactions starting spontaneously in the pre-conditioned sediment used in the column experiment and after a short lag time in the halotolerance test suggest that the unspecified natural microbial communities in the aquifer material were ready to use high concentrations of hydrogen as electron donor as well as sulfate and inorganic carbon as electron acceptors. Furthermore, the results show that at $p(H_2)$ higher than 2 bars the increasing dissolved hydrogen concentration had no effect on the type nor on the velocity of the established redox reactions. The results of the halotolerance test combined with the column experiment supported the idea of a fast establishment of microbially catalyzed redox reactions in case of a hydrogen gas leakage into shallow or medium deep aquifers, even in a scenario including salt water intrusion accompanying the gas leakage. Storage of hydrogen gas in porous aquifers will probably also initiate these redox reactions, if the salt content in the aquifer does not exceed some tenner grams per liter.

4.5. Kinetics

In the column experiment the decrease of sulfate as well as calcium concentrations along the flow path follow a pseudo zeroth order kinetics, while the acetate formation suggests a first order dependency from dissolved TIC. A descriptive process model composed of the combination of zeroth and first order rate equations and stoichiometric balance equations was developed and used to determine the rate coefficients (Table 4.5). An explicit model (Eqs. 4.1 to 4.5) was simultaneously fitted to associated concentration profiles of Ca^{2+}, SO_4^{2-}, acetate ($[Ac^-]$), TIC, and dissolved hydrogen by variation of the zeroth order rate coefficients for the formation of calcium carbonate (k_{Prec}) and the reduction of sulfate (k_{SR}), respectively, as well as the first order rate coefficient with respect to TIC for the formation of acetate (k_{AcG}).

$$-\frac{d[Ca^{2+}]}{dt} = k_{Prec} \qquad \text{Equation 4.1}$$

$$-\frac{d[SO_4^{2-}]}{dt} = k_{SR} \qquad \text{Equation 4.2}$$

$$-\frac{d[Ac^-]}{dt} = k_{AcG} \cdot [TIC] \qquad \text{Equation 4.3}$$

Consumption rates of dissolved hydrogen and TIC were defined from stoichiometric balance equations using Eq. 4.4 and Eq. 4.5, respectively.

$$-\frac{d[H_2]}{dt} = 4\frac{d[Ac^-]}{dt} + 4\frac{d[SO_4^{2-}]}{dt} \qquad \text{Equation 4.4}$$

$$-\frac{d[TIC]}{dt} = 2\frac{d[Ac^-]}{dt} + \frac{d[Ca^{2+}]}{dt} \qquad \text{Equation 4.5}$$

The model fits well to the concentration profiles (Figure 4.4) with rate coefficients for sulfate reduction and acetogenesis between 9 and 26 μM h^{-1} (average 18±5) and 0.015 and 0.033 h^{-1} (average 0.030±0.006), respectively (Table 4.5). The fitted calcite precipitation rate coefficients vary between 39 and 88 μM h^{-1} (average 57±17).

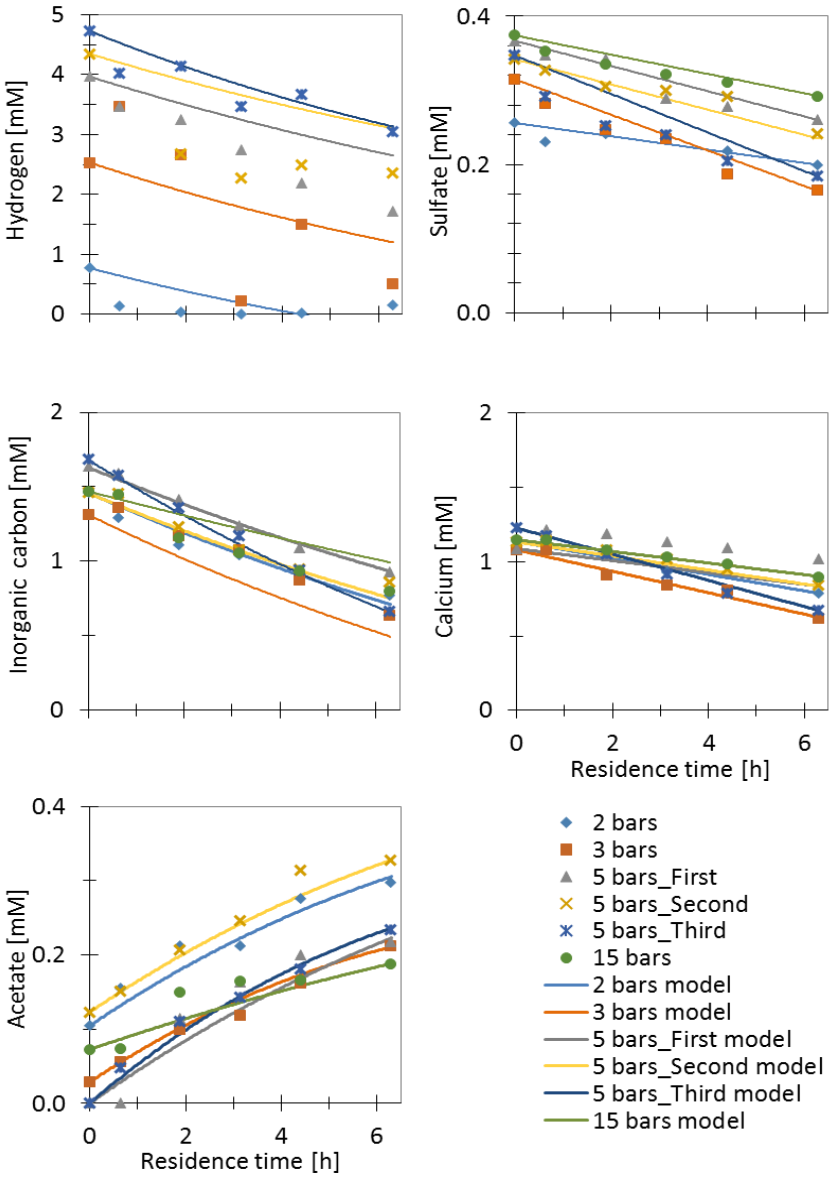

Figure 4.4: Fitted model results (lines) and dissolved concentrations of hydrogen, sulfate, TIC, calcium, and acetate (symbols) along the flow path of the high pressure column experiment during different experimental phases. The residence time was calculated using mean flow and porosity; dispersion was neglected.

The consistent model fit supports the assumption that the simultaneously proceeding and microbially catalyzed hydrogenotrophic sulfate reduction and acetogenesis were the main redox processes established in the column experiment, accompanied by carbonate precipitation induced by the increasing pH-value. Nevertheless, sulfate reduction by acetate oxidation is also a well-known microbial metabolic process (Jesußek et al., 2012) and a model considering this process instead of direct hydrogenotrophic sulfate reduction could also be fitted to the results of the column experiment. However, such a model would be under-parameterized using the available data set, because acetotrophic sulfate reduction would consume acetate and produce carbon dioxide, which is then reduced again to acetate by oxidizing hydrogen. Consequently, the acetate oxidation rate would be twice as high as the sulfate reduction rate for stoichiometric reasons and the rate of acetogenesis would increase by the same value, resulting in identical model results. The experimental results support a parallel and not a sequential occurrence of acetogenesis and sulfate reduction, as both processes started immediately at the beginning of the flow path, thereby providing no evidence for sulfate reducing processes other than hydrogenotrophic sulfate reduction. However, an appearance of acetotrophic sulfate reduction cannot be totally ruled out.

Table 4.5. Pseudo zeroth order rate coefficients for hydrogenotrophic sulfate reduction (k_{SR}) and calcium carbonate precipitation (k_{Prec}), and pseudo first order rate coefficient with respect to TIC for acetogenesis (k_{AcG}).

	k_{SR} ($\mu M \cdot h^{-1}$)	k_{AcG} (h^{-1})	k_{Prec} ($\mu M \cdot h^{-1}$)
average	18±5	0.030±0.006	57±17
2bar	9	0.030	55
3bar	24	0.033	72
5bar_First	17	0.028	40
5bar_Second	17	0.030	47
5bar_Third	26	0.033	88
15bar	13	0.015	39

A model based on Monod kinetics (Appelo and Postma, 2005) could also describe the experimental data, but this model would also be strongly under-parameterized due to the large number of variables usually needed for describing Monod kinetics. On the other hand, Monod kinetics reflect either zeroth or first order kinetic behavior in case of steady-state microbial activity and if reactant concentrations are way higher or lower than the Monod-concentrations, respectively (Dale et al., 2006; Schäfer et al., 2007; Schäfer et al., 1998). The results of the column experiment suggest more or less constant metabolic rates for both sulfate reduction and acetogenesis over time and independently from the dissolved hydrogen concentration (Figure 4.5), indicating a quasi-steady state of the microbial community. Furthermore, the sulfate and hydrogen concentrations are higher than the known Monod-concentrations (Dale et al., 2006; Schäfer et al., 2007; Schäfer et al., 1998). The first order dependency of the acetate formation with respect to TIC would then indicate that the TIC content was in the range of or smaller than the Monod-concentration. Overall, for further applications we suggest the more robust assumption of pseudo first and zeroth order kinetics, as these were directly supported by the experimental results. For including further or different pathways of the reduction of inorganic carbon species, Eq 5. can be extended by terms representing reactions such as methane or formate production.

The rate coefficients gathered by fitting the model may be plotted against the initial dissolved hydrogen concentration (Figure 4.5). For the rate coefficients, the model input data were the six concentration profiles along the flow path as well as all concentration differences between the inflow and outflow solution. The averaged values considering the in- and outflow concentrations from each experimental period are in good agreement with the results provided by the concentration profiles. Overall, the rate coefficients may vary by a factor of two or three, but no dependency on the initial hydrogen concentration was indicated. The mean specific sulfate reduction rate of 42 $nM \cdot cm^{-3}_{sediment} \cdot h^{-1}$ or the mean acetogenesis of 85 $nM \cdot cm^{-3}_{sediment} \cdot h^{-1}$, which were calculated from the column experiment, are smaller than rates described for other aquatic environments exhibiting high dissolved hydrogen concentrations. Experimental studies (Krumholz et al., 1999; Nevatalo et al., 2010; Vallero et al., 2005) on bioreactors yielded sulfate reduction rates between 3060 and 79 500 $nM \cdot cm^{-3}_{sediment} \cdot h^{-1}$. A study (Krumholz et al., 1999) on acetogenesis in a Cretaceous shale and sandstone environment showed rates reaching from 110 to 160 $nM \cdot cm^{-3}_{sediment} \cdot h^{-1}$. While the acetogenesis rate was at least in a similar range, the sulfate reduction was two or three orders of magnitude smaller in the column experiment. Several reasons might be responsible for the comparatively low metabolic activity, e. g. a lack of nutrients, composition of the established microbial community, or the comparatively high pH-value.

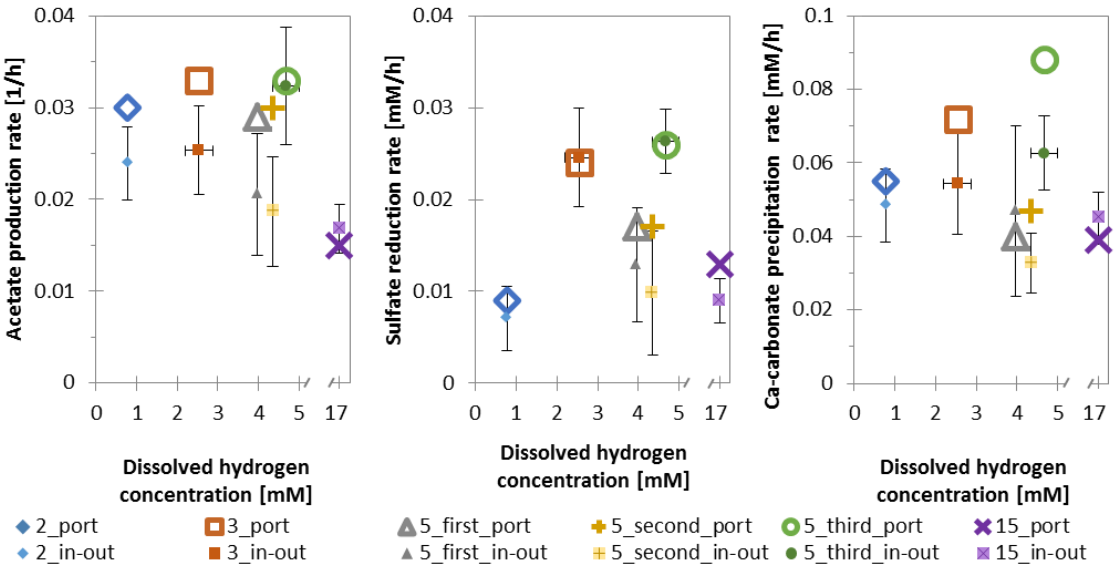

Figure 4.5: Rate coefficients describing sulfate reduction, acetate formation, and calcium carbonate precipitation in the column experiment versus the initial dissolved concentration of hydrogen. Vertical and horizontal error bars represent standard deviations in the measured hydrogen concentrations, and in reaction rate constants fitted for every in- and outflow concentration ("_in-out"), respectively. The larger symbols ("_port") represent the six fits based on concentrations over the flow path (Table 4.5, Figure 4.4).

4.6. Implications

In the investigated hydrogen-rich groundwater environment simultaneously proceeding redox reactions were identified, instead of a redox sequence consisting of separate metabolic zones. This poses a sharp contrast compared to the hydrogen-limited groundwaters in pristine or contaminated aquifers known from the literature so far. These findings can be relevant for large scale modeling attempts, design of monitoring networks at hydrogen gas storage sites, or for laboratory investigations serving a site specific risk assessment. Using pressure-independent elementary kinetics instead of sophisticated rate equations in large scale transport reaction models will probably save computational efforts and may enable easier scenario modeling. Zeroth or simple first order kinetics might overestimate the metabolic rate in case of exhausting reaction partners, but this effect should be small at conditions with high initial reactant concentrations. Furthermore, the independence of the observed redox reactions from the dissolved hydrogen concentration implies in a converse argument that laboratory investigations on hydrogen leakage scenarios can be performed at system pressures lower than in-situ conditions, which will drastically reduce laboratory efforts. Thereby, the presented halotolerance test provides an easy procedure to estimate the effect of a salt water intrusion accompanying a hydrogen leakage into shallow or medium deep aquifers, if the natural material from a particular site is available. The results of the halotolerance test should not be transferred directly to any other groundwater environment, because deep saline aquifers might have a well-adapted and highly halotolerant microbial community possibly enabling the consumption of newly introduced hydrogen even if the salinity of the groundwater in such an aquifer is higher than 35 $g \cdot l^{-1}$. However, in less saline aquifers a rapid hydrogenotrophic sulfate reduction as well as a CO_2-reduction has to be expected, and the reaction products will modify the groundwater and the stored gas. Therefore, targets of a monitoring network covering a hydrogen gas storage site should be focused on the reaction products instead of the stored gas dissolved in shallow aquifers, in order to detect a gas leakage. Moreover, the stored hydrogen gas will probably be contaminated by the gaseous reaction products, i.e. H_2S or methane, which should also be considered for project planning.

4.7. Additional experimental characterization of hydrogen-consuming redox reactions

4.7.1. Motivation for three further aspects

The work presented in the Chapters 4.1-4.6. and included in the manuscript submitted to Environmental Science and Technology has been extended with three further experimental phases to characterize a wider range of reactive geochemical environments influenced by a hydrogen intrusion. These efforts were made in order to better support the development of corresponding hydrogeochemical models, to further improve the process understanding on hydrogenotrophic reactions, and to characterize additional geochemical aspects of hydrogen storage operations and potential leakage monitoring.

In order to create experimental conditions answering these novel questions, certain modifications were carried out in the described apparatuses and also new set-ups were also developed. If not indicated else, the laboratory routine (e. g. analytics, sampling, etc.) was consistent with the methods followed earlier and described in Chapter 4.3.

The results of this supplementary study were also used for evaluating the applicability of the three experimental setups for characterizing biogeochemical changes triggered by hydrogen at different conditions. However, the goal of this additional chapter is merely to shortly present the most important preliminary results as well as results from ongoing experiments. A detailed study including more results along with their adequate evaluation and interpretation may be prepared and published in 2018-19.

4.7.2. Effects of lowered pH and increased concentration of C_{inorg}

Further high pressure column experiments were carried out to represent aquifers which are intruded by a hydrogen plume and which contain a groundwater having a lower pH value and a higher concentration of total dissolved inorganic carbon species compared to the already investigated conditions representing a shallow Pleistocene aquifer. Such aquifers are still potentially used for drinking water production (TrinkwV), and they can be characterized by a higher partial pressure of CO_2 compared to the shallow groundwaters investigated so far (Table 4.3). These new experiments aimed to evaluate potential changes in the hydrogen-induced reactions discussed in Chapters 4.1-4.6, namely sulfate reduction, carbonate precipitation and acetate production. A special focus was laid on the investigation of changes in rates and products of inorganic carbon reduction, because indications from batch pre-experiments and literature sources suggested two major changes. First, at increased inorganic carbon concentrations the reaction rates of inorganic carbon reduction may increase (Berger, 2015; Mascus, 2015). Second, the decrease in pH would result in inorganic carbon reduction producing end products other than acetate: production of formate and methane shall take place (Metzgen, 2016). Moreover, lowering the pH value causes a significant shift in the speciation of the members of the carbonate buffer system (Appelo and Postma, 2010). Therefore, the precipitation and dissolution of carbonates may also be expected to change compared to the high pressure experiments with an unchanged partial pressure of CO_2.

Improvements in methods and concept

To lower the pH of the groundwater percolated through the sediment column and to increase its total inorganic carbon concentration at the same time, the gas supply system of the high pressure experimental apparatus was switched to a gas mixture containing 1% CO_2 and 99% H_2 instead of the pure hydrogen used before. The total gas pressure was set to 5 bars, and the same operation and sampling routine was followed as before (Metzgen, 2016).

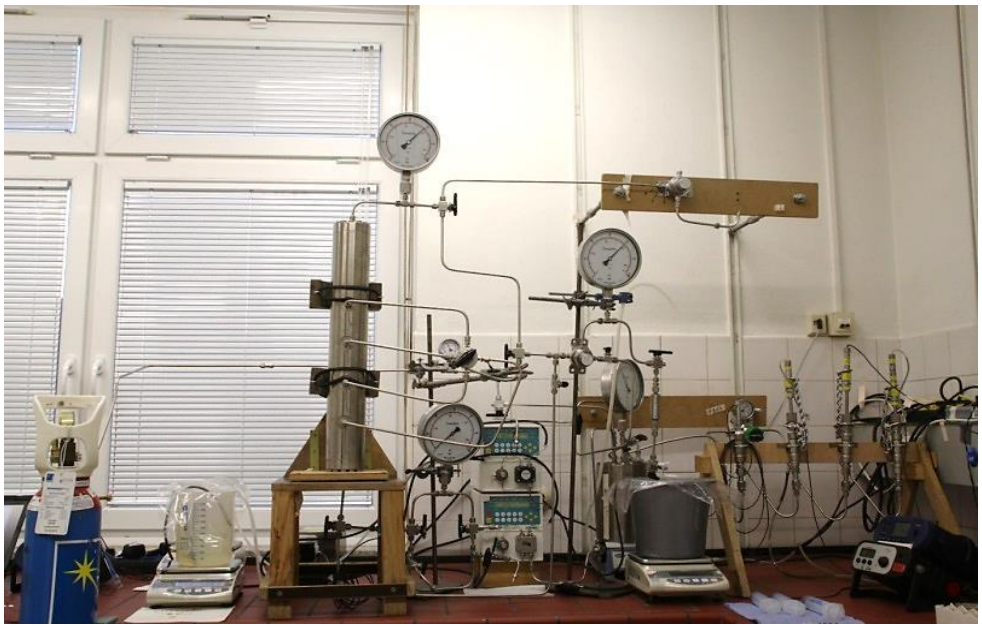

Figure 4.6: An overview photo showing the high pressure experimental apparatus in operation. For a conceptual sketch of a similar set-up see Figure 2.2.

Results of the high pressure experiment with added CO_2

The addition of CO_2 to the gas applied to saturate the inflow water for the high pressure experiments had three major effects (Figure 4.8). First, it decreased the pH of the inflowing groundwater, which resulted in the second effect: the precipitation of carbonates turned into a dissolution of carbonates. Third, the main product of carbonate reduction changed from acetate alone to major amounts of formate and minor amounts of methane. On the other hand, sulfate reduction rates did not show any change within the investigated pH conditions.

Dissolution of previously precipitated $CaCO_3$ was indicated by increasing inorganic carbon and calcium concentrations of up to 2.9 mM and 2.11 mM, respectively. The dissolution of carbonates is one of the reasons why the pH values decreased only by ca. 1, instead of a higher drop compared to equilibrium calculations prepared using PHREEQC (Parkhurst and Appelo, 2013). The surplus concentration of inorganic carbon observed after switching to the gas mixture containing CO_2 is most probably composed by the re-eluted carbonates and by the carbon dioxide supplied additionally to the inflowing groundwater (Figure 4.8).

Formate production was found to commence within a few days after switching to the gas mixture containing CO_2 and thus decreasing the pH by rising the partial pressure of CO_2. The appearance of formate production resulted in formate concentrations of 0.75 ± 0.2 mM. The immediate start of formate production was accompanied by a similarly sharp drop in acetogenesis (Figure 4.8) causing acetate concentrations of only 0.06 ± 0.03 mM measured in the outflow of the high pressure column. Formate is a rather unusual end product in groundwater environments, because it mostly serves as an intermediate in microorganisms synthetizing larger organic molecules, starting at acetate (Ragsdale and Pierce, 2008). Interestingly though, the summarized amount of inorganic carbon reduced into acetate and formate together is higher than the amount of acetate produced at the lowest pH levels realized by the experiments with pure hydrogen. Therefore the results gathered in experiments with added CO_2 may support the hypothesis that the overall rate of inorganic carbon reduction increases with increasing inorganic carbon concentration.

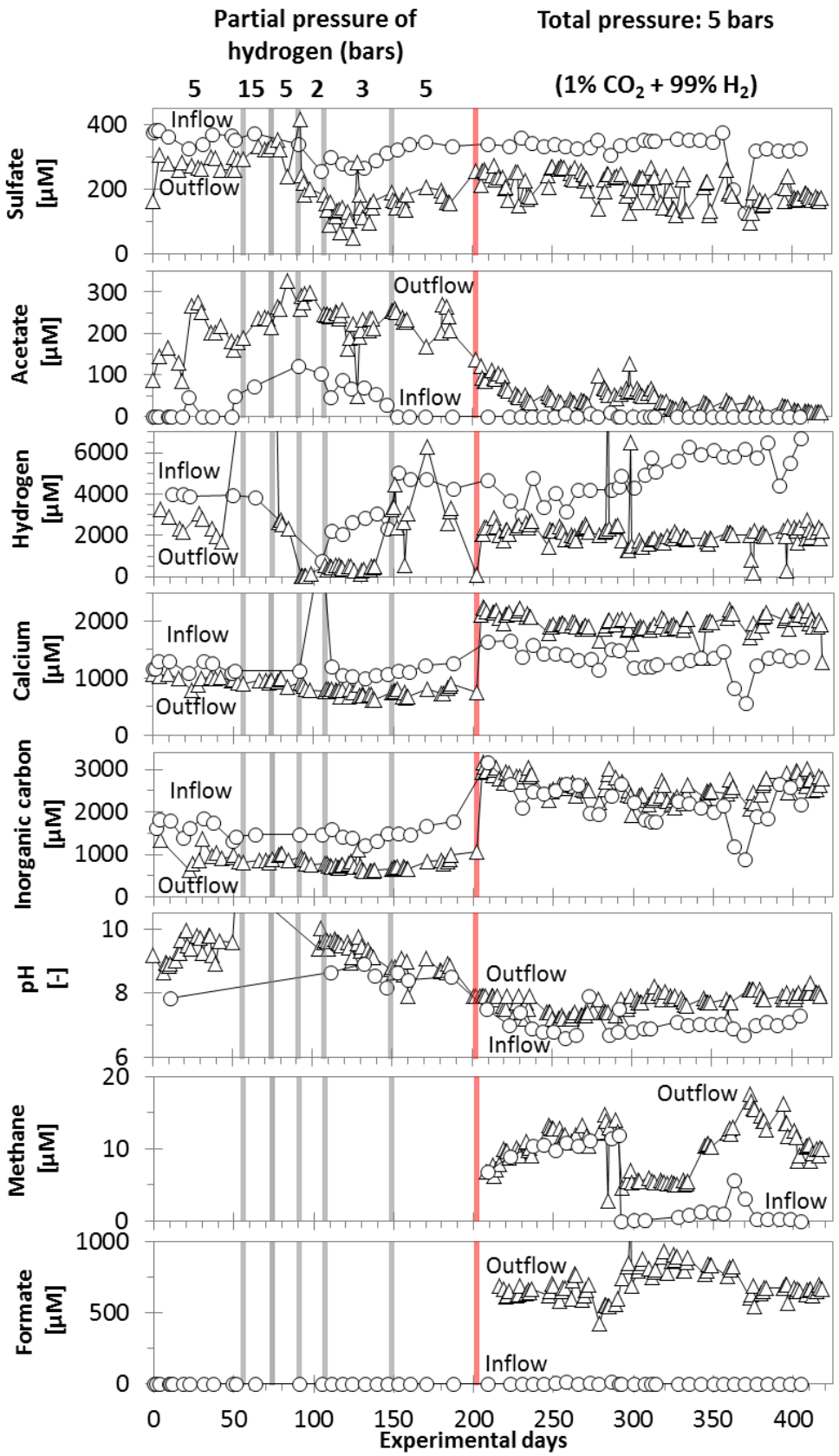

Figure 4.7: Dissolved concentrations of sulfate, acetate, hydrogen, calcium, inorganic carbon methane, and formate as well as the pH value measured in the in-, and outflows of the high pressure experimental column plotted versus the experimental run time. The red line represents the time of switching to the CO_2-containing hydrogen gas, the grey lines mark the switches between different hydrogen partial pressures in the first experimental phase. Note the changes compared to the experiments with pure hydrogen (Figure 4.1).

Methane concentration increased in the outflow of the high pressure column after switching to the gas mixture. The produced amount showed a slowly growing trend and fluctuations similar to concentrations of sulfate or acetate. However, methanogenic activity apparently took place not only within the sediment column, but also on a filter, built in the high pressure experimental set-up for technical purposes. Methanogenesis on the filters was demonstrated in additional batch incubations using the filter material gathered when exchanging filter inlets and the same gas and groundwater which were used for the experiments. After replacing the filter, the methane concentrations measured in the inflow dropped to nearly zero, therefore the methane concentrations measured in the outflow only represented the methane produced in the high pressure column (see Figure 4.8 around 300 days). Based on samples taken after eliminating these artifacts, a methane production rate of 1.1 μM/h was determined for the sediment column at the represented conditions.
Formate production has not been found in the relevant literature in such a context. Therefore the presented experimental results potentially identified an additional reaction to be considered when evaluating geochemical aspects of hydrogen storage, which otherwise would have not been expected for the case if a hydrogen plume intrudes an aquifer. These conclusions offer the possibility for completing the reaction model described in Chapter 4.5 by considering the dependency of rates and products of inorganic carbon reduction (methane, acetate, and formate) on pH and inorganic carbon concentration. The simultaneous dependency on inorganic carbon concentration and pH suggests that for numerical process model development the partial pressure (or saturation index) of CO_2 might be a better parameter than considering inorganic carbon concentration and pH as separate variables.

4.7.3. Effects of sediment and groundwater characteristics

The experiments carried out and discussed in Chapters 4.1-4.6 applied a sediment and a groundwater from a shallow Pleistocene aquifer. However, for a more general validity of the presented results it is useful to perform comparative investigations including further unconsolidated sediments with different properties potentially influencing the metabolic response of the incumbent microbial community to a hydrogen surplus. Such differences in the chosen sediments may be focused on the depth and age of the sampled aquifer, the total organic carbon content of the solid phase, and the way the sediment sample has been stored before starting the experiments. Investigating two further sediments in comparison with the Pleistocene sand can reveal the potential qualitative influences of the respective parameters on hydrogen-oxidizing reactions identified in the experiments.

Improvements in methods and concept

Microcosm batch experiments are an adequate tool for qualitatively investigating microbially mediated anaerobic redox reactions in an aquifer environment. When using batch incubations it can be identified which reactions can be expected to take place in which sediment and groundwater combinations under the influence of a hydrogen surplus. The rates of the identified reactions can then be directly compared between the observed batch series. However, as the transport conditions are not representative to an aquifer, their results may not be as reliable for upscaling as the quantitative results from column experiments.

The preparation of the batches for this experimental series was identical to the preparation of the batch experiments with varied TDS concentrations (Chapter 4.3), but instead of using the same Pleistocene sediment and groundwaters with various salinities different sediments and different groundwaters were combined. Additionally to the Pleistocene ("NMS shallow" or "NMS-f") sediment and groundwater (characterized in Chapter 4.3) two additional sediments (Table 4.6) and one additional groundwater (Table 4.8) were used. First, a Tertiary lignite sand and groundwater were taken from the same aquifer on the site where the "NMS shallow" sediment and groundwater were also taken from, but from a deeper depth interval of 61-80 mbgl ("NMS deep" or "NMS-t"). Second, another Pleistocene sand from 58-74 mbgl in the Kuden region, Germany ("Kuden" or "Ku") was taken from another site (N54.0055, E9.1514). The combinations compiled from these materials for the batch experimental series are listed in Table 4.7. Additionally to those combinations, blank batch series purged with Ar instead of H_2 were also prepared parallel for all incubations.

Table 4.6. Solid phase characteristics of the sediments used for this study (Lüders et al., 2016, accepted).

Abbreviation of sediment name	**NMS-f**	**NMS-t**	**Ku**
Sedimentary unit	Pleistocene sand	Upper lignite sand	Pleistocene sand
Depth under GOK [m]	4-14	67-77	50-84, 125-127
Σ(Na, K, Ca, Mg, Fe, Mn) [mmol/kg]	1070	135	383
C_{org} [mg/kg]	142	1078	346
Pyrite [mg/kg]	221	723	262

Table 4.7. Sediment and groundwater combinations applied in the microcosm experiments.

Sediment	**Water**
Commercial quartz sand (Quartz)	Deionized water (dest)
Shallow Pleistocene sediment (NMS_f)	Shallow Pleistocene groundwater (NMS_f)
Deep Miocene sediment (NMS_t)	Deep Miocene groundwater (NMS_t)
Organic-rich sand (Ku)	Shallow Pleistocene groundwater (NMS_f)

Both sediments from the "NMS" site were gathered from drilling cores, they were mixed and stored wet under Ar-atmosphere to keep the conditions as anaerobic as possible, although the experiments were filled with the sediment at normal atmosphere conditions. The "Ku" sediment was stored dry under atmospheric and aerobic conditions for months. The groundwater was produced through the same well the drilling cores were taken from, and was stored in gas tight Al-impregnated bags (Tesseraux). No additional inoculation with microorganisms was performed and no nutrients were added, similarly to all other experiments discussed in this Thesis.

Table 4.8. Composition of the "NMS-t" groundwater based on analysis from standard well sampling (Lüders et al., 2016, accepted). Note the differences compared to Table 4.3.

Parameter	Unit	"NMS-t" groundwater
Electric conductivity	[µS/cm]	307 ± 6
pH	[-]	7.6 ± 0.1
Dissolved oxygen	[mg/l]	0.011 ± 0.004
Redox potential (EH-SHE)	[mV]	-104 ± 39
Temperature	[°C]	10.1 ± 0.2
Na^+	[mM]	0.317 ± 0.009
K^+	[mM]	0.0267 ± 0.0007
Ca^{2+}	[mM]	1.38 ± 0.02
Mg^{2+}	[mM]	0.065 ± 0.001
Fe^{tot}	[mM]	0.0132 ± 0.0006
Mn^{tot}	[µM]	1.60 ± 0.03
Si^{tot}	[mM]	0.401 ± 0.006
Non-purgable $C_{organic}$	[mM]	0.12 ± 0.04
Total $C_{inorganic}$	[mM]	2.7 ± 0.5
F^-	[µM]	5.3 ± 5.3
Cl^-	[mM]	0.31 ± 0.01
Br^-	[µM]	1.25 ± 1.25
NO_3^-	[µM]	6 ± 40
PO_4^{3-}	[µM]	1.05 ± 1.05
SO_4^{2-}	[mM]	0.148 ± 0.009
CH_4	[µM]	1.3 ± 0.7

Results of microcosm incubations with varying sediments and groundwaters

All three series of microcosms containing sediment and groundwater from three different geological settings showed the same hydrogen consuming and terminal electron accepting processes (Figure 4.9) as the high pressure experiments did (Figures 4.1-2), such as simultaneous sulfate reduction and acetate production coupled to hydrogen oxidation. The observed net decrease rates in dissolved hydrogen concentrations varied between 0.15 and 0.27 $\mu M \cdot h^{-1}$ and sulfate concentrations varied between 0.30 and 0.55 $\mu M \cdot h^{-1}$, as well as the overall increase rates in acetate concentrations varying between 0.09 and 40 $\mu M \cdot h^{-1}$. These values were typically within the same order of magnitude in all three series of microcosms containing different sediment - groundwater combinations. Compared to the reaction rates observed in the high pressure experiments (Figures 4.4-5, Table 4.5), the rates estimated for the microcosms were significantly lower, probably due to the different fluid transport conditions. Considering that all other experiments were carried out using the "NMS-s" sediment and groundwater, the results of the microcosm experiments suggested that the origin of the sediments and groundwaters applied had no major qualitative impact, but caused a difference of up to a factor of four in the rates of the same reactions. Therefore, it can be suggested that the batch incubations are only suitable for preliminary studies needing less experimental effort or to test site-specific materials for process identification as well as for a comparative estimation of the reaction rates. Column experiments on the other hand, represent more realistic reactive transport conditions. Therefore, the reaction rates observed using a column setup are closer to values expected in an aquifer but column experiments also require more laboratory infrastructure. However, column experiments require higher amount of efforts and more laboratory infrastructure, especially when working with high pressures.

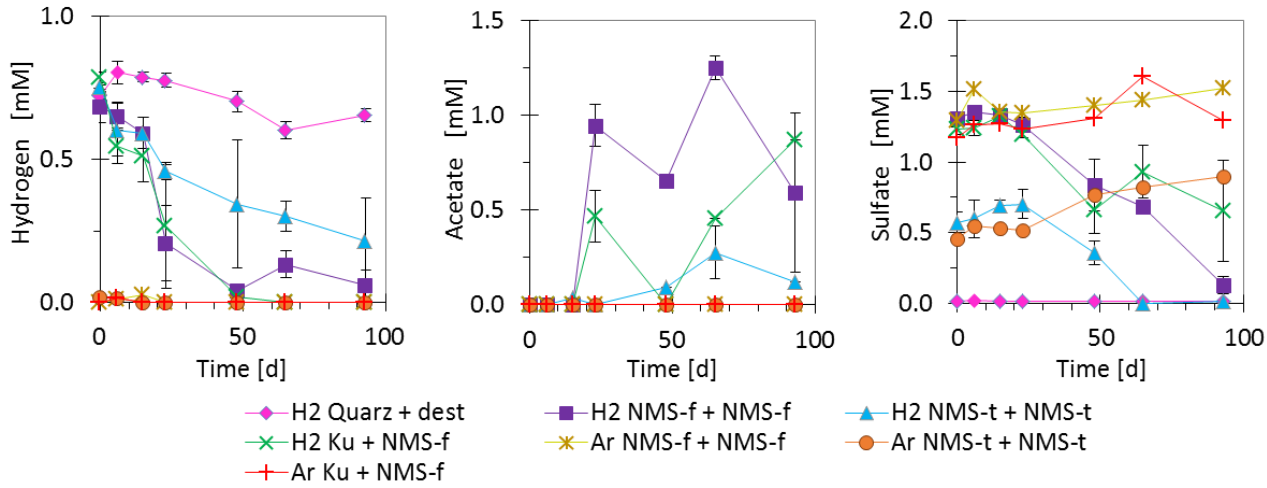

Figure 4.8: Concentrations of dissolved hydrogen (left), acetate (middle) and sulfate (right) versus the incubation time in the microcosm experiments. Each line represents a series of microcosms: "H_2" were experiments prepared with hydrogen, "Ar" were blanks flushed with argon. pH and the concentration of Ca did not show any major changes, except a 30% decrease in Ca in the "NMS-f" series. Interestingly, no methane was found in any of the experiments, but formate concentrations of up to ca. 0.4 mM appeared at the end (93 days) of the "NMS-t" series.

A series of microcosms filled with "NMS shallow" sediment and groundwater showed an increase in dissolved Fe^{tot} and Mn^{tot} concentrations between days 10 and 20, reaching maxima of 10-16 µM and 6-7 µM, respectively, before decreasing again. This temporary appearance of dissolved Fe^{tot} and Mn^{tot} suggests initial reduction of Fe^{III} and Mn^{IV} (hydr)oxides, while the produced Fe^{II} and Mn^{II} could have precipitated as carbonates or as sulfides after sulfate reduction releasing sulfide ions had started. Dissolved Fe^{tot} and Mn^{tot} was temporarily appearing in all other microcosm series as well, but the development of their concentrations did not show such clear redox sequence patterns (data not shown).

4.7.4. Effects of increased flow speed and increased nitrate concentration

Amongst the hydrogen leakage scenarios considered, a hydrogen plume intruding a shallow, unconfined aquifer is of particular interest, because such an aquifer can potentially contain major amounts of nitrate. Based on the Gibbs free energy yields of different aqueous redox reactions coupled to hydrogen oxidation (Table 4.1) hydrogenotrophic nitrate reduction is expected to be the preferred and the fastest amongst the reactions potentially taking place in an aquifer. This hypothesis is supported by pre-experiments (Berger, 2015; Mascus, 2015) finding the rates of nitrate reduction to be significantly higher than the rates of acetate production or sulfate reduction. Hydrogen oxidation coupled to nitrate reduction, typically producing N_2/N_2O, is known mostly from hydrogenotrophic groundwater denitrification technologies (Ergas and Reuss, 2001; Ergas et al., 1999; Liessens et al., 1992; Smith et al., 1994; Xia et al., 2010). However, for an improved understanding of hydrogenotrophic redox reactions as a consequence of a hydrogen leakage into the groundwater, hydrogen oxidation coupled to nitrate reduction, along with its kinetics, has to be characterized directly at aquifer conditions. In order to create flow conditions corresponding to the assumed high hydrogenotrophic denitrification rates the flow speed of the groundwater streaming through the sediment columns has to be way higher than in usual aquifer environments. The results gathered using such an approach will, therefore, enable the investigation of the quick nitrate reduction kinetics at a high time resolution.

Improvements in methods and concept

Nitrate reduction coupled to hydrogen oxidation was investigated using an experimental set-up providing a minutes-scale time resolution. Four glass columns (Ø=2.35 cm) with lengths of 5, 10, 15, and 20 cm, respectively, were filled with the "NMS shallow" sediment and were percolated with the "NMS shallow" groundwater, enriched in nitrate to 1 mM (Berger, 2015). The column lengths were proportional to the residence time because the columns were treated identically (Figure 4.7). The inflowing solution was equilibrated with $p(H_2)$=1 bar in a mixing vessel before it was pumped through the sediment columns via glass tubes using Ismatec peristaltic pumps with Viton pumping tubes. The flow velocity in these experiments was set to up to 20 $m \cdot d^{-1}$, which is extremely fast compared to any natural groundwater flow and even compared to groundwater flow velocities in the vicinity of a potential gas intrusion. Anyway, the high flow velocity was necessary in order to properly investigate the rapid hydrogenotrophic nitrate reduction. Despite the short residence time within the columns, a most probably diffusive loss in hydrogen of up to 13% was identified in control runs (Berger, 2015). Blank experiments without adding hydrogen to the inflow solution were also performed in an equivalent column setup, but realizing a larger residence time of 30 h within the columns. Samples were taken from the mixing cell and from the outflows of each column. Reaction rates were calculated by dividing the difference in concentrations measured by the elapsing residence time needed for that change.

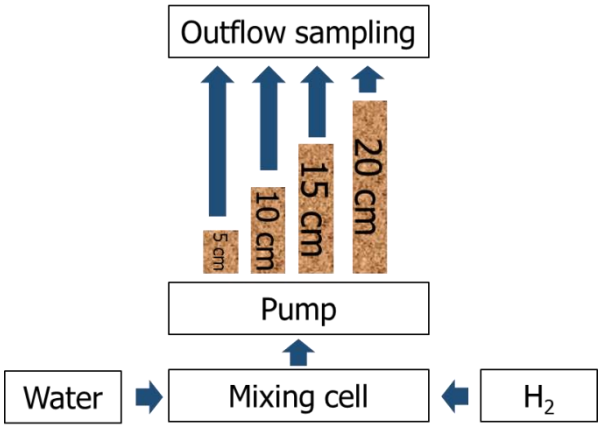

Figure 4.9: Sketch of the low pressure-high flow speed column experiments

Results of fast-flow columns with nitrate-enriched groundwater

The concentration profiles (Figure 4.10) compiled from the fast flow-through experiments revealed that both, hydrogen of up to 0.6 mM as well as nitrate of up to 0.24 mM depleted within minutes. The parallel depletion of dissolved hydrogen and nitrate indicates that hydrogenotrophic denitrification was the dominant redox reaction in these experiments. The pseudo zeroth order rate constants for the hydrogenotrophic nitrate reduction found in the high flow speed column experiments were as high as up to 10400 $nM \cdot cm^{-3}_{sediment} \cdot h^{-1}$. This reaction rate is higher than the rates reported in the literature on traditional and membrane bioreactors as well as geological environments, which were between 23 and 4510 $nM \cdot cm^{-3}_{sediment} \cdot h^{-1}$ (Chang et al., 1999; Ergas and Reuss, 2001; Haugen et al., 2002; Smith et al., 2005b; Smith et al., 1994; Xia et al., 2010).

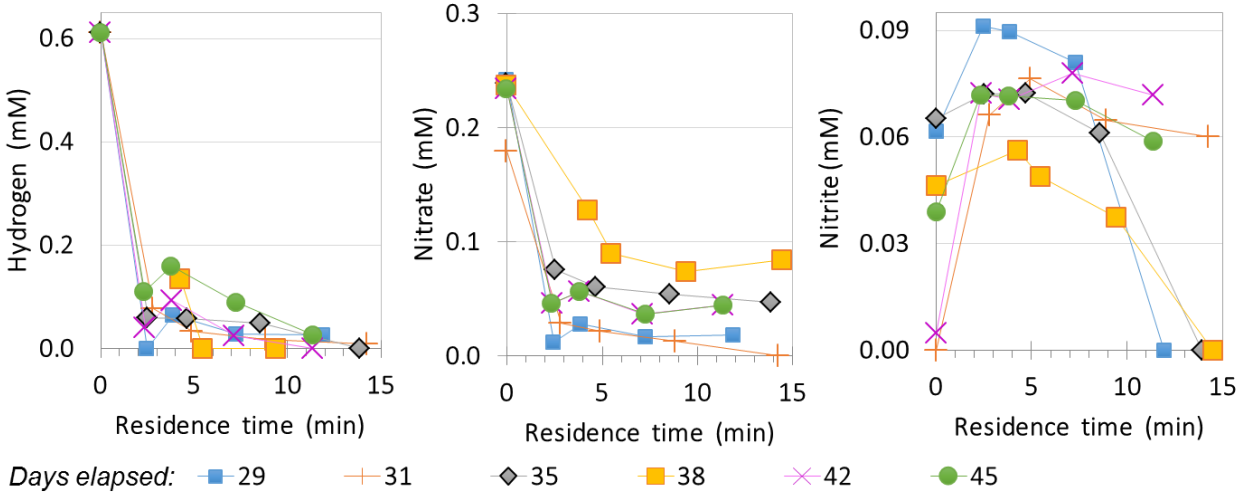

Figure 4.10: Concentrations of dissolved hydrogen, nitrate, and nitrite versus the residence time of the groundwater in the columns show fast nitrate reduction and temporary nitrite production.

The concentration profiles of nitrite show that up to a third of the reduced nitrate temporarily accumulates as nitrite. The presence of nitrite is usually of particular importance when assessing groundwater quality (TrinkwV). The nitrite concentrations increased to up to 0.09 mM, which is clearly above the usual 0.01 mM threshold limit for drinking waters (TrinkwV). In the presented experiments nitrite was found to be a short-lived intermediate of nitrate reduction, and then it was also reduced to N_2O/N_2. However, accumulation of nitrite within such a multi-step reaction path can often be enhanced by higher pH (Lee and Rittmann, 2000; Liessens et al., 1992; Smith et al., 2005b), which might be considered when evaluating potential metabolites in a nitrate-containing aquifer intruded by a gaseous hydrogen plume.

Nitrate and nitrite were apparently not reduced into ammonium, which is indicated by constant ammonium concentrations of up to 33 µM. Dissolved concentrations of other redox-sensitive parameters like sulfate, Fe^{tot}, or Mn^{tot} and of pH-sensitive species like total inorganic carbon species, Ca^{2+} and Mg^{2+} also showed no significant changes related to the aqueous redox reactions triggered by hydrogen. Acetate was not found in any of the samples.

The electron balance calculated based on the nitrate-consuming redox reactions equaled to up to 18% surplus in hydrogen consumption, which discrepancy could be explained by diffusive hydrogen losses identified when testing the low pressure experimental setup. Additionally, no nitrate consumption occurring in hydrogen-free control experiments supported that the nitrate reduction is coupled to hydrogen oxidation in the presented experiments (Mascus, 2015).

4.7.5. Supplementary considerations and conclusions

The high pressure experiment applying hydrogen enriched with 1% CO_2 showed that the lowering of the pH level and the increase in the dissolved concentration of total inorganic carbon species results in methanogenesis and formate production commencing, and in acetate production declining. These changes represent a significant dependency on the end products of carbonate reduction on the partial pressure of CO_2, which shall be considered when improving process models, such as the model described by Eqs. 4.1-4.5. Therefore, further investigations at an even wider range may be necessary to deliver a deeper process understanding for considering geochemical and even geomicrobiological aspects in subsurface hydrogen storage scenarios.

The microcosm incubations suggest that microbial hydrogen consumption and the coupled consumption of electron acceptors can take place at every aquifer condition represented in the experiments described here. The investigated sediment-groundwater combinations showed the same reactions, although their rates were different by up to a factor of four. Nevertheless, site- and sediment specific reaction rates can be revealed only by targeted investigations for evaluating potential consequences of an accidental hydrogen leakage.

Reductive hydrogeochemical reactions can have an influence on the porous aquifer matrix as well. These effects may include precipitation and dissolution of sulfides and carbonates as well as the reductive dissolution of Fe^{III} and Mn^{IV} from the solid phase. Such reactions may change the porosity and permeability of an aquifer sediment. However, the Fe^{III} and Mn^{IV} potentially reduced to Fe^{II} and Mn^{II} most probably precipitates as sulfide near the original mineral phase, if such a reduction takes place at all. The cumulative amount of the carbonate precipitates, however, can be estimated to account for 4-5% of the total pore volume during the experimental run time. Therefore, carbonate precipitation possibly changes the porosity after several months-years.

Apart from potentially influencing the aquifer environment around a hydrogen intrusion the identified reactions may also support the development of new monitoring strategies. For monitoring gas storage sites as well as locating potential gas leakages geoelectric methods have been discussed in the literature (al Hagrey et al., 2016; Dethlefsen et al., 2013). The decrease in electric conductivity (Figure 4.1) may offer a fundament for novel methods to track reactions triggered by dissolved hydrogen at aquifer conditions.

Nearly stoichiometrical consumption of nitrate and dissolved hydrogen within a few minutes suggests that the kinetics of nitrate reduction may be neglected if the time scale of the investigated scenario is considerably longer and both, nitrate and hydrogen concentrations, are in the mM range. The requirement for such a simplification can be fulfilled for instance in a leakage or site remediation scenario typically lasting for time spans between a few days and several years. Therefore, fast hydrogenotrophic nitrate reduction suggests that applying geochemical steady state models instead of kinetic reaction equations could considerably reduce modeling efforts when evaluating scenarios numerically (Hagemann et al., 2014, 2016; Pfeiffer et al., 2016). Apart from characterizing redox reactions potentially taking place after a hydrogen leakage, these considerations may also contribute to advancing in-situ groundwater treatment technologies using hydrogen.

These efforts shall support the proceeding of the model development process as well as contribute to its implementation when evaluating different energy storage scenarios using site-scale computer models. Overall, the inclusion of these further hydrogeochemical redox reactions into the ANGUS+ Guidelines may also support improvements in the sustainability of subsurface energy storage within the concurrent ways of using the subsurface space.

5. Conclusions

5.1. Summary and significance

Integrating energy storage facilities in power networks is potentially a prerequisite for increasing the share of solar and wind energy in the energy supply mix without risking the stability of such networks. These solutions may help to provide energy from renewable sources, and, therefore, support the global climate change mitigation efforts. Geological energy storage has the potential to participate in a cooperative system of various energy storage technologies covering a wide range both in storage capacity and in response time together. Assessing environmental and operational impacts of energy storage technologies integrated in future energy networks is a necessary requirement for technologies aiming to a sustainable operation. Geological energy storage technologies, which are better characterized, potentially represent a safer and more predictable element in future energy networks including a major amount of energy storage capacities.

The presented doctoral project experimentally characterized gas-specific geochemical reactions following a leakage of compressed air, methane or hydrogen into a shallow aquifer from a gas storage reservoir. The outcomes presented here include the identification of the corresponding redox reactions, the description of their kinetic behavior with respect to various environmental conditions, and the development of reaction models potentially deployable in further investigations. Although detailed microbial investigations were beyond the scopes of this study, it can also be generally concluded that most redox processes investigated here are carried out, or at least potentially mediated, by microbial communities.

The characterization of hydrogeochemical reactions described in the presented experimental workflow provides insights beyond the state of the literature about the processes to be expected if a gas leakage would intrude a shallow aquifer. The identification and parameterization of such reactions, and geochemical aspects in general, represent a significant contribution to numerical models dealing with the thermal, hydraulic, mechanic, and chemical effects the use of the subsurface can potentially have. When these models are applied to describe and evaluate possible scenarios of subsurface use, and particularly the use of the subsurface for energy storage, such new geochemical insights can result in more realistic outcomes of such studies. Apart from modeling, geochemical leakage monitoring is also supported by a more adequate characterization of reactions potentially triggered by a gas intrusion into an aquifer, because if the geochemical patterns created by such reactions are known form experimental investigations, and later potentials also from pilot site studies, a localization and management of a potential leakage event can be done more efficiently.

Gas storage facilities are expected to be constructed as a part of the global energy transition in the upcoming decades, along with other emerging uses of the subsurface space for geological energy storage. Conflicts potentially rising between various ways of using the subsurface space are often evaluated by considering numerical scenarios considering various combinations of technologies, geological settings, and operational boundary conditions. A special case amongst scenarios including a conflict of use is represented by the unwanted interactions between gas storage facilities and protected shallow groundwater resources found in aquifers overlying such facilities. The potential geochemical consequences of a leakage scenario were characterized in details in this PhD Thesis for three different gases. The outcomes therefore contribute to improvements in the knowledge on the geochemical effects energy storage facilities and, most importantly, an accidental leakage from such gas storage systems can cause in the subsurface, supporting the planning and operation workflows for geological energy storage facilities.

5.2. Aims reached

The outcomes presented in this Thesis provide detailed experimental parameterization of pyrite oxidation kinetics, completed by a passivation effect and a model function describing and transferring reaction rates from experimental to in situ conditions. Regarding methane, the current process understanding was supported by experiments showing no methane oxidation coupled to reduction of any electron acceptors within ca. a year. In contrast, for hydrogen intrusions, an improved process understanding describes the quickly proceeding reactions by their reaction rates and integrating them into a descriptive process model containing parallel acetogenesis and sulfate reduction. All these outcomes contribute to the answers provided to the initial questions:

1. How does pyrite oxidation by oxygen change the groundwater in a shallow aquifer after a leakage of compressed air?

    a. *How do the products of pyrite oxidation decrease pyrite reactivity? What factors influence this passivation?*

The rate of pyrite oxidation, the main process to be expected after a compressed air leakage, is slowed down to a few percent by the oxidation products. This passivation layer precipitates onto the surface of the pyrite grains and insulates them from the oxygen-rich groundwater. The development of this iron-oxihydroxide coating has a stronger effect at higher oxygen partial pressures and forms linearly as pyrite is being oxidized. This passivation effect has not been characterized in such an extent so far, therefore its inclusion in the development of the presented reactive transport model represents an improvement compared to currently available reaction model schemes.

    b. *What transfer function can scale up the results from lower, athmospherical pressure experiments to higher, in situ conditions?*

Based on the experimental results with 0-11 bars of oxygen partial pressure, a reactive transport model was developed, describing the observed reaction kinetics of pyrite oxidation. This model extends and adjusts previously published reaction concepts and equations to the conditions to be expected in a shallow aquifer influenced by a compressed air leakage, such as higher oxygen partial pressures, lower temperatures and neutral pH. Carrying out experiments at lower partial pressures, and then using the presented transfer function for upscaling can save a considerable amount of effort compared to experiments at *in situ* conditions.
The changes in groundwater composition provided by the model and the experimental results are limited to an up to 0.5 mM increase in sulfate and a slight decrease in pH, which is, under the investigated conditions, not a significant risk to water resources potentially utilized as sources of drinking water. However, a higher pyrite content or specific surface area as well as different transport conditions may cause a more significant effect.

2. How can methane be oxidized in a shallow aquifer after a methane leakage and what reaction rates should be considered?

    a. *What does the state-of-the-art literature reveal on microbial redox reactions oxidizing methane in aqueous environments?*

Although methane and its potential electron acceptors are unlikely to be found simultaneously in aqueous environments, methane is a comparatively unfavorable electron donor for microbial metabolism. Therefore, anaerobic methane oxidation coupled to sulfate reduction is a reaction found mostly in marine and freshwater environments where similar conditions (concentrations of methane and sulfate) are stable for at least several or several tens of years, which is a long time compared to most sudden gas leakage scenarios. Reasons for this slow response can be i) the doubling time of up to 7 months of the microorganisms carrying out the reaction; ii) the ca. 1% rate of assimilation of the carbon taken up by these microorganisms; and iii) the very low (ca. 1 ATP) energy yield of the reactions.

b. *What is the expected time scale for starting a reaction involving reduction of sulfate or nitrate coupled to methane oxidation?*

Our experiments showed that the oxidation of methane coupled to the reduction of sulfate, nitrate or ferric iron must take at least a year to show the first recognizable signs at the conditions represented in this study. Such conditions represented a methane intrusion into an aquifer in which no microbial community mediating these reactions was established previously.

c. *What should be in the focus of monitoring and modeling efforts for fugitive methane?*

Monitoring of methane leakages should focus on methane itself, as no reactions and reaction products are to be expected to be produced at considerable reaction rates. No biogeochemical methane oxidation coupled to any of the potential electron acceptors also means that the spreading of fugitive methane plumes may not be limited by chemical reactions. Therefore, a conservative behavior may be considered when modeling numerical scenarios. However, experiments with site-specific sediments and groundwaters may yield reaction rates and lag times explicitly valid for a given gas storage facility and its locally overlying aquifers.

3. What biogeochemical redox reactions do elevated hydrogen partial pressures trigger in shallow aquifers and at what rates do these reactions take place?

a. *Is nitrate, sulfate and carbonate reduction dependent on hydrogen concentration?*

If in an aquifer a hydrogen concentration is provided, which is around a million times higher than the concentrations found in natural environments, then prompt and simultaneous reduction of nitrate (if available), sulfate and carbonate can take place. In the presented experiments such reactions resulted in rising concentrations of nitrite and N_2/N_2O, sulfide and acetate, along with a near-stoichiometrical depletion of hydrogen. All of these reactions imply a significant and immediate change of groundwater composition, and all reactions were found to be independent from the hydrogen partial pressures applied. In case the partial pressure of CO_2 is comparatively higher, production of formate and methane may be expected.

b. *Are the observed reactions potentially transferable to deeper aquifer environments?*

Hydrogen, in strong contrast to methane, triggers immediate redox reactions which were, in contrast to pyrite oxidation by oxygen, independent from the partial pressure of hydrogen and from the experimental run time. Investigations of sediments from deeper aquifers and with elevated salinities suggest that the consequences of hydrogen intrusion into a shallow aquifer characterized here are potentially transferable for those environments as well. A particularly important aspect of this outcome is that even hydrogen storage facilities constructed in saline aquifers potentially show the reactions characterized here, which would mean a loss from the stored hydrogen and changes in its composition.

Based on the reactions characterized using the high pressure column experiments a descriptive process model was developed, which can serve as input for further experimental and modeling studies involving various aquifer environments. In terms of applications and project deliverables, this model is one of the major outcomes of the investigations on redox reactions consuming hydrogen.

5.3. Outlook and potential future aspects

In order to provide additional insights on the behavior of the redox reactions characterized here, new efforts may be focused on a series of fields. Further research may include parallel experiments on pyrite oxidation at wider pressure, temperature and pH conditions. For methane, an experimental investigation of a sediment-groundwater system from a methane leakage site with proven aerobic or anaerobic methane oxidizing activity could specifically characterize the reactions and also the microbial community responsible for redox reactions potentially changing the groundwater composition. The experimental investigation of such microbial reactions may be reinforced by adding nutrient mixtures potentially needed by the microorganisms. Further efforts on hydrogen-driven, strongly reductive redox reactions can include investigation of the effects on minerals composing the solid phase, especially those containing Fe^{III}, Mn^{IV} or toxic trace elements in oxidized states (microbial reduction of metals); and the exploration of potential pH-, temperature-, or nutrient (for instance phosphate, inorganic and organic trace nutrients) dependency of basically all redox reactions mentioned in this Thesis. Correlating the "reactivity" of a representative number of sediments from different origins to one or more of their properties (age, organic carbon content, pristine geochemical conditions, salinity, and degree of consolidation) could return precious input for general site or sediment characterization projects. Furthermore, investigating geomechanical changes, like changes in rock stability or permeability, following the reactions characterized in this Thesis may provide further insights into operational and safety implications of subsurface gas storage.

However, new efforts can also be recommended to be focused on pilot scale field studies instead of more laboratory experiments to deliver more realistic results. For example, hydrogen or compressed air injection limited in space and time into a model shallow aquifer could yield valuable further characterization of the response of the subsurface valid for that site but also allowing to improve the processes described in this Thesis towards a more general process understanding. Regarding reservoir conditions, a similar experimental workflow may yield comparable results, possibly relevant for companies planning such facilities, or other civil or governmental stakeholders. Creating environments representing deeper aquifers used for storage may require setting the corresponding pressure, temperature and salinity conditions, which may have an influence on the processes observed. As a leakage of methane, but also a more extensive leakage of can potentially reach levels very close to the surface, experiments representing very shallow, unsaturated conditions may be carried out using special experimental set-ups percolated by water-saturated gas instead of gas-saturated water. Such optimized experimental and sampling methods may deliver a characterization valid to near-surface systems, similar to the results gathered on saturated aquifers here. Those results could also contribute to the development of near-surface leakage monitoring methods.

In order to follow the reactions taking place, the microbial community shall be regularly, selectively, and quantitatively monitored due to the deciding role these living organisms play in mediating the reactions both in experiments and on the field. Due to the culturing routines for these species ranging from difficult to unknown, *in situ* sampling and investigations can yield results more convenient to apply into biogeochemical models. The identification process can possibly include methods based on nucleic acids or various biomarkers. A further recommendation for the analytic efforts of future studies may be to also follow the changes in the isotopic composition of the dissolved hydrogen, carbon, sulfur, oxygen and nitrogen species involved in the redox reactions triggered by a gas leakage. Isotope methods have the potential to deliver further insights to the actual pathways of the redox reactions characterized within this Thesis, and thereby supporting decisions during process model development.

Implementations already in process include the integration of the characterized geochemical reactions into 3D multiphase reservoir scale numerical reactive transport models. These new inputs for these thermal-hydraulic-mechanic-chemical models will support the analysis of simulated scenarios and contribute to the ANGUS+ Guidelines for the sustainable and conflict-free use of the subsurface space.

References

Al Hagrey SA, Schäfer D, Köhn D, Wiegers CE, Chung D, Dahmke A, Rabbel W (2016): Monitoring gas leakages simulated in a near surface aquifer of the Ellerbek paleo-channel. Environ Earth Sci 75:1083.

Appelo CAJ, Postma D (2010): Geochemistry, groundwater and pollution. Balkema Publishers, Leiden, The Netherlands. ISBN 04 1536 4280

Apps JA, Zheng L, Zhang Y, Xu T, Birkholzer JT (2010): Evaluation of potential changes in groundwater quality in response to CO_2 leakage from deep geologic storage. Transport Porous Med 82, 215-246.

Audigane P, Ebrahimiyekta A, Pichavant M (2015): Evaluation of hydrogen migration and geochemical reactivity into underground. 6th International Conference on Fundamentals & Development of Fuel Cells. HAL, Toulouse, France

Bauer S. (2015a): Presentation and personal communication at the ANGUS+ meeting, 7-9. September 2015, Asendorf, Germany.

Bauer S, Pfeiffer W, Boockmeyer A, Dahmke A, Beyer C (2015b): Quantifying induced effects of subsurface renewable energy storage. Energy Procedia 76, 633-641.

Bauer S, Beyer C, Dethlefsen F, Dietrich P, Duttmann R, Ebert M, Feeser V, Gorke U, Köber R, Kolditz O, Rabbel W, Schanz T, Schäfer D, Würdemann H, Dahmke A (2013): Impacts of the use of the geological subsurface for energy storage: An investigation concept. Environ Earth Sci 70, 3935–3943.

Basso O, Lascourrèges J-F, Jarry M, Magot M (2005): The effect of cleaning and disinfecting the sampling well on the microbial communities of deep subsurface water samples. Environ Microbiol 7, 13–21.

Beal EJ, House CH, Orphan VJ (2009): Manganese- and iron-dependent marine methane oxidation. Science 325(5937), 184-187.

Becker A (2014): Fortführung von Langzeitsäulenversuchen zur Untersuchung geochemischer Folgereaktionen infolge von Methanintrusionen in oberflächennahe Aquifere. BSc Thesis at the Institute of Geosciences, Christian-Albrechts University Kiel.

Beckmann A, Gerhardt M, Zittwitz M, Martiensse M, Krieg R, Geistlinger H, Schirmer M (2007): Das OXYWALL-Projekt: Anwendung eines Verfahrens zur Direktgasinjektion von Sauerstoff zur in situ Sanierung von organisch kontaminierten Grundwässern. Altlasten Spektrum 4, 153-159.

Berest P, Brouard B, Durup G (2002): Tightness tests in salt cavern wells. Oil Gas Sci Technol 56, 451-469.

Berger S (2015): Laborversuche zur Quantifizierung von Wasserstoff-Oxidationsreaktionen in Aquifer-Sedimenten. MSc Thesis at the Institute of Geosciences, Christian-Albrechts University Kiel.

Berta M, Becker A, Dethlefsen F, Ebert M, Koch S, Dahmke A (2015a): Experiments showed no reactions coupled to methane leaked into shallow aquifers. First Break 33, 93-95.

Berta M, Becker A, Dethlefsen F, Ebert M, Koch S, Dahmke A (2015b): No Short-term Attenuation of Methane Leaked into Shallow Aquifers - An Experimental Study. The Third Sustainable Earth Sciences Conference and Exhibition, EarthDoc.

Berta M, Dethlefsen F, Ebert M, Gundske K, Dahmke A (2016): Surface passivation model explains pyrite oxidation kinetics in column experiments with up to 11 bars $p(O_2)$. Environ Earth Sci 75:1175.

Berta M, Dethlefsen F, Ebert M, Schäfer D. (2017): Integrated experimental and modeling assessment of potential effects of gas leakages on groundwater composition. Abstract submitted to the European Geosciences Union General Assembly, Vienna, 23-28. April.

Blight K, Ralph DE, Thurgate S (2000): Pyrite surfaces after bio-leaching: a mechanism for bio-oxidation. Hydrometallurgy 58, 227–237.

BMUB (2013): Report of the German Federal Ministry for the Environment, Nature Conservation, Building and Nuclear Safety.

Boetius A, Ravenschlag K, Schubert CJ, Rickert R, Widdel F, Gieseke A, Amann R, Jorgensen BB, Witte U, Pfannkuche O (2000): A marine microbial consortium apparently mediating anaerobic oxidation of methane. Nature 407, 623-626.

Bolliger C, Schroth MH, Bernasconi SM, Kleikemper J, Zeyer J (2001): Sulfur isotope fractionation during microbial sulfate reduction by toluene-degrading bacteria. Geochim Cosmochim Ac 65, 3289-3298.

Bossel U (2006): Wasserstoff löst keine Energieprobleme. Technikfolgenabschätzung – Theorie und Praxis Nr 1–15:27-34.

Brantley SL, Yoxtheimer D, Arjmand S, Grieve P, Vidic R, Pollak J, Llewellyn GT, Abad J, Simon C (2014): Water resource impacts during unconventional shale gas development: the Pennsylvania experience. Int J Coal Geol 126, 140-156.

Brigmon RL (2001): Methanotrophic bacteria: use in bioremediation. Westinghouse Savannah River Company, WSRC-MS-2001-00058.

Bundesnetzagentur (2013): Monitoringbericht. Bundesnetzagentur für Elektrizität, Gas, Telekommunikation, Post und Eisenbahnen; Bundeskartellamt, p 319.

Bünger U, Michalski J, Crotogino F, Kruck O (2016): 7 - Large-scale underground storage of hydrogen for the grid integration of renewable energy and other applications A2 - Veziroğlu, Michael BallAngelo BasileT. Nejat. Compendium of Hydrogen Energy. Woodhead Publishing, Oxford. pp 133-163

Bussman I, Suess E (1998): Groundwater seepage in Eckernförde Bay (Western Baltic Sea): Effect on methane and salinity distribution of the water column. Cont Shelf Res 18, 1795-1806.

Bussman I, Dando PR, Niven SJ, Suess E (1999): Groundwater seepage in the marine environment: Role for mass flux and bacterial activity. Mar Ecol Prog Ser 178, 169–177.

Buzek F, Onderka V, Vancura P, Wolf I (1994): Carbon isotope study of methane production in a town gas storage reservoir. Fuel 73, 747-752.

Cai ML, Liu JX, Wei YS (2004): Enhanced biohydrogen production from sewage sludge with alkaline pretreatment. Environ Sci Technol 38, 3195-3202.

Canfield D, Raiswell R, Westrich JT, Reaves C, Berner RA (1986): The use of Chromium reduction in the analysis of reduced inorganic sulfur in sediments and shales. Chem Geol 54, 149-155.

Chang CC, Tseng SK, Huang HK (1999): Hydrogenotrophic denitrification with immobilized Alcaligenes eutrophus for drinking water treatment. Bioresource Technol 69, 53-58.

Chapelle FH, Lovley DR (1992): Competitive exclusion of sulfate reduction by Fe(III)-reducing bacteria: a mechanism for producing discrete zones of high-iron ground water. Ground Water 30, 29-36.

Chapelle FH, Haack SK, Adriaens P, Henry MA, Bradley PM (1996): Comparison of Eh and H_2 measurements for delineating redox processes in a contaminated aquifer. Environ Sci Technol 30, 3565-3569.

Chapelle FH, O'Neill K, Bradley PM, Methe BA, Ciufo SA, Knobel LL, Lovley DR (2002): Hydrogen-based subsurface microbial community dominated by methanogens. Nature 415, 312-315.

Chiquet P (2015): Personal communication by e-mail.

Cirpka OA, Chiogna G, Rolle M, Bellin A (2014): Transverse mixing in three-dimensional nonstationary anisotropic heterogeneous porous media. Water Resour Res 51, 241-260.

Conrad R (1999): Contribution of hydrogen to methane production and control of hydrogen concentrations in methanogenic soils and sediments. FEMS Microbiol Ecol 28, 193-202.

Conrad R (2016): Personal Communication. EGU Wien

Conrad R, Goodwin S, Zeikus JG (1987): Hydrogen metabolism in a mildly acidic lake sediment (Knaack Lake). FEMS Microbiol Ecol 45, 243–249.

Conrad R, Wetter B (1990): Influence of temperature on energetics of hydrogen metabolism in homoacetogenic, methanogenic, and other anaerobic bacteria. Arch Microbiol 155, 94-98.

Cord-Ruwisch R, Seitz HJ, Conrad R (1988): The capacity of hydrogenotrophic anaerobic bacteria to compete for traces of hydrogen depends on the redox potential of the terminal electron acceptor. Arch Microbiol 149, 350-357.

Courtin-Nomade A, Bril H, Bény JM, Kunz M, Tamura N (2010): Sulfide oxidation observed using micro-Raman spectroscopy and micro-X-ray diffraction: The importance of water/rock ratios and pH conditions. Am Mineral 95, 582-591.

Crotogino F, Mohmeyer KU, Scharf R (2001): Huntorf CAES: More than 20 years of successful operation. Spring 2001 Meeting Orlando, Florida, USA 15 -18 April 2001.

Dale AW, Regnier P, van Cappellen P (2006): Bioenergetic controls on anaerobic oxidation of methane (AOM) in coastal marine sediments: a theoretical analysis. Am J Sci 306, 246-294.

Descourvières C., Hartog, N., Patterson, B. M., Oldham, C., Prommer, H. (2009): Geochemical controls on sediment reactivity and buffering processes in a heterogeneous aquifer. Appl Geochem 25, 261-275.

Dethlefsen F, Bauer S, Dahmke A (2015): Current Status and Further Needs in Parameterization for an Underground Land Use Planning. The Third Sustainable Earth Sciences Conference and Exhibition. EarthDoc.

Dethlefsen F, Beyer C, Feeser V, Köber R (2016a): Parameterizability of processes in subsurface energy and mass storage - Supported by a review of processes, codes, parameters, and a regional example: Schleswig-Holstein, Germany. Environ Earth Sci 75:885.

Dethlefsen F, Köber R, Schäfer D, al Hagrey SA, Hornbruch G, Ebert M, Beyer C, Großmann J, Dahmke A (2013): Monitoring approaches for detecting and evaluating CO_2 and formation water leakages into near-surface aquifers. Energy Procedia 37, 4886-4893.

Dethlefsen F, Nolde M, Schäfer D, Dahmke A (2016b): Basic parameterization of Schleswig-Hostein's shallow geological formations for numerical reactive transport simulations based on existing data. Envir Earth Sci 75:885.

Dethlefsen F, Nolde M, Schäfer D, Dahmke, A. (2017): Basic parameterization of Schleswig–Holstein's shallow geological formations for numerical reactive transport simulations: representative groundwater compositions. Environ Earth Sci 76:59.

Deutzmann JS (2011): Aerobic and anaerobic oxidation of methane in sediments of Lake Constance. PhD Thesis, Universität Konstanz, p. 111.

Deutzmann JS, Schink B (2011): Anaerobic oxidation of methane in sediments of Lake Constance, an oligotrophic freshwater lake. Appl Env Microbiol 77, 4429–4436.

Devol AH, Anderson JJ, Kuivila K, Murray JW (1984): A model for coupled sulfate reduction and methane oxidation in the sediments of Saanich Inlet. Geochim Cosmochim Acta 48, 993-1004.

Dincer AR, Kargi F (2001): Salt inhibition kinetics in nitrification of synthetic saline wastewater. Enzyme Microb Tech 28, 661-665.

Dusseault M, Jackson R (2013): Seepage pathway assessment for natural gas to shallow groundwater during well stimulation, production and after abandonment. GeoMontreal conference 2013

Ebert, M. (2004): Elementares Eisen in permeablen reaktiven Barrieren zu in-situ Grundwassersanierung – Kenntnisstand nach zehn Jahren Technologieentwicklung. Habilitation - Institut für Geowissenschaften, CAU Kiel.

Edwards EA, Wills LE, Reinhard M, Grbic-Galic D (1992): Anaerobic degradation of toluene and xylene by squifer microorganisms under sulfate-reducing conditions. Appl Environ Microb 58:794-800.

Eisentraeger A, Klag P, Vansbotter B, Heymann E, Dott W (2001): Denitrification of groundwater with methane as sole hydrogen donor. Water Res, 35, 2261–2267.

Engle MA, Rowan EL (2014): Geochemical evolution of produced waters from hydraulic fracturing of the Marcellus Shale, northern Appalachian Basin: A multivariate compositional data analysis approach. Int J Coal Geol 126, 45-56.

Ergas SJ, Shumway L, Fitch MW, Neemann J (1999): Membrane process for biological treatment of contaminated gas streams. Biotechnol Bioeng 63, 431–441.

Ergas SJ, Reuss AF (2001): Hydrogenotrophic denitrification of drinking water using a hollow fibre membrane bioreactor. J Water Supply Res T 50, 161-171.

Ettwig KF, Butler MK, Le Paslier D, Pelletier E, Mangenot S, Kuypers M, Schreiber F, Dutilh D, Zedelius J, De Beer D, Gloerich J, Wessels HJ, Van Alen CT, Luesken F, Wu ML, Van De Pas-Schoonen KT, Op Den Camp HJ, Janssen-Megens EM, Francoijs KJ, Stunnenberg H, Weissenbach J, Jetten MS, Strous M (2010): Nitrite-driven anaerobic methane oxidation by oxygenic bacteria. Nature 464, 543-548.

Ettwig KF, Zhu B, Speth D, Keltjens JT, Jetten MSM, Kartal B (2016): Archaea catalyze iron-dependent anaerobic oxidation of methane. PNAS 113, 12792–12796.

European Parliament, European Council (2000): Directive 2000/60/EC of the European Parliament and of the Council of 23 October 2000 establishing a framework for the Community action in the field of water policy.

Evans DJ (2008): An appraisal of underground gas storage technologies and incidents, for the development of risk assessment methodology. British Geological Survey for the Health and Safety Executive.

Evans DJ (2009): A review of underground fuel storage events and putting risk into perspective with other areas of the energy supply chain. In: Evans, D. J., Chadwick, R. A. (eds): Underground gas storage: worldwide experiences and future development in the UK and Europe. The Geological Society, London, Special Publications, 313, 173-216.

Feisthauer S, Seidel M, Bombach P, Traube S, Knöller K, Wange M, Fachmann S, Richnow HH (2012): Characterization of the relationship between microbial degradation processes at a hydrocarbon contaminated site using isotopic methods. J Contam Hydrol 133, 17–29.

Fraunhofer ISE: https://www.energy-charts.de/energy.htm (in 2016)

Gao D, Jiang DF, Liu P, Li Z, Hu SG, Xu H (2014): An integrated energy storage system based on hydrogen storage: process configuration and case studies with wind power. Energy 66, 332-341.

Girguis PR, Cozen AE, DeLong EF (2005): Growth and population dynamics of anaerobic methane-oxidizing archaea and sulphate-reducing bacteria in a continuous flow bioreactor. Appl Environ Microbiol 71, 3725-3733.

Gleisner M, Herbert RB, Frogner Kockum PC (2006): Pyrite oxidation by *Acidithiobacillus ferrooxidans* at various concentrations of dissolved oxygen. Chem Geol 225, 16-29.

Gniese, C., Bombach, P., Rakoczy, J., Hoth, N., Schlömann, M., Richnow, H-H., Krüger, M. (2014): Relevance of deep-subsurface microbiology for underground gas storage and geothermal energy production. Adv Biochem Eng Biotechnol 142, 95-121.

Grossman EL, Cifuentes LA, Cozzarelli IM (2002): Anaerobic methane oxidation in a landfill-leachate plume. Environ Sci Technol 36, 2436-2442.

Gundske, K. (2013): Determination of the pyrite oxidation kinetics at elevated O_2 partial pressures in column experiments. Masterarbeit am Institut für Geowissenschaften der CAU Kiel.

Haase C, Dahmke A, Ebert M, Schäfer D, Dethlefsen F (2014): Suitability of existing numerical model codes and thermodynamic databases for the prognosis of calcite dissolution processes in near-surface sediments due to a CO_2 leakage investigated by column experiments. Aquat Geochem 20, 639–661.

Hagemann B, Rasoulzadeh M, Panfilov M, Ganzer L, Reitenbach V (2014): Hydrogenization of underground storage of natural gas - Impact of hydrogen on biochemical transformations of stored gas. 14th European Conference on the Mathematics of Oil Recovery Catania, Sicily, Italy

Hagemann B, Rasoulzadeh M, Panfilov M, Ganzer L, Reitenbach V (2016): Hydrogenization of underground storage of natural gas. Computational Geosciences 20, 595-606.

Hammack RW, Watzlaf GR (1990): The effect of oxygen on pyrite oxidation. Mining and Reclamation Conference and Exhibition, Charleston, WV, April 23 -26, 1990.

Hansen, LB, Finster K, Fossing H, Iversen N. (1998): Anaerobic methane oxidation in sulfate depleted sediments: effects of sulfate and molybdate additions. Aquat Microb Ecol 14, 195-204.

Harris SH, Smith RL, Suflita JM (2007): In situ hydrogen consumption kinetics as an indicator of subsurface microbial activity. FEMS Microbiol Ecol 60, 220–228.

Haugen KS, Semmens MJ, Novak PJ (2002): A novel in situ technology for the treatment of nitrate contaminated groundwater. Water Res 36, 3497–3506.

Hassannayebi N, Azizmohammadi S (2015): Does Injected H_2 Induce Interactions among Brine and Minerals in Reservoir? An Equilibrium Geochemical Modelling Approach. The Third Sustainable Earth Sciences Conference and Exhibition, EarthDoc.

Haugen KS, Semmens MJ, Novak PJ (2002): A novel in situ technology for the treatment of nitrate contaminated groundwater. Water Res 36:3497-3506.

Heimann A, Blodau C, Postma D, Larsen F, Viet PH, Nhan PQ, Jessen S, Duc MT, Hue NTM, Jakobsen R (2007): Hydrogen thresholds and steady state concentrations associated with microbial arsenate respiration. Environ Sci Technol 41, 2311–2317.

Heimann A, Jakobsen R, Blodau C (2010): Energetic constraints on H_2-dependent terminal electron accepting processes in anoxic environments: a review of observations and model approaches. Environ Sci Technol 44:24–33.

Heron G, Crouzet C, Bourg ACM, Christensen TH (1994): Speciation of Fe(II) and Fe(III) in contaminated aquifer sediments using chemical extraction techniques. Environ Sci Technol 28, 1698-1705.

Hoehler TM, Alperin MJ, Albert DB, Martens CS (1994): Field and laboratory studies of methane oxidation in an anoxic marine sediment: Evidence for a methanogen-sulfate reducer consortium. Glob Biogeochem Cycles 8, 451-463.

Hoehler TM, Alperin MJ, Albert DB, Martens CS (1998): Thermodynamic control on hydrogen concentrations in anoxic sediments. Geochim Cosmochim Ac 62, 1745-1756.

Holzman DC (2012): Methane found in well water near fracking sites. Environ Health Persp 119:289.

Hrsak D, Begonja A (2000): Possible interactions within a methanotrophic-heterotrophic groundwater community able to transform linear alkylbenzenesulfonates. Appl Environ Microbiol 66, 4433–4439.

Huminicki DMC, Rimstidt JD (2009): Iron oxyhydroxide coating of pyrite for acid mine drainage control. Appl Geochem 24, 1626–1634.

Iannotti EL, Kafkewitz D, Wolin MJ, Bryant MP (1973): Glucose fermentation products in *Ruminococcus albus* grown in continuous culture with Vibrio succinogenes: changes caused by interspecies transfer of H_2. J Bacteriol 114, 1231-1240.

IPCC (2014): Climate Change 2014: Synthesis Report. Contribution of Working Groups I, II and III to the Fifth Assessment Report of the Intergovernmental Panel on Climate Change [Core Writing Team, R.K. Pachauri and L.A. Meyer (eds.)]. IPCC, Geneva, Switzerland, 151 pp.

Islas-Lima S, Thalasso F, Gomez-Hernandez J (2004): Evidence of anoxic methane oxidation coupled to denitrification. Water Res 38, 13-16.

Iversen N, Jørgensen BB (1985): Anaerobic methane oxidation rates at the sulfate-methane transition in marine sediments from Kattegat and Skagerrak (Denmark). Limnol Oceanogr 30, 944-955.

Iversen N, Oremland RS, Klug MJ (1987): Big Soda Lake (Nevada). 3. Pelagic methanogenesis and anaerobic methane oxidation. Limnol Oceanogr 32, 804-814.

Jackson RE, Gorody AW, Mayer B, Roy JW, Ryan MC, van Stempvoort DR (2013a): Groundwater protection and unconventional gas extraction: the critical need for field-based hydrogeological research. Groundwater 51, 488-510.

Jackson RB, Vengosh A, Darrah TH, Warner NR, Down A, Poreda RJ, Osborn SG, Zhao K, Karr JD (2013b): Increased stray gas abundance in a subset of drinking water wells near Marcellus shale gas extraction. PNAS 28, 11250–11255.

Jakobsen R, Albrechtsen HJ, Rasmussen M, Bay H, Bjerg PJ, Christensen TH (1998): H_2 concentrations in a landfill leachate plume (Grindsted, Denmark): in situ energetics of terminal electron acceptor processes. Environ Sci Technol 32, 2142-2148.

Jesußek A, Köber R, Grandel S, Dahmke A (2012): Aquifer heat storage: sulphate reduction with acetate at increased temperatures. Environ Earth Sci 69, 1763-1771.

Joye SB, Boetius A, Orcutt BN, Montoya JP, Schulz HN (2004): The anaerobic oxidation of methane and sulfate reduction in sediments from Gulf of Mexico cold seeps. Chem Geol 205, 219-38.

Jørgensen BB (2000): Bacteria and marine biogeochemistry. In: Schultz, H. D., Zabel, M. (eds): Marine Geochemistry, Springer-Verlag, ISBN 3-540-664-53-X.

Jørgensen BB, Weber A, Zopfi A (2001): Sulfate reduction and anaerobic methane oxidation in Black Sea sediments. Deep-Sea Res PT I 48, 2097-2120.

Jørgensen CJ, Jacobsen OS, Elberling B, Aamand J (2009): Microbial oxidation of pyrite coupled to nitrate reduction in anoxic groundwater sediment. Environ Sci Technol 43, 4851-4857.

Kabuth A, Dahmke A, Beyer C, Dethlefsen F, Dietrich P, Duttmann R, Ebert M, Feeser V, Görke U, Köber R, Kolditz O, Rabbel W, Schanz T, Schäfer D, Würdemann H, Bauer S (2017) Energy storage in the geological subsurface: dimensioning, risk analysis and spatial planning – The ANGUS+ project. Environ Earth Sci. 76, 23.

Kasten S, Jørgensen BB (2000): Sulfate reduction in marine sediments. In: Schultz, H. D., Zabel, M. (eds): Marine Geochemistry, Springer-Verlag, ISBN 3-540-664-53-X.

Kelly WR, Matisoff G, Fisher JB (1985). The effects of a gas well blow out on ground water chemistry. Envir Geol Water S 7, 205-213.

Kotelnikova S (2002): Microbial production and oxidation of methane in deep subsurface. Earth Sci Rev 58, 367–395.

Knab NJ, Dale AW, Lettmann K, Fossing H, Jørgensen BB (2008): Thermodynamic and kinetic control on anaerobic oxidation of methane in marine sediments. Geochim Cosmochim Ac 72, 3746-3757.

Kneeshaw TA, McGuire JT, Smith EW, Cozzarelli IM (2007): Evaluation of sulfate reduction at experimentally induced mixing interfaces using small-scale push–pull tests in an aquifer–wetland system. Appl Geochem 22, 2618-2629.

Knittel K, Boetius A (2009): Anaerobic oxidation of methane: progress with an unknown process. Annu Rev Microbiol 63, 311-34.

Kleinitz W, Boehling E (2005): Underground gas storage in porous media—operating experience with bacteria on gas quality. Paper SPE 94248 at the SPE Europec/EAGE Annual Conference, Madrid 13–16 June 2005.

Koch S (2014): Experimental study on geochemical effects of methane leakages into groundwater. MSc-Thesis at the Institute of Geosciences, Christian-Albrechts University Kiel.

Koenigsberg SS, Sandefur CA (1999): The use of hydrogen release compound for the accelerated bioremediation of anaerobically degradable contaminants: the advent of time-release electron donors. Remed J 10, 31-53.

Koisur DR, Warford AL (1979): Methane production and oxidation in Santa Barbara basin sediments. Estuarine and Coastal Marine Science 8, 379-385.

Krooss B (2008): Evaluation of database on gas migration through clayey host rocks. Research report to Belgian National Agency for radioactive waste and enriched fissile material (ONDRAFNIRAS), RWTH Aachen.

Krumholz LR, Harris SH, Tay ST, Suflita JM (1999): Characterization of two Subsurface H_2-utilizing bacteria, *Desulfomicrobium hypogeiumsp. nov.* and *Acetobacterium psammolithicumsp. nov.*, and their ecological roles. Appl Environ Microbiol 65, 2300-2306.

Krumholz LR, Mckinley JP, Ulrich GA, Suflita JM (1997): Confined subsurface microbial communities in Cretaceous rock. Nature 386, 64-66.

Krüger M, Wolters H, Gehre M, Joye, SB, Richnow HH (2008): Tracing the slow growth of anaerobic methane-oxidizing communities by ^{15}N-labelling techniques. FEMS Microbiol Ecol 63, 401–411.

Leak DJ, Dalton H (1986): Growth yields of methanotrophs 2: A theoretical analysis. Appl Microbiol Biotechnol 23, 477-481.

Lee KC, Rittmann BE (2000): A novel hollow-fibre membrane biofilm reactor for autohydrogenotrophic denitrification of drinking water. Wat Sci Technol 41, 219–226.

Lefticariu L, Schimmelmann A, Pratt LM, Ripley EM (2007): Oxygen isotope partitioning during oxidation of pyrite by H_2O_2 and its dependence on temperature. Geochim Cosmochim Ac 71, 5072-5088.

Leon EA, Rate AW, Hinz C, Campbell GD (2004): Weathering of sulphide minerals at circum-neutral-pH in semi-arid/arid environments: influence of water content. 3rd Australian New Zealand Soils Conference, 5-9. December 2004, University of Sydney, Australia.

Levenspiel O. (1972): Chemical Reaction Engineering. John Wiley & Sons. New York, Chichester, Brisbane, Toronto.

Lienen T, Westphal A, Würdemann H. (2014): Mikrobiologische Parametrisierung und experimentelle Untersuchungen zum Verhalten von Mikroorganismen an geothermischen Anlagen (AP1.9). ANGUS+ Meeting, 1-3. September 2014, Travemünde, Germany.

Liessens J, Vanbrabant J, De Vos P, Kersters K, Verstraete W (1992): Mixed culture hydrogenotrophic nitrate reduction in drinking water. Microb Ecol 24, 271-290.

Lin LH, Slater GF, Sherwood Lollar B, Lacrampe-Couloume G, Onstott TC (2005): The yield and isotopic composition of radiolytic H_2, a potential energy source for the deep subsurface biosphere. Geochim Cosmochim Ac 69, 893-903.

Long H, Dixon DG (2004): Pressure oxidation of pyrite in sulfuric acid media: a kinetic study. Hydrometallurgy 73, 335-349.

Lovley DR (1985): Minimum threshold for hydrogen metabolism in methanogenic bacteria. Appl Environ Microbiol 49, 1530-1531.

Lovley DR, Klug MJ (1986): Model for the distribution of sulfate reduction and methanogenesis in freshwater sediments. Geochim Cosmochim Ac 50, 11-18.

Lovley DR, Goodwin S (1988): Hydrogen concentrations as an indicator of the predominant terminal electron-accepting reactions in aquatic sediments. Geochim Cosmochim Ac 52, 2993-3003.

Lovley DR, Phillips EJP (1988): Novel mode of microbial energy metabolism: organic carbon oxidation coupled to dissimilatory reduction of iron or manganese. Appl Environ Microbiol 54, 1472-1480.

Lovley DR, Chapelle FH, Woodward JC (1994): Use of dissolved H_2 concentrations to determine distribution of microbially catalyzed redox reactions in anoxic groundwater. Environ Sci Technol 28, 1205-1210.

Lüders K., Firmbach L, Ebert M, Dahmke A, Dietrich P, Köber R (2016, accepted): Gas phase formation during thermal energy storage in near surface aquifers - experimental and modeling results. Environ Earth Sci.

Luo J, Im JH, Mayer MT, Schreier M, Nazeeruddin MK, Park NG, Tilley SD, Fan JH, Grätzel M (2014): Water photolysis at 12.3% efficiency via perovskite photovoltaics and Earth-abundant catalysts. Science 26, 1593-1596.

Mascus C (2015): Laboratory experiments evaluating geochemical reactions in aquifers due to hydrogen intrusion. MSc-Thesis at the Institute of Geosciences, Christian-Albrechts University Kiel.

McCarty PL (1971): Energetics and bacterial growth. In S. D. Faust and J. V. Hunter (ed.): Organic compounds in aquatic environments, 495-531. Marcel Dekker, Inc., New York.

McCray JE (2010): Mathematical modeling of air sparging for subsurface remediation: state of the art. J Hazard Mat 72, 237-263.

McIntosh JC, Grasby SE, Hamilton SM, Osborn SG (2014): Origin, distribution and hydrogeochemical controls on methane occurrences in shallow aquifers, southwestern Ontario, Canada. Appl Geochem 50, 37-52.

McKibben MA, Barnes HL (1986): Oxidation of pyrite in low temperature acidic solutions: Rate laws and surface textures. Geochim Cosmochim Ac 50, 1509-1520.

Meckenstock RU, Elsner M, Griebler C, Lueders T, Stumpp C, Aamand J, Agathos SN, Albrechtsen HJ, Bastiaens L, Bjerg PL, Boon N, Dejonghe W, Huang WE, Schmidt SI, Smolders E, Sørensen SR, Springael D, van Breukelen BM (2015): Biodegradation: updating the concepts of control for microbial cleanup in contaminated aquifers. Environ Sci Technol 49, 7073−7081.

Melchers C (2009): Methan im südlichen Münsterland: Genese, Migration und Gefahrenpotenzial. PhD Thesis, Univ. Münster, p 198.

Metzgen A (2016): Einfluss des pH-Wertes auf die Reduktion gelöster Grundwasserinhaltsstoffe durch Wasserstoff in Hochdruck-Laborversuchen. BSc Thesis at the Institute of Geosciences, Christian-Albrechts University Kiel.

Meulepas RJW, Jagersma CG, Gieteling J, Buisman CJN, Stams AJM, Lens PNL (2009): Enrichment of anaerobic methanotrophs in sulfate-reducing membrane bioreactors. Biotechnol Bioeng 104, 458-470.

Michaelis W, Seifert R, Nauhaus K, Treude T, Thiel V (2002): Microbial reefs in the Black Sea fueled by anaerobic oxidation of methane. Science 297, 1013-15.

Modin O, Fukushi K, Nakajima F, Yamamoto K (2010): Aerobic methane oxidation coupled to denitrification: kinetics and effect of oxygen supply. J Environ Eng 136, 211-219.

Molofsky LJ, Connor JA, Wylie AS, Wagner T, Farhat SK (2013): Evaluation of methane sources in groundwater in northeastern Pennsylvania. Groundwater 53, 333-349.

Mommsen R (2013): Geochemical aspects of pyrite oxidation under high pressure conditions. BSc Thesis at the Institute of Geosciences, Christian-Albrechts University Kiel.

Morozova D, Zettlitzer M, Let D, Würdemann H, and the CO_2SINK group (2011): Monitoring of the microbial community composition in deep subsurface saline aquifers during CO_2 storage in Ketzin, Germany. Energy Procedia 4, 4362-4370.

Moses CO, Herman JS (1991): Pyrite oxidation at circumneutral pH. Geochim Cosmochim Ac 55, 47l-482.

Müller K, Städter M, Rachow F, Hoffmannbeck D, Schmeißer D (2013): Sabatier-based CO_2-methanation by catalytic conversion. Environ Earth Sci 70, 3771-3778.

Nagy A. (2008): Edelmetallrecycling beim Rückbau sulfidhaltiger Erzabgänge. Dissertation an die Fakultät für Energie- und Wirtschaftswissenschaften der Technischen Universität Clausthal.

Nauhaus, K, Boetius A, Krüger M, Widdel F (2002): In vitro demonstration of anaerobic oxidation of methane coupled to sulphate reduction in sediment from a marine gas hydrate area. Environ Microbiol 4, 296-305.

Nauhaus K, Albrecht M, Elvert M, Boetius A, Widdel F (2007): In vitro cell growth of marine archaeal-bacterial consortia during anaerobic oxidation of methane with sulfate. Environ Microbiol 9:187-196.

Neal C, Stanger G (1983): Hydrogen generation from mantle source rocks in Oman. Earth Planet Sc Lett 66, 315-320.

Nedwell DB, Banat IM (1981): Hydrogen as an electron donor for sulfate-reducing bacteria in slurries of salt marsh sediment. Microb Ecol 7, 305-313.

Nevatalo LM, Bijmans MF, Lens PN, Kaksonen AH, Puhakka JA (2010): Hydrogenotrophic sulfate reduction in a gas-lift bioreactor operated at 9°C. J Microbiol Biotechnol 20, 615-621.

Niewöhner C, Hensen C, Kasten S, Zabel M, Schulz HD (1998): Deep sulfate reduction completely mediated by anaerobic methane oxidation in sediments of the upwelling area off Namibia. Geochim Cosmochim Ac 62, 455-464.

Niemann H, Elvert M, Hovland M, Orcutt B, Judd A (2005): Methane emission and consumption at a North Sea gas seep (Tommeliten area). Biogeosciences 2, 335-51.

Niemann H, Duarte J, Hensen C, Omoregie E, Magalhaes VH (2006a): Microbial methane turnover at mud volcanoes of the Gulf of Cadiz. Geochim Cosmochim Ac 70, 5336-5355.

Niemann H, Lösekann T, DeBeer D, Elvert M, Nadalig T (2006b): Novel microbial communities of the Haakon Mosby mud volcano and their role as a methane sink. Nature 443, 854-858.

Nordstrom DK, McCleskey RB, Ball JW (2009): Sulfur geochemistry of hydrothermal waters in Yellowstone National Park: IV Acid-sulfate waters. Appl Geochem 24, 191-207.

Omar SA, Abdelsater MA, Khallil AM, Abdalla MH (1994): Growth and enzyme-activities of fungi and bacteria in soil salinized with sodium-chloride. Folia Microbiol 39, 23-28.

Omoregie EO, Mastalerz V, de Lange G, Straub KL, Kappler A (2008): Biogeochemistry and community composition of iron- and sulfur-precipitating microbial mats at the Chefren Mud volcano (Nile Deep Sea Fan, Eastern Mediterranean). Appl Environ Microbiol 74, 3198-3215.

Oren A (2001): The bioenergetic basis for the decrease in metabolic diversity at increasing salt concentrations: implications for the functioning of salt lake ecosystems. Hydrobiologia 466, 61-72.

Oren A (2008): Microbial life at high salt concentrations: phylogenetic and metabolic diversity. Saline Syst 4, 1-13.

Oritz L, Volckaert G, Mallants D (2001): Gas generation and migration in Bloom Clay, a potential host rock formation for nuclear waste storage. Elsevier, Nuclear Research Center, Belgium.

Osborn SG, Vengosh A, Warner NR, Jackson RB (2011): Methane contamination of drinking water accompanying gas-well drilling and hydraulic fracturing. PNAS 108, 8172-8176.

Panfilov M (2010): Underground storage of hydrogen: self-organisation and methane generation. Transport in Porous Med 85, 841-865.

Panfilov M (2015): Underground and pipeline hydrogen storage. In: Ram Gupta R, Basile A, Nejat TN, Veziroglu: Compendium of Hydrogen Energy: Hydrogen Storage, Distribution and Infrastructure, Woodhead Publishing, 3 Sep 2015, p 438.

Papangelakis VG, Demopoulos GP (1991): Acid pressure oxidation of pyrite: reaction kinetics. Hydrometallurgy 26, 309-325.

Parkes RJ, Cragg BA, Banning N, Brock F, Webster G (2007): Biogeochemistry and biodiversity of methane cycling in subsurface marine sediments (Skagerrak, Denmark). Environ Microbiol 9, 1146-1161.

Parkhurst DL, Appelo CAJ (2013): Description of input and examples for PHREEQC version 3—A computer program for speciation, batch-reaction, one-dimensional transport, and inverse geochemical calculations: U.S. Geological Survey Techniques and Methods, Book 6, A43, 497 p.

Pedersen K (2012): Subterranean microbial populations metabolize hydrogen and acetate under in situ conditions in granitic groundwater at 450 m depth in the Äspö Hard Rock Laboratory, Sweden. FEMS Microbiol Ecol 81, 217-229.

Pelak AJ, Sharma S (2014): Surface water geochemical and isotopic variations in an area of accelerating Marcellus Shale gas development. Environ Pollut 195:91-100.

Pérez-López R, Cama J, Nieto JM, Ayora C, Saaltink MW (2009): Attenuation of pyrite oxidation with a fly ash pre-barrier: reactive transport modelling of column experiments. Appl Geochem 24, 1712-1723.

Pfeiffer WT, Al Hagrey SA, Köhn D, Rabbel W, Bauer S (2016): Porous media hydrogen storage at a synthetic, heterogeneous field site - Numerical simulation of storage operation and geophysical monitoring. Environ Earth Sci 75, 1177.

Raghoebarsing AA, Pol A, Van De Pas-Schoonen KT, Smolders AJP, Ettwig KF, Rijpstra WIC, Schouten S, Sinninghe S, Damstè JS, Op Den Camp HJM, Jetten MSM, Strous M (2006): A microbial consortium couples anaerobic methane oxidation to denitrification. Nature 440, 918-921.

Ragsdale SW, Pierce E (2008): Acetogenesis and the Wood–Ljungdahl pathway of CO_2 fixation. Biochim Biophys Acta 1784, 1873-1898.

Rasigraf O, Vogt C, Richnow HH, Jettena, MSM, Ettwig KF (2012): Carbon and hydrogen isotope fractionation during nitrite-dependent anaerobic methane oxidation by *Methylomirabilis oxyfera*. Geochim Cosmochim Ac 89, 256-264.

Reardon EJ (2005): Zerovalent irons: styles of corrosion and inorganic control on hydrogen pressure buildup. Environ Sci Technol 39, 7311-7317.

Reitenbach V, Ganzer L, Albrecht D, Hagemann B (2015): Influence of added hydrogen on underground gas storage: a review of key issues. Environ Earth Sci 73, 6927-6937.

Reeburgh WS (1980): Anaerobic methane oxidation: rate depth distributions in Skan bay sediments. Earth Planet Sci Lett 47, 345-352.

Reeburgh WS (2007): Oceanic Methane Biogeochemistry. Chem Rev 107:486−513.

Rimstidt JD, Vaughan DJ (2003): Pyrite oxidation: a state-of-the-art assessment of the reaction mechanism. Geochim Cosmochim Ac 67, 873-880.

Roy N, Molson J, Lemieux J-M, Van Stempvoort D, Nowamooz A (2016): Three-dimensional numerical simulations of methane gas migration from decommissioned hydrocarbon production wells into shallow aquifers. Water Resour Res 52.

Safaei H, Keith DW, Hugo RJ (2013): Compressed air energy storage (CAES): with compressors distributed at heat loads to enable waste heat utilization. Appl Ener 103, 165-179.

Sandefur CA, Koenigsberg SS (1999): The Use of Hydrogen Release Compound for the Accelerated Bioremediation of Anaerobically Degradable Contaminants: The Advent of Time-Release Electron Donors. Remed J 10, 31-53.

Schäfer D, Schäfer W, Kinzelbach W (1998): Simulation of reactive processes related to biodegradation in aquifers: 1. Structure of the three-dimensional reactive transport model. J Contam Hydrol 31:167-186.

Schäfer D, Hornbruch G, Schlenz B, Dahmke A (2007): Contaminant spreading assuming different kinetic approaches to simulate microbial degradation. Grundwasser 12:15-25.

Schäfer D, al Hagrey SA, Auken E, Bahr A, Beyer C, Dahmke A, Dumke I, Foged N, Furche M, Gräber M, Großmann J, Helkjaer M, Köber R, Poggenburg J, Naue G, Schlömer S, Seeger C, Tischler L, Vidal A, Wiegers CE, Wöhrl C (2013): Environmental and Process Monitoring. In: CLEAN - CO_2 Large-Scale Enhanced Gas Recovery in the Altmark Natural Gas Field. Kühn M, Münch U (Eds.), Springer, Geotechnologien Science Report 19, 131-167.

Schloemer S, Elbracht J, Blumenberg M, Illing CJ (2016): Distribution and origin of dissolved methane, ethane and propane in shallow groundwater of Lower Saxony, Germany. Appl Geochem 67, 118-132.

Schubert CJ, Durisch-Kaiser E, Holzner CP, Klauser L, Wehrli B (2006): Methanotrophic microbial communities associated with bubble plumes above gas seeps in the Black Sea. Geochem Geophys Geosyst 7, 1-8

Schütz MK, Libert M, Schlegel ML, Lartigue JE, Bildstein O (2013): Dissimilatory iron reduction in the presence of hydrogen: a case study of microbial activity and nuclear waste disposal. Procedia Earth and Planetary Science 7, 409-412.

Schwartz F (2014): Folk Beliefs and Fracking. Keynote at the FH-DGG meeting, 28-31. May 2014, Bayreuth, Germany.

Sherwood Lollar B, Frape SK, Weise LS, Fritz P, Macko SA, Welhan JA (1993): Abiogenic methanogenesis in crystalline rocks. Geochim Cosmochim Ac 57, 5087-5097.

Siegert M, Krüger M, Teichert B, Wiedicke M, Schippers A (2011): Anaerobic oxidation of methane at a marine methane seep in a forearc sediment basin off Sumatra, Indian Ocean. Front Microbiol 2:249.

Segarra KEA, Schubotz F, Samarkin V, Yoshinaga MY, Hinrichs K-U, Joye SB (2015): High rates of anaerobic methane oxidation in freshwater wetlands reduce potential atmospheric methane emissions. Nature Communications 6:7477.

Sivan O, Schrag DP, Murray RW (2007): Rates of methanogenesis and methanotrophy in deep-sea sediments. Geobiology 5, 141-151.

Smigáň P, Greksák M, Kozánková J, Buzek F, Onderka V, Wolf I (1990): Methanogenic bacteria as a key factor involved in changes of town gas stored in an underground reservoir. FEMS Microbiol Lett 73, 221-224.

Smith RL, Ceazan ML, Brooks MH (1994): Autotrophic, hydrogen-oxidizing, denitrifying bacteria in groundwater, potential agents for bioremediation of nitrate contamination. Appl Environ Microbiol 60, 1949-1955.

Smith RL, Howes BL, Garabedian SP (1991): *In situ* measurement of methane oxidation in groundwater by using natural-gradient tracer tests. Appl Env Microbiol 57, 1997-2004.

Smith NJP, Shepherd TJ, Styles MT, Williams GM (2005a): Hydrogen exploration: a review of global hydrogen accumulations and implications for prospective areas in NW Europe. In: Dore, A. G.; Vining, B. A., (eds.) Petroleum geology: north-west Europe and global perspectives: proceedings of the 6th Petroleum Geology Conference. Geological Society of London, 349-358.

Smith RL, Buckwalter SP, Repert DA, Miller DN (2005b): Small-scale, hydrogen-oxidizing-denitrifying bioreactor for treatment of nitrate-contaminated drinking water. Water Res 39, 2014-2023.

Steeb P, Linke P, Treude T (2014): A sediment flow-through system to study the impact of shifting fluid and methane flow regimes on the efficiency of the benthic methane filter. Limnol Oceanogr-Meth 12, 25-45.

Sterner M, Stadler I (2014): *Energiespeicher – Bedarf, Technologien, Integration*. Springer-Verlag Berlin Heidelberg, p 785.

Stevens T, McKinley JP (1995): Lithoautotrophic microbial ecosystems in deep basalt aquifers. Science 270, 450-454.

Stumm W, Morgan JJ (1981): Aquatic Chemistry. New York: J. Wiley & Sons, 1981.

Taylor JB, Alderson JEA, Kalyanam KM, Lyle AB, Phillips LA (1986): Technical and economic assessment of methods for the storage of large quantities of hydrogen. Int J Hydrogen Energy 11, 5-25.

Telling J, Boyd ES, Bone N, Jones EL, Tranter M, MacFarlane JW, Martin PG, Wadham JL, Lamarche-Gagnon G, Skidmore ML, Hamilton TL, Hill E, Jackson M, Hodgson DA (2015): Rock comminution as a source of hydrogen for subglacial ecosystems. Nature Geosci 8, 851-855.

Thauer RK, Jungermann K, Decker K (1977): Energy conservation in chemotrophic anaerobic bacteria. Bacteriol Rev 41, 100-180.

Thauer RK, Möller-Zinkham D, Spormann AM (1989): Biochemistry of acetate catabolism in anaerobic chemotrophic bacteria. Annu Rev Microbiol. 43, 43-67.

Thomson NR, Johnson RL (2010): Air distribution during in situ air sparging: an overview of mathematical modeling. J Hazard Mater 72, 265-282.

Tichomirowa M, Junghans M (2009): Oxygen isotope evidence for sorption of molecular oxygen to pyrite surface sites and incorporation into sulfate in oxidation experiments. Appl Geochem 24, 2072-2092.

Treude T, Boetius A, Knittel K, Wallmann K, Jørgensen BB (2003): Anaerobic oxidation of methane above gas hydrates at Hydrate Ridge, NE Pacific Ocean. Mar Ecol Prog Ser 264, 1-14.

Treude T, Krüger M, Boetius A, Jørgensen BB (2005a): Environmental control on anaerobic oxidation of methane in the gassy sediments of Eckernförde Bay (German Baltic). Limnol Oceanogr 50, 1771-1786.

Treude T, Niggemann J, Meyer J, Wintersteller P, Schubert CJ, Boetius A, Jørgensen BB (2005b): Anaerobic oxidation of methane and sulfate reduction along the Chilean continental margin. Geochim Cosmochim Ac 69, 2767-2779.

Treude T, Orphan V, Knittel K, Gieseke A, House C, Boetius A (2007): Consumption of methane and CO_2 by methanotrophic microbial mats from gas seeps of the anoxic Black Sea. Appl Environ Microbiol 73, 2271-2283.

TrinkwV: Trinkwasserverordnung (2001): Verordnung über die Qualität von Wasser für den menschlichen Gebrauch, BGBl-I-S 2977 and 3154. *(German law on drinking water, in German)*

Truche L, Jodin-Caumon M-C, Lerouge C, Berger G, Mosser-Ruck R, Giffaut E, Michau N (2013): Sulphide mineral reactions in clay-rich rock induced by high hydrogen pressure. Application to disturbed or natural settings up to 250 °C and 30 bar. Chem Geol 351, 217-228.

UBA (Umweltbundesamt) (2010): Energieziel 2050: 100% Strom aus erneuerbaren Quellen. (eds. T. Klaus, C. Vollmer, K. Werner, H. Lehmann and K. Muschen; in German), Dessau-Roßlau, Germany.

Uygur A, Kargi F (2004): Salt inhibition on biological nutrient removal from saline wastewater in a sequencing batch reactor. Enzyme Microb Tech 34, 313-318.

Valentine DL (2002): Biogeochemistry and microbial ecology of methane oxidation in anoxic environments: a review. Antonie van Leeuwenhoek 81, 271-282.

Vallero MVG, Lettinga G, Lens PNL (2005): High rate sulfate reduction in a submerged anaerobic membrane bioreactor (SAMBaR) at high salinity. J Membrane Sci 253, 217-232.

Van Houten BHGW, Meulepas RJW, van Doesburg W, Smidt H, Muyzer G, Stams AJM (2009): *Desulfovibrio paquesiisp. nov.*, a hydrogenotrophic sulfate-reducing bacterium isolated from a synthesis-gas-fed bioreactor treating zinc- and sulfate-rich wastewater. Int J Syst Evol Micr 59, 229-233.

Van Stempvoort D, Maathuis H, Jaworski E, Mayer B, Rich K (2005): Oxidation of fugitive methane in ground water linked to bacterial sulfate reduction. Groundwater, 43, 187-99.

Varekamp JC, Ouimette AP, Herman SW, Flynn KS, Bermudez A, Delpino D (2009): Naturally acid waters from Copahue volcano, Argentina. Appl Geochem 24, 208-220.

Vignais PM, Colbeau A (2004): Molecular biology of microbial hydrogenases. Curr Iss Mol Biol 6, 159-188.

Wang G, Spivack AJ, D'Hondt S (2010): Gibbs energies of reaction and microbial mutualism in anaerobic deep subseafloor sediments of ODP Site 1226. Geochim Cosmochim Ac 74, 3938-3947.

Wankel SD, Adams MM, Johnston DT, Hansel CM, Joye SB, Girguis PR (2012): Anaerobic methane oxidation in metalliferous hydrothermal sediments: influence on carbon flux and decoupling from sulfate reduction. Environ Microbiol 10, 2726-2740.

Wegener G, Shovitri M, Knittel K, Niemann H., Hovland M, Boetius A (2008): Biogeochemical processes and microbial diversity of the Gullfaks and Tommeliten methane seeps (Northern North Sea). Biogeosciences 5, 1127-1144.

WHO (1996): Hydrogen Sulfide in Drinking-water: Background document for development of World Health Organization (WHO) Guidelines for Drinking-water Quality. In: Guidelines for drinking-water quality, 2nd ed. Vol. 2. Health criteria and other supporting information. World Health Organization, Geneva.

Wichern J, Wichern F, Joergensen RG (2006): Impact of salinity on soil microbial communities and the decomposition of maize in acidic soils. Geoderma 137, 100-108.

Windey K, De Bo I, Verstraete W (2005): Oxygen-limited autotrophic nitrification–denitrification (OLAND) in a rotating biological contactor treating high-salinity wastewater. Water Res 39, 4512-4520.

Williamson MA, Rimstidt JD (1994): The kinetics and electrochemical rate determining step of aqueous pyrite oxidation. Geochim Cosmochim Ac 58, 5443-5454.

Xia S, Zhong F, Zhang Y, Li H, Yang X (2010): Bio-reduction of nitrate from groundwater using a hydrogen-based membrane biofilm reactor. J Environ Sci 22, 257-262.

Yan N, Marschner P, Cao W, Zuo C, Qin W (2015): Influence of salinity and water content on soil microorganisms. International Soil and Water Conservation Research 3, 316-323.

Yuan HY, Chen YG, Zhang HX, Jiang S, Zhou Q, Gu GW (2006): Improved bioproduction of short-chain fatty acids (SCFAs) from excess sludge under alkaline conditions. Environ Sci Technol 40, 2025-2029.

Zhang C, Grossman EL, Ammermann JW (1988): Factors influencing methane distribution in Texas ground water. Ground Water 36, 58-66.

Ziemkiewicz PF, He YT (2015): Evolution of water chemistry during Marcellus Shale gas development: A case study in West Virginia. Chemosphere 13, 224-231.

Zinder SH (1993): Physiological ecology of methanogens. In: Methanogenesis, Chapman & Hall, New York, 128-206.

Zhukov VV, Laari A, Koiranen T (2015): Kinetic modeling of high-pressure pyrite oxidation with parameter estimation and reliability analysis using the Markov chain Monte Carlo method. Ind Eng Chem Res 54, 9920−9930.

List of figures

List of tables

Unpublished appendix (on CD only)

1. PhD Thesis
    a. This dissertation (version approved for printing in .pdf format)
    b. Slides presented at the defense talk in Kiel on 11. April 2017 (in .pdf format)
2. Papers constituting this Thesis in their published or submitted forms (in .pdf format)
    a. Berta M, Dethlefsen F, Ebert M, Gundske K, Dahmke A (2016): Surface passivation model explains pyrite oxidation kinetics in column experiments with up to 11 bars p(O2). Environmental Earth Science 75:1175.
    b. Berta M, Becker A, Dethlefsen F, Ebert M, Koch S, Dahmke A (2015): Experiments showed no reactions coupled to methane leaked into shallow aquifers. First Break 33:93-95.
    c. Berta M, Dethlefsen F, Ebert M, Berger S, Dahmke A (submitted): Geochemical effects of millimolar hydrogen concentrations in groundwater - an experimental study in the context of geological hydrogen storage. Environmental Science and Technology.
3. Conference presentation slides on parts of this Thesis (in .pdf format)
    a. Berta, M., Dethlefsen, F., Ebert, M. (2013): Concept of column experiments on pyrite oxidation at 1bar O_2 partial pressure in a near-surface sediment. 23. Doktorandentreffen der Hydrogeologen, BGR Hannover, 7-8. March.
    b. Berta, M., Dethlefsen, F., Ebert, M. (2014): Geochemical Effects of Gas Leakages from Storage Systems into Shallow Aquifers. 24. Doktorandentreffen der Hydrogeologen, CAU Kiel, 9-11. April.
    c. Berta, M., Dethlefsen, F., Ebert, M., Dahmke, A. (2014): Scaling the Geochemical Effects of Potential Gas Leakages from Deep Underground Storage Systems into Shallow Aquifers. Tagung der Fachsektion Hydrogeologie in der DGG, Universität Bayreuth, 28.-31. May. ISSN 0944-4122
    d. Berta, M., Ebert, M., Dethlefsen, F., Dahmke A. (2014): Geochemical Effects of Gas Leakages on Shallow Aquifers. ANGUS+ Meeting, Travemünde, 1-3. September.
    e. Berta, M., Ebert, M., Dethlefsen, F., Dahmke A. (2015): Underground science: Investigating the capabilities of the largest battery under our feet. Science Show, Kieler Uni Live, Kieler Woche, 27. June 2015.
    f. Berta, M., Ebert, M., Dethlefsen, F., Dahmke A. (2015): AP1.7: Updates on Geochemical Effects of Gas Leakages in Shallow Aquifers. ANGUS+ Meeting, Asendorf, 07.-09. September.
    g. Berta, M., Ebert, M., Dethlefsen, F., Berger, S., Mascus, C., Dahmke, A. (2015): Reductive biogeochemical sequence triggered by hydrogen in experiments using aquifer sediment and groundwater. Talk at the GeoBerlin Conference, Berlin, 4-7. October.
    h. Berta, M., Dethlefsen, F., Ebert, M., Schäfer, D. (2017): Integrated experimental and modeling assessment of potential effects of gas leakages on groundwater composition. Abstract submitted to the European Geosciences Union General Assembly, Vienna, 23-28. April 2017.

4. Conference posters on parts of this Thesis (in .pdf format)
    a. Berta, M., Ebert, M., Dethlefsen, F., Dahmke A. (2013): Reactions in shallow potable aquifers caused by leakage of gases stored in the subsurface. ANGUS+ Meeting, Kiel 19-20. June.
    b. Berta, M., Becker, A., Dethlefsen, F., Ebert, M., Koch, S., Dahmke, A. (2015): No Short-term Attenuation of Methane Leaked into Shallow Aquifers - An Experimental Study. 3rd Sustainable Earth Sciences Conference & Exhibition, 13-15 October, Celle, Germany.
    c. Berta, M., Dethlefsen, F., Ebert, M., Dahmke, A. (2016): Hydrogeochemical aspects of a compressed air, methane, or hydrogen intrusion into shallow aquifers. European Geosciences Union General Assembly, Vienna, 17-22. April, ISSN 1607-7962.
5. Raw and evaluated hydrogeochemical data this Thesis is based on (in .xlsx and .xls format)
    a. Experimental results and modeling on pyrite oxidation kinetics
        i. PHREEQC code on pyrite oxidation kinetics (in .phr format)
        ii. Plots on experiments with 0-1 bars $p(O_2)$
        iii. Raw data on experiments with 0-1 bars $p(O_2)$
        iv. Tracer test results on low $p(O_2)$ column experiments
        v. Plots, calculations and raw data on pyrite oxidation at up to 11 bars $p(O_2)$
        vi. 3D site-scale multiphase reactive transport model results with no passivation (in .mp4 format)
        vii. 3D site-scale multiphase reactive transport model results with passivation (in .mp4 format)
        viii. Trace element data and plots on $p(O_2)$=1 bar experiments
    b. Experimental results on potential anaerobic methane oxidation
        i. Plots, calculations and raw data on the initial phase of the experiments
        ii. Plots, calculations and raw data the experiments after improving methods
        iii. Results of post-monitoring of the experimental columns
    c. Experimental results and model development on reactions triggered by hydrogen
        i. Plots, calculations and raw data on flow-through experiments
        ii. Plots, calculations and raw data on fast-flow experiments with nitrate added
        iii. Plots, calculations and raw data on hydrogen oxidation at up to 15 bars $p(O_2)$
        iv. Process model developed on hydrogen oxidation at up to 15 bars $p(O_2)$
        v. Plots, calculations and raw data on batch tests with varied sediments
        vi. Plots, calculations and raw data on batch tests with varied salinities

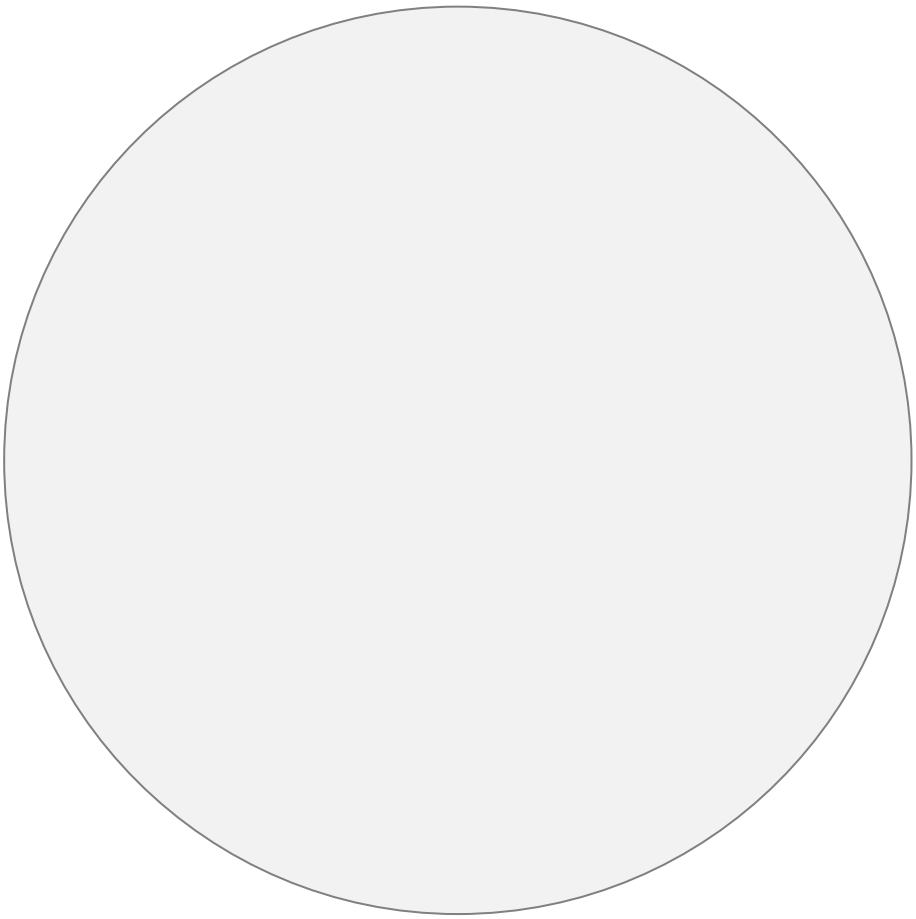

Eidesstattliche Erklärung nach § 8 Abs. 1 der Promotionsordnung

der Mathematisch-Naturwissenschaftlichen Fakultät und Technischen Fakultät der Christian-Albrechts-Universität zu Kiel (vom 2012)

und

nach Abs.4. c) des Merkblattes über die Vervielfältigung von Dissertationen der Mathematisch-Naturwissenschaftlichen Fakultät der Christian-Albrechts-Universität zu Kiel

- Diese Abhandlung ist - abgesehen von der Beratung durch die Betreuern und von der Beiträge anderer Coauthoren - nach Inhalt und Form meine eigene Arbeit.
- Diese Arbeit wurde nicht auf einer anderen Stelle im Rahmen eines Prüfungsverfahrens vorgelegen, veröffentlicht oder zur Veröffentlichung eingereicht.
- Diese Arbeit ist unter Einhaltung der Regeln guter wissenschaftlicher Praxis der Deutschen Forschungsgemeinschaft entstanden.

Kiel, 24. Feburar 2017

Márton Berta